Interstitially Insulated Coaxial Pipe

by

Dong K. Kim

Ed Marotta, Ph.D.

Skip Fletcher, Ph.D., P.E.

Thermal Conduction Laboratory

Department of Mechanical Engineering

Texas A&M Univeristy

Final Project Report – Phases Two & Three

Analytical and Experimental Studies of the Performance Characteristics for an Interstitially Insulated Coaxial Pipe

Prepared for the Minerals Management Service
Under the MMS/OTRC Cooperative Research Agreement
1435-01-04-CA-35515
Task Order 35663
Project Number 509

June 2007

OTRC Library Number: 5/07A181

For more information contact:

Offshore Technology Research Center
Texas A&M University
1200 Mariner Drive
College Station, Texas 77845-3400
(979) 845-6000

or

Offshore Technology Research Center
The University of Texas at Austin
1 University Station C3700
Austin, Texas 78712-0318
(512) 471-6989

A National Science Foundation Graduated Engineering Research Center

ABSTRACT

Oil consumption has been steadily increasing around the world; consequently, the petroleum industries have been endeavoring to keep up with the demand through exploration in deeper ocean environments. At current seafloor depths, pipeline insulation is essential to prevent pipeline blockage resulting from the solidification of paraffin waxes that exist as in the crude oil. To maintain crude oil temperatures above the paraffin solidification point, new and better insulation techniques are essential to minimize pipeline heat loss and maintain crude oil temperatures. The main objective of this project was to determine whether or not the thermal resistance of a new insulation concept involving interstitial screen-wire insulation would translate directly into comparable values for a prototype fabricated pipe segment. In other words, whether the reduction in heat transfer observed for small laboratory samples was realistic for application to a pipeline configuration.

This phase of the project involved both an analytical modeling study and a series of experimental verification tests. The analytical model for the interstitial insulation contained both conforming and nonconforming interfaces within the wire screen contacts in the interstitial space between the coaxial pipes. The experimental study of this novel insulation technology consisted of a prototype coaxial pipe fabricated with two layers of low conductivity wire-screen (stainless steel) as the interstitial insulation material. Both the inner and outer surface temperatures of the coaxial pipes were measured in order to evaluate the effective thermal conductivity and thermal diffusivity of the insulation

concept. The predicted results from the model compared favorably with the experimental results, confirming both the trends and magnitudes of the experimental data.

With the experimental results for thermal conductivity and thermal diffusivity from the prototype pipe segment, this study has confirmed the feasibility and performance of the insulation concept and demonstrated the thermal competitiveness of the interstitially insulated coaxial pipe technology.

TABLE OF CONTENTS

TABLE OF FIGURES AND TABLES

NOMENCLATURE

A	=	*Area,* (m^2)
$A+B$	=	*Geometric parameter related to radius of curvature,* $(1/m)$
Bi	=	*Biot number, Dimensionless*
C	=	*Coefficient, dimensionless*
D	=	*Diameter,* (m)
E	=	*Modulus of elasticity,* (N/m^2)
E'	=	*Effective modulus of elasticity,* (N/m^2)
F	=	*Applied load,* (N)
H	=	*Hardness,* (MPa)
I_g	=	*Gap conductance integral, dimensionless*
K	=	*Complete elliptic integral of first kind, dimensionless*
L	=	*Length,* (m)
M	=	*Gas parameter,* (m)
N	=	*Number of microcontacts, dimensionless*
Nu	=	*Nusselt Number, Dimentionless*
P	=	*Pressure,* $(N/m^2, Pa)$
Pr	=	*Prandtl number, Dimensionless*
$\dot{Q}$	=	*Heat rate,* (W)
R	=	*Thermal resistance,* (K/W)
Ra	=	*Rayleigh number, Dimensionless*

Ra^*	=	Modified *Rayleigh number, Dimensionless*
T	=	*Temperature,* (K)
Y	=	*Mean plane separation,* (m)
a	=	*Semi-major diameter of ellipse,* (m)
a_c	=	*Microcontact radius,* (m)
b	=	*Semi-minor diameter of ellipse,* (m)
c	=	*Length between nodes,* (m)
c_1	=	*Correlation coefficient, dimensionless*
c_2	=	*Correlation coefficient,* (GPa)
f	=	*Combination of terms, dimensionless*
g	=	*Gravitatational Acceleration,* (m/s^2)
h	=	*Thermal conductance,Heat transfer coefficient,* $(W/m^2 \cdot K)$
k	=	*Thermal conductivity,* $(W/m \cdot K)$
m	=	*Absolute asperity slope, radian*
		Semimajor axis parameter, dimensionless
n	=	*Number density of contact spot* $(1/m^2)$
r^*	=	*Dimensionless Radious, Dimensionless*
t	=	*Elapsed cooling time,* (s)
		Wall thickness, (m)
α	=	*Ratio of semi-major axes, dimensionless*
		Thermal diffusivity, (m^2/s)

δ = *Normal deformation of surface, (m)*

ε = *Relative contact spot size, dimensionless*

θ^* = *Dimensionless temperature, dimensionless*

κ = *Parameter, dimensionless*

ζ = Eigen value, *dimensionless*

λ = *Relative mean plane separation, dimensionless*

ν = *Poisson's ratio, dimensionless*

Kinematic viscosity, (m^2 / s)

ρ = *Minimum Radius of curvature, (m)*

ρ' = *Maximum Radius of curvature, (m)*

σ = *Effective surface roughness, (m)*

ψ = *Constriction parameter, dimensionless*

Δ = *Physical parameter, (m / N)*

Subscript

$1-2$ = *Surface 1 and 2*

a = *Apparent*

c = *Constriction, Contact, Coolant*

ct = *Elapse cooling*

e = *Elliptic, elastic*

eff = *Effective*

g = *Gas*

i	=	*Inner*
is	=	*Inner Surface*
iw	=	*Inner wall*
mc	=	*Microcontact*
n	=	*Order*
o	=	*Outer*
ow	=	*Outer wall*
os	=	*Outer surface*
p	=	*Plastic*
r	=	*Real*
ss	=	*Cooing bath surface*
tmc	=	*Total microcontact*
tot	=	*Total*
w	=	*Wire of screen mesh, Water*

INTRODUCTION

The high demand for oil has come from an exponential increase in transportation's use of the internal combustion engine within developed and developing countries. To meet this high demand, oil industries have explored more offshore locations for more oil products. But within the deep sea environment, temperatures can range from 0°C to 2°C (32°F to 35°F), thus pipe insulation is obligatory to prevent blockage in the pipe due paraffin and hydrate build-up. Crude oil often contains a type of wax that begins to form solid paraffin deposits on the inner surface of the pipe when the oil temperature reaches the paraffin cloud point (68°C or 155°F); therefore, blockage can and does occur. When paraffin waxes block the inside of the pipe, an additional process is needed to remove it which translates to reduced production efficiency. Crude oil production temperatures are typically above 70°C (159°F) and to maintain the inner wall temperature above the paraffin formation point, the heat loss from the pipe wall must be minimized. Several insulation techniques have been developed to overcome the thermal issue by the addition of low conductivity materials and coatings on the external pipe surface. However, these techniques often have had severe limitations such as damage due to large hydrostatic pressure differentials and installation concerns.[1,2,3] With insertion of one or more layers of a wire screen as an interstitial material within the annulus of a coaxial pipe, a reduction in the heat transfer rate, and thus retardation in paraffin build-up, can be achieved without the limitations previously stated. Moreover, the manufacture and installation process for sub-sea piping will be greatly simplified[4]. Within the interstitially insulated coaxial pipe, the interstitial fluid is air which remains stagnant with conduction heat transfer dominating however, other gases can be

employed to achieve greater insulation performance. This is due to the fact that the air space between the coaxial pipes is small enough to prevent natural convection from occurring within the space. The dominate heat transfer mechanism for this system is conduction through nonconforming contacts between the wall and wire screen. In addition, conforming microcontacts within the screen wire and pipe wall itself provide an additional resistance heat flow path between contacting interfaces. Both macro contact and micro contact models were reviewed and employed to develop a proper joint resistance model. To aid in the model development, a thermal network circuit was drawn to help visualize the heat path and aid in the joint model development.

A review of the literature on thermal contact resistance shows an extensive number of publications for both experimental and analytical studies. There exist numerous papers which detail correlations and analytical models for contact resistance for rough, conforming surfaces and nonconforming contacting surfaces. These studies take various approaches; however, little work has been performed for a joint that contains both contacts simultaneously such as a wire screen.[5]

An initial analytical study by Cividino et al. [6] analyzed joint conductances for a woven wire screen utilizing only Hertzian theory[7] to predict the macro contact area when the wire screen contacts a solid surface. The contacting surfaces follow Hertzian theory for deformation. The authors neglected bulk resistance of wire-to-wire contacts, and micro resistances. However, to obtain more accurate predictions, micro contact analysis under the formed macro contact area is required as well. This investigation develops an analytical

model that combines both macro and micro contact theory to predict the overall joint resistance for contacting surfaces containing a wire screen.

Lambert and Fletcher[8] reviewed contact resistance models for various cases under vacuum condition while Sridhar and Yovanovich[9] reviewed elastic and plastic models which showed that smooth, contacting surfaces deform elastically and rough surfaces deform plastically. Also, Savija et al.[10] contained an excellent review for thermal conductance models with interstitial substances inserted at the joint.

In the present investigation, the analytical model for an interstitially insulated coaxial pipe that includes both macro and micro contact resistances along with fluid gap resistances was developed. Predictions from the model were compared with experimental data from a previous experimental study[4]. The interstitial material was a low conductivity wire screen inserted in the annulus of a simulated coaxial pipe.

From the previous phase of this project, an insulation system incorporating a low thermal conductivity screen mesh between a pipe and an interior liner was shown to be an effective passive thermal insulation solution for deepwater flow lines and risers. It has been established that a thermal resistance (due to the metrology of the contacting surfaces) was created at an interface between two materials, in this case a pipe and a liner. If the two contacting surfaces are further separated by a screen wire or mesh at the pipe and liner interface, then a higher thermal interface resistance will result, which will significantly increase the resistance to thermal transport characteristics. The screen wire reduces the heat transfer by restricting the path for conduction and forms a stagnant air gap to minimize convective heat transfer. Heat transfer can be further reduced by adding an insulation layer

(Between the screen mesh and interior liner) and minimized by optimizing the total number of layers for actual applications. As an intermediate stage toward the actual size pipe test, an experimental investigation with a prototype pipe insulation system was conducted.

ANALYTICAL MODEL

Thermal Circuit Modelling

Cividino et al. [6] developed an analytical model for a woven wire screen contacting a solid wall, but in this study the bulk resistance, through the screen wire, and the microcontact resistances within the wires were neglected. Moreover, to have a more accurate model the contact points among wire screen materials must be account for as well. In the present experimental study, the actual specimen diameter was 1 inch (2.54 cm) as shown by Fig. 1 a).

To properly build the thermal circuit, the nominal area was specified, and then divided into a unit cell area. Each unit cell area had four nodes. Figs. 1 a) and b) are top view of the actual wire screen and thermal flow paths, respectively. The heat flow path from the inner pipe wall to the outer pipe wall was simplified as shown in Figs. 2 a) and b).

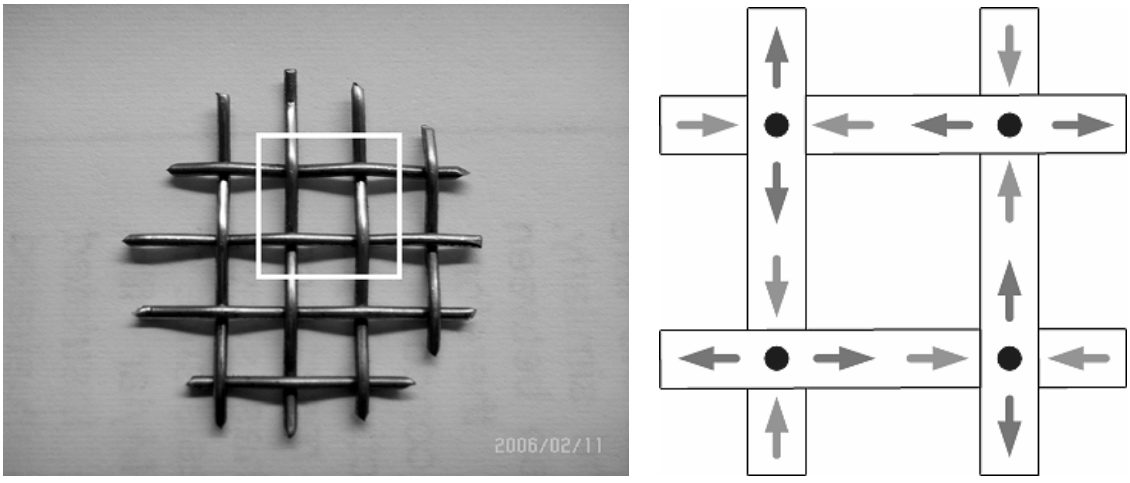

a) **b)**

Fig. 1 a) Top view of unit cell of the Screen Wire, b) Schematic of heat flow in a unit cell.

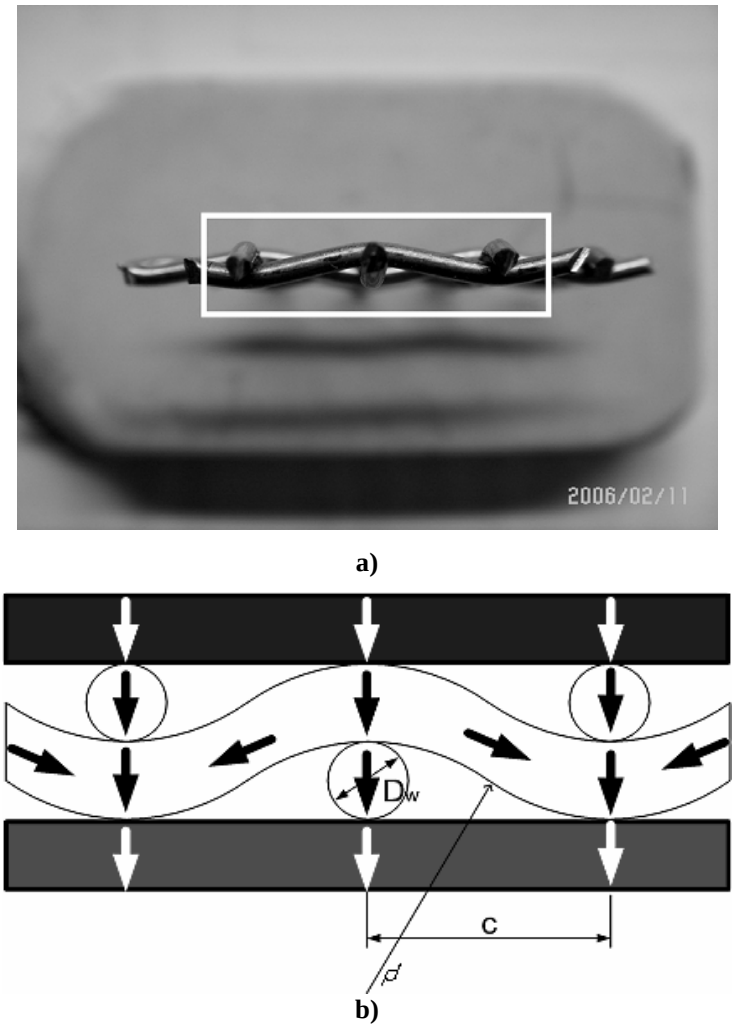

Fig. 2 a) Side view of unit cell of the Screen Wire, b) Schematic of heat flow path.

For a given unit cell, four nodes were connected in parallel connection while each node has both serial and parallel paths (resistances).[11] The overall thermal resistance for the unit cell can be written as a parallel circuit of each node as shown in Fig. 3.

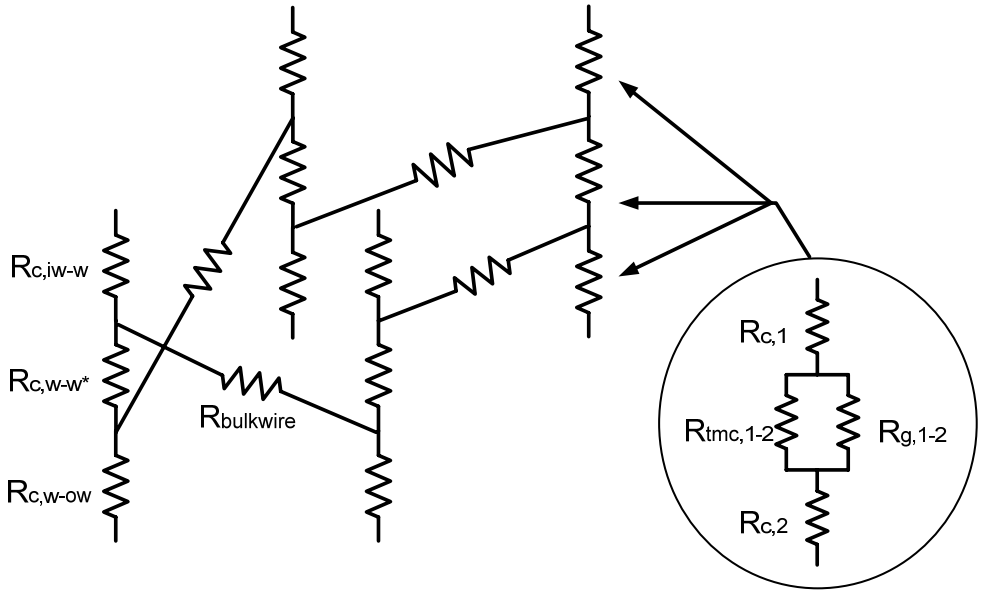

a)

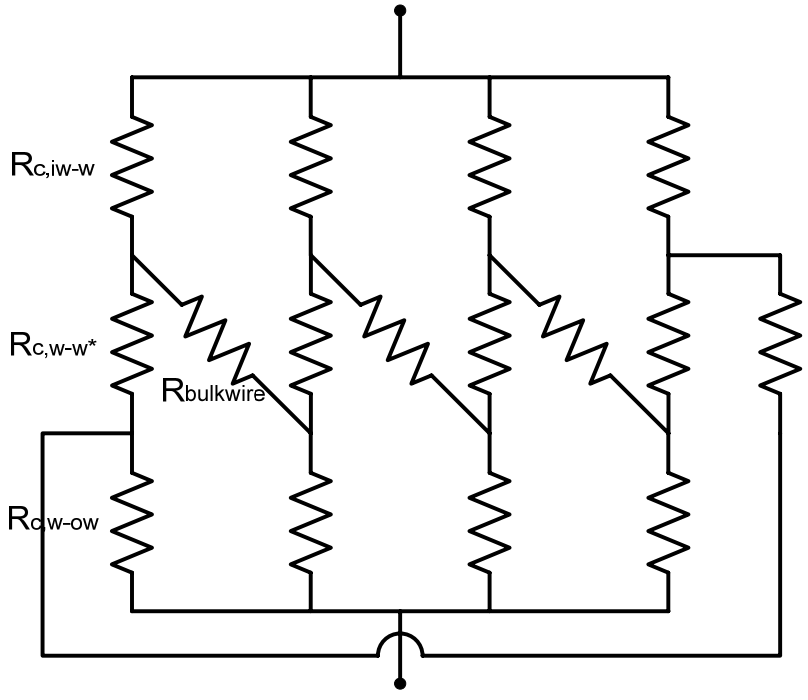

b)

Fig. 3 a) Thermal circuit in a unit cell, b) Thermal circuit in a unit cell in a closed form.

Contact Resistance Model

The joint analytical model was based on a combination of macro contact resistance, micro contact resistance, micro gap resistance, bulk resistance and air resistance for each node in the unit cell, and then programmed with the use of Matlab™ Software.

Macro Contact Model

Nonconforming contact modeling was the first step in developing the model, and was based on expressions for macro contact resistance developed by Yovanovich.[12] To obtain the contact area formed by the applied load on each nodal contact, geometrical parameters for screen wire and walls[13] as shown in Fig. 2. b) were calculated with the following expressions,

$$\alpha = \frac{c}{D_w} \tag{1}$$

$$\rho = \frac{D_w}{2} \tag{2}$$

$$\rho' = \frac{D_w}{4}(1+\alpha^2) \tag{3}$$

where ρ', ρ are the maximum and minimum of radius of curvature (for flat surface $\rho' = \rho = \infty$), c and D_w are the distances between nodes and the wire screen diameter, respectively.

The inner and outer walls were assumed to be flat surfaces so that their curvatures were considered to be infinite. Each contact point forms an elliptical contact area with semi-major and semi-minor axes *a* and *b* computed as follow.

$$a = m\left[\frac{3}{4}F\Delta\right]^{\frac{1}{3}}, \quad b = n\left[\frac{3}{4}F\Delta\right]^{\frac{1}{3}} \tag{4}$$

where m and n are dimensionless parameters obtained from the expressions[13] below for the range of values $2 < \alpha < 8$, F is the applied force on each node and Δ is a geometric-physical parameter shown below,

$$m = 0.830\alpha^{0.735}, \quad \frac{m}{n} = 0.7905\alpha^{1.18} \tag{5}$$

$$F = PA_{apparent} = Pc^2 \tag{6}$$

$$\Delta_{1-2} = \frac{\left[\frac{1-\nu_1^{\,2}}{E_1} + \frac{1-\nu_2^{\,2}}{E_2}\right]}{A+B} \tag{7}$$

$$A+B = \frac{1}{2}\left[\frac{1}{\rho_1} + \frac{1}{\rho_1'} + \frac{1}{\rho_2} + \frac{1}{\rho_2'}\right] \tag{8}$$

Since the formed elliptical contact area is very small when compared with the nodal area, the thermal resistance in the contact area can be modeled as a thermal constriction-spreading resistance within half-space[12]. With the calculated semi-major and semi-minor axes, the thermal constriction resistance for the contact area of each node can be determined as,

$$R_{constriction} = \frac{\psi_e^{\,T}}{4ka} \tag{9}$$

where $\psi_e^{\,T}$ is the spreading/constriction parameter defined[13] as,

$$\psi_e^{\,T} = \frac{2}{\pi}K(\kappa) \tag{10}$$

and $K(\kappa)$ is the complete elliptic integral of the first kind with κ defined as,

$$\kappa = \left[1 - \left(\frac{b}{a}\right)^2\right]^{1/2} \tag{11}$$

The constriction-spreading resistance between the two different materials is the summation of each resistance,

$$R_{constriction12} = R_{c1} + R_{c2} \tag{12}$$

A total of three constriction-spreading resistances exist for each nodal contact (e.g. $R_{iw-w}, R_{w-w}, R_{w-ow}$).

Bulk resistance (wire)

In the thermal circuit, some portion of the heat flow within wire itself between each node must be taken into account as shown in Fig. 3. Analyzing the circuit network via Kirchhoff's Law[14], the amount of heat out flow and in flow must be identical, and can be modeled as a parallel resistance with the wire to wire constriction resistance and bulk resistance. The bulk resistance through the wire was defined as,

$$R_{bulkwire} = \frac{2L}{k_w A_w} \tag{13}$$

where A_w (defined below) and L are the wire cross-sectional area and wire length, respectively.

$$A_w = \frac{\pi D_w^{\,2}}{4}, L = \sqrt{c^2 + D_w^{\,2}} \tag{14}$$

Micro contact resistance

Within the elliptical contact area formed by the applied load, a number of conforming microcontacts are also formed; therefore, micro constriction/spreading and gap resistances coexist in parallel. Generally, each surface has roughness where all contacting asperities were assumed be isotropic and randomly distributed over the contacting surfaces, i.e., Gaussian surface.[15]

Between two Gaussian surfaces, the contact can be simplified as a flat/rough surface with an effective roughness and slope. The effective RMS surface roughness and effective absolute mean asperity slope were computed as,

$$\sigma = \sqrt{\sigma_1^2 + \sigma_2^2}, \quad m = \sqrt{m_1^2 + m_2^2} \tag{15}$$

Depending on the deformation mode of the contacting asperities, two model types are available - plastic or elastic. With geometric parameters obtained from each model, the contact resistances can be obtained with the use of the following relationships[16]

$$h_c = \frac{2nak_s}{\psi(\varepsilon)} \tag{16}$$

$$k_s = \frac{2k_1k_2}{k_1 + k_2} \tag{17}$$

$$\psi(\varepsilon) = (1-\varepsilon)^{1.5}, \varepsilon = \sqrt{\frac{A_r}{A_a}} \tag{18}$$

Details of plastic and elastic model are further explained in the following sections below,

Plastic model

If contacting asperities are deformed plastically, then the following relationships via Cooper et al.[16, 17] are applicable with appropriate geometric parameters,

$$\lambda = \left(\frac{Y}{\sigma}\right)_p = \sqrt{2} erfc^{-1}\left(\frac{2P}{H_p}\right) \tag{19}$$

$$a_c = \sqrt{\frac{8}{\pi}}\frac{\sigma}{m}\exp\left(\frac{\lambda^2}{2}\right) erfc\left(\frac{\lambda}{\sqrt{2}}\right) \tag{20}$$

$$n = \frac{1}{16}\left(\frac{m}{\sigma}\right)^2 \frac{\exp(-\lambda^2)}{erfc(\lambda/\sqrt{2})} \tag{21}$$

$$\frac{A_r}{A_a} = \frac{1}{2} erfc(\frac{\lambda}{\sqrt{2}}) \tag{22}$$

where λ, a_c, n and A_r / A_a are the relative mean plane separation, radius of microcontact, number density of contact, and the ratio of actual contact area to nominal area, respectively. In Eq. (19), H_p is the microhardness of the softer contacting asperities.

An appropriate microhardness can be obtained from the relative contact pressure P / H_P relationship developed by Song et. al.[18],

$$\frac{P}{H_p} = \left[\frac{P}{c_1 (1.62\sigma / m)^{c_2}}\right]^{1/(1+0.071 c_2)} \tag{23}$$

$$\begin{aligned} \frac{c_1}{3178} &= 4.0 - 5.77 H_B^{\,*} + 4.0 (H_B^{\,*})^2 - 0.61 (H_B^{\,*})^3 \\ H_B^{\,*} &= \frac{H_B}{3178} \\ c_2 &= -0.370 + 0.442 (\frac{H_B}{c_1}) \end{aligned} \tag{24}$$

where c_1, c_2 are the correlation coefficients which are obtained from Vickers microhardness measurements. Equivalent Vickers microhardness can be computed from Brinell hardness values H_B.

Elastic Model

The Elastic deformation model for contacting asperities was initially proposed by Mikic[19] as follows,

$$\lambda = \left(\frac{Y}{\sigma}\right)_e = \sqrt{2} erfc^{-1}\left(\frac{4P}{H_e}\right) \tag{25}$$

$$a_c = \frac{2}{\sqrt{\pi}} \frac{\sigma}{m} \exp\left(\frac{\lambda^2}{2}\right) erfc\left(\frac{\lambda}{\sqrt{2}}\right) \tag{26}$$

$$n = \frac{1}{16}\left(\frac{m}{\sigma}\right)^2 \frac{\exp(-\lambda^2)}{erfc(\lambda/\sqrt{2})} \tag{27}$$

$$\frac{A_r}{A_a} = \frac{1}{4} erfc(\frac{\lambda}{\sqrt{2}}) \tag{28}$$

$$H_e = CmE', C = 0.7071 \tag{29}$$

$$\frac{1}{E'} = \frac{1-\nu_1^2}{E_1} + \frac{1-\nu_2^2}{E_2} \tag{30}$$

where H_e, $\frac{1}{E'}$ are the equivalent elastic hardness and the effective Young's modulus, respectively.

With appropriate geometrical parameters and either the plastic or elastic model, the microcontact thermal resistance can be computed as,

$$R_{mc} = \frac{1}{h_c \pi a_c^2} \tag{31}$$

For a given nodal area, the total microcontact resistance was calculated with the following expression,

$$R_{tmc} = \frac{R_{mc}}{N_{mc}} \tag{32}$$

where ($N_{mc} = n \times A_e, A_e = \pi ab$) N_{mc} is the number of micro contacts within the nodal area A_{node}.

Micro Gap resistance

In the present investigation, the space within the wall and wire screen and the micro-gap between the contacting interfaces was filled with air, which is the media of conduction across the gap. The gap conductance model was first developed by Yovanovich[17] as

$$h_g = \frac{k_g}{\sigma} I_g \tag{33}$$

A correlation equation for the gap integral I_g was developed by Negus et al.[20] which depends on two dimensionless parameters, the relative mean planes separation Y/σ and the relative gas rarefaction parameter M/σ.

$$I_g = \frac{f_g}{\frac{Y}{\sigma} + \frac{M}{\sigma}} \tag{34}$$

where $f_g = 1.063 + 0.0471\left(4 - \frac{Y}{\sigma}\right)^{1.68}\left(\ln\frac{\sigma}{M}\right)^{0.84}$.

The gas's dependence on pressure and temperature for the gas parameter M was presented by Yovanovich et al.[21] in Eq. (35).

$$M = 0.373 \times 10^{-6} \times \frac{T_{air}}{323} \times \frac{P_{g,1atm}}{P_g} \tag{35}$$

With these parameters, the micro-gap resistance for a node was obtained as

$$R_g = \frac{1}{h_g \pi ab} \tag{36}$$

In Eq. (36), πab is the formed contact area in a node.

Air Resistance in the space within wall and wire screen

The interstitial area between the inner and outer wall was occupied with air and wire screen, and the area not occupied by the wire screen is the cross-sectional area occupied by trapped air. The area of the unit cell is $A_{node} = c^2$. Thus the occupied air cross-sectional area was computed as,

$$A_{air} = A_{node} - \left(2 \times c \times D_w - D_w^{\,2}\right) \tag{37}$$

When the load was applied to the node, each contact point was deformed in the same direction as the applied whose deformation can be obtained from the expression developed by Johnson[7],

$$\delta = \frac{3F}{2\pi abE'} bK(\kappa) \tag{38}$$

Therefore, the thermal resistance through the air in the space for each deformed node and air space can be expressed as ,

$$R_{air} = \frac{2D_w - \delta_{iw-w} - \delta_{w-w} - \delta_{w-ow}}{k_{air} A_{air}} \tag{39}$$

This expression takes into account the wire deformation and its influence on the gap of the air space.

Total resistance

The total contact resistance for each node from the inner wall to the wire mesh, and then the outer wall is a summation of all the resistances which are in serial and parallel as shown in Fig. 4.

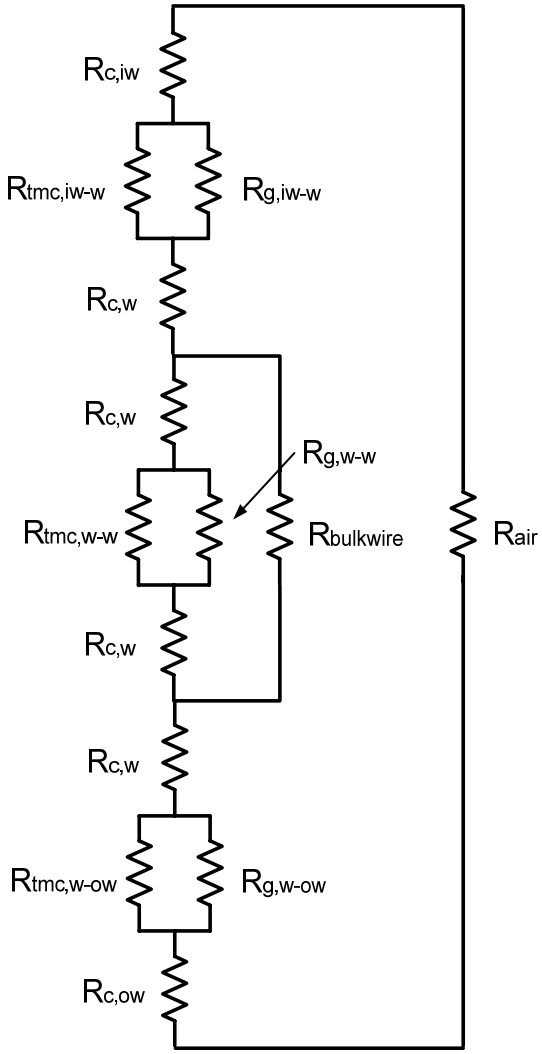

Fig. 4 Total Thermal Circuit for a node.

The following expressions detail the equations used to calculate each component. For the inner or outer wall and wire screen, the following expressions were used,

$$R_{c,iw-w} = R_{c,iw} + \left(\frac{1}{R_{tmc,iw-w}} + \frac{1}{R_{g,iw-w}} \right)^{-1} + R_{c,w} \tag{40}$$

$$R_{c,w-ow} = R_{c,w} + \left(\frac{1}{R_{tmc,w-ow}} + \frac{1}{R_{g,w-ow}} \right)^{-1} + R_{c,ow} \tag{41}$$

For the resistance of the wire screen, the following expression was employed,

$$R_{c,w-w} = \left(\frac{1}{\left(R_{c,w} + \left(\frac{1}{R_{tmc,w-w}} + \frac{1}{R_{g,w-w}} \right)^{-1} + R_{c,w} \right)} + \frac{1}{R_{bulkwire}} \right)^{-1} \tag{42}$$

The total contact resistance of each node was calculated from the summation of the contact points as follow,

$$R_{tot,c} = R_{c,iw-w} + R_{c,w-w} + R_{c,w-ow} \tag{43}$$

The total contact resistance was in parallel with the air space resistance shown in Fig. 4 and computed as,

$$R_{tot,node} = \left(\frac{1}{R_{tot,c}} + \frac{1}{R_{air}} \right)^{-1} \tag{44}$$

One unit cell has four nodes, which exist as parallel resistances; therefore, the total resistance for the unit cell becomes,

$$R_{tot,cell} = \left(\frac{4}{R_{tot,node}} \right)^{-1} \tag{45}$$

The number of unit cells in an actual area can obtained from the following expression,

$$N_{cell} = \frac{A_{actual}}{A_{cell}} \tag{46}$$

In a similar manner, actual joint thermal resistance can obtained as,

$$R_{actual} = \left(\frac{N_{cell}}{R_{tot,cell}} \right)^{-1} \tag{47}$$

Finally, conductance for the actual area can be expressed as,

$$h_{actual} = \frac{1}{R_{actual} A_{actual}} \tag{48}$$

In this expression, actual area is a coupon area which has one (1) inch diameter.

As mentioned above, thermal resistance of a node which includes all resistance components such as macro contact resistance, micro gap resistance, bulk resistance, micro resistance (plastic or elastic), micro gap resistance and air resistance and presents as parallel and serial resistance combination form as shown in Fig. 4. Four resistances of a node forms a resistance of a unit cell as a parallel form and finally, unit cells in actual coupon area forms actual resistance as a parallel form as in Eq. (47). From the analytical model, the characteristics of IICP will be shown in the Results and Discussions section.

EXPERIMENTAL INVESTIGATION

Phase 3 of this project involved the construction, assembly, and testing of an initial prototype pipe section as an intermediate stage towards a conventional size pipe for actual applications. The test pipe, manufactured by Stress Engineering Houston, TX, is three feet long and is made of common pipe steel. The inner diameter of the inner pipe is 3 inch, the outer diameter of the outer pipe is 4 inch and the length is three feet long. As shown in Fig. 5, two stainless steel wire meshes, divided by a thin aluminium layer that acts as a radiation heat transfer barrier comprise the prototype piping, on one end a flange was welded onto the pipe to connect it with the test apparatus. While on the other end there was a drill hole containing threading for attachment to an exterior pipe fitting.

Fig. 5: IICP-test-section & Cross-section view of the test pipe.

Purpose

The objective of the prototype experiments was to investigate the performance characteristic of the insulation technology that is named “The Interstitial Insulated Coaxial

Pipe (IICP)". Its performance can be represented by following the thermo-physical properties;

1) Thermal conductivity, k, is the intensive property of a material that indicates its ability to conduct heat. However, it is more useful to represent the heat transfer ability using effective thermal conductivity, k_e, when heat transfer through any of these insulation systems may include several modes: conduction through the solid materials; conduction or convection through the air in the void spaces; and, if the temperature is sufficiently high, radiation exchange between the surfaces. Effective thermal conductivity depends on the thermal conductivity and surface radiative properties of the solid material, as well as the nature and volumetric fraction of air or void space. And 2) Thermal diffusivity, α, the ratio of the thermal conductivity to the volumetric heat capacity is an important property which measures the ability if a material to conduct thermal energy relative to its ability to store thermal energy. Material of large, α, will respond quickly to change in their thermal environment, while small , α, will respond more slowly, taking longer to reach a new equilibrium condition. These properties are highly depend on a special parameter of the system, bulk density (solid mass/total volume), which depends strongly on the manner in which the solid materials are interconnected.

The experimental facility was appropriate for simulating deepwater thermal applications. The tests consisted of two parts to measure the thermal properties stated above, 1) steady state and 2) transient testing. The details of the experimental procedure and experimental plans are described below.

In each test run, the inner and outer surface temperature were measured with an Omega 30 gauge – SLE (Special Limited Error) thermocouple. Each surface had 12 temperature reading locations which were spaced at 3 inch intervals along with the axial direction from inlet to outlet. Fig. 6 shows the prototype pipe after all the thermocouple wires were attached. These thermocouples were used to measure the axial temperature distributions on the surfaces every second (i.e., the reading rate of the data logger).

Fig. 6 Prototype pipe with thermo couples.

Steady State Test

Steady state tests, simulating the flow of hot oil through an operating pipeline, were conducted at several temperatures which were set with the use of a hot water heater. The temperatures were 50, 60, 70, 75 and 80°C with a preset mass flow rate (0.05-0.4 GPM) that allowed the control of the heat flux. At each given inlet temperature, the heat flux could be controlled by the inlet hot water valve and the flow meter which were connected

to the hot loop inlet line. With data from the steady state tests, the effective thermal conductivities were completed (see the result and discussion section).

Transient Test

Transient tests were conducted under prescribed hot water temperatures that maintained a free inner pipe flow volume with no mass flow variations to simulate conditions following a pipeline shutdown to demonstrate the change in thermal resistance of a pipeline with time. Each test was run at 50, 60, 70, 73, 75 and 80°C for the initial hot water temperature. The temperature measurements were recorded as a function of time, and then the thermal diffusivities were calculated which will be shown in the result and discussion section.

Under the above two test conditions, the temperature of the inner and outer surface of the pipe and the hot water and coolant inlet and outlet temperatures were measured with a data acquisition system every one (1) second.

In summary, the results from the steady state tests were plotted as thermal conductivity as a function of heat flux under a given inlet hot water temperature. And for the transient tests, the thermal diffusivity was plotted as a function of temperature. With the data obtained from these experimental tests, the performance of the IICP was ascertained.

Apparatus Design Overview

The experiment setup was constructed with cold and hot loops to simulate actual working environment with the hot water as the crude oil and the coolant as the seawater.

The hot loop was designed so as to control the input heat load by using a hot water inlet valve with a flow meter connected to the hot water source. A built in temperature controller maintained the hot loop inlet temperature while the cold loop was connected to a coolant bath to maintain the outer surface environment. A schematic of the test apparatus and loops is shown in Fig. 7. Twelve "T" type thermocouples were attached to the inner surface and outer surfaces to measure the temperature. For the cold and hot loops, the inlet and outlet temperatures were measured with two thermocouples within each loop flow line. Preliminary test results, with a relatively large cooling bath, indicated that a new design was required to meet the cooling loads. Therefore, a new cooling bath design was fabricated to satisfy the proper capacity of the coolant bath. The new cooling bath design was a plug-in type cooling bath (i.e., prototype IICP was insert and placed in the coaxial PVC cooling bath).

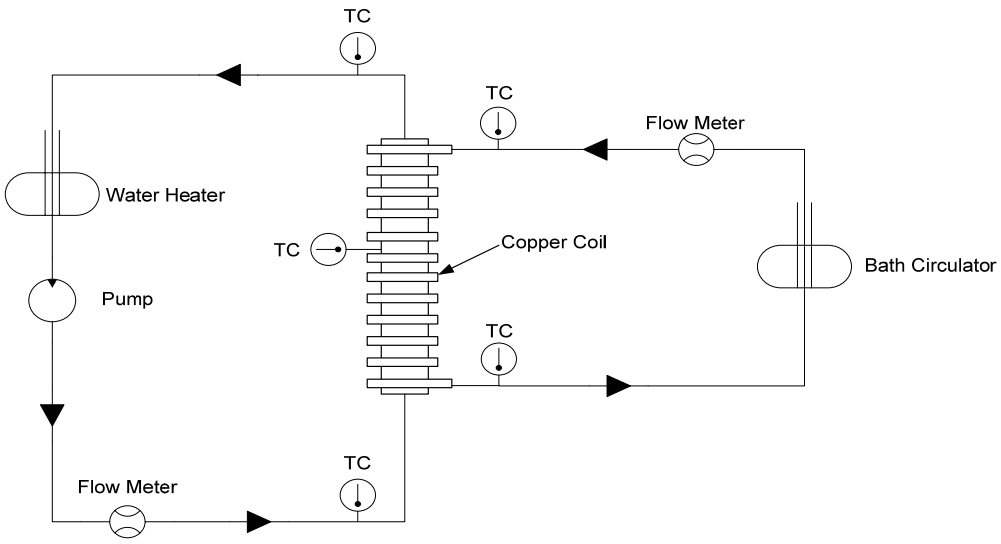

Fig. 7: Schematic of Test Apparatus.

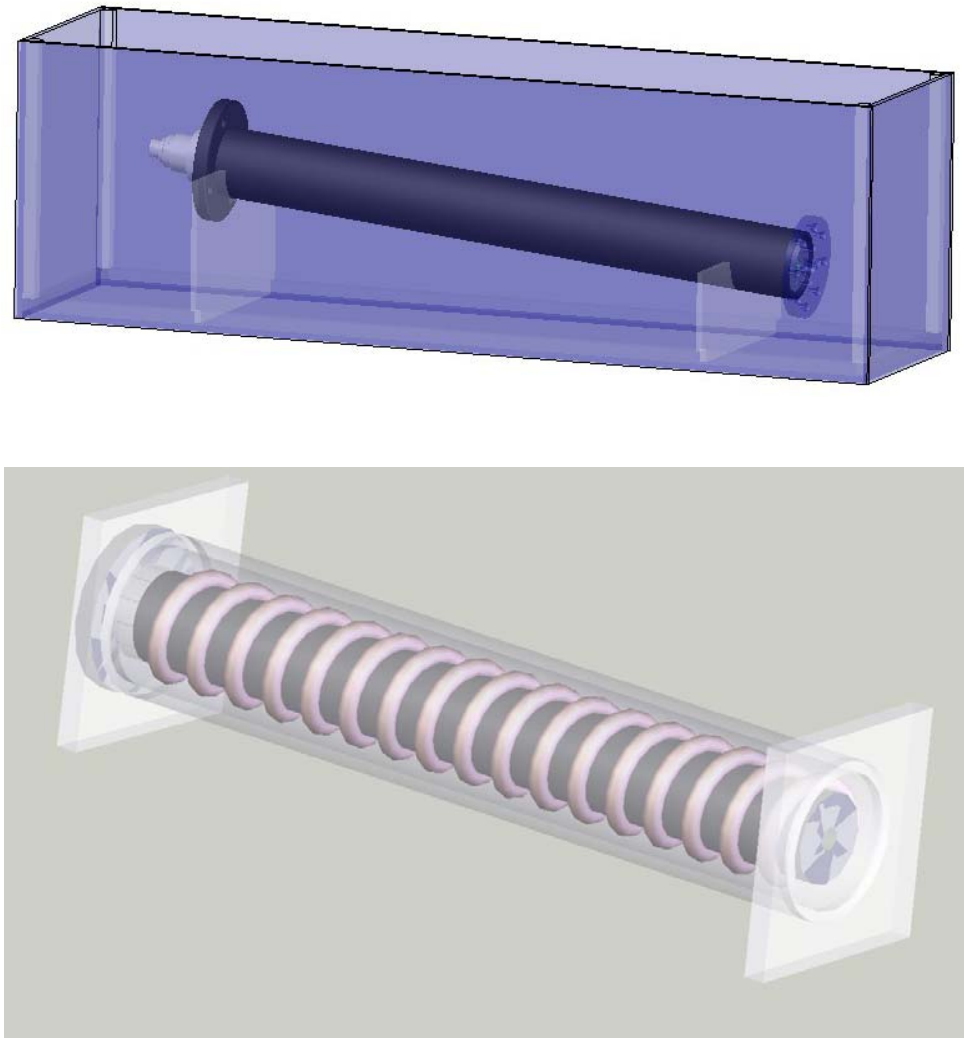

Fig. 8: Old (upper) and New Design (lower) of Cooling Bath

A six (6) inch inner diameter PVC pipe was used for the coolant bath. The prototype pipe was inserted to PVC pipe with copper coil wrapping which was connected to low temperature circulator, assembly is shown in Fig. 8.

Fig. 9: Before(upper) and after(lower) application of insulation

The gap between the prototype piping and the PVC pipe was filled with ethylene glycol. To minimize heat loss, the coolant bath (PVC pipe) and all connected lines were entirely enclosed with air bubble/ fiberglass insulation as shown in Fig. 9.

Fig. 10 Hot Water Heater(left) and Low temperature Circular(right).

For the hot loops source, an A.O. Smith water heater was used which had a 66 gallon capacity for a given temperature setting (Fig. 2). For the cold loop source, a NESLAB UTL-95 Low Temperature Circulator was employed as shown in Fig. 10.

Data Acquisition System

For the temperature data collection a National Instruments TC-2095 Data Board was used, which provided 32 channels for thermo couples. All measurements were displayed via Lab View 7.1. Lab View is a graphical programming development environment based on "G programming" language. It offers interactive control for data

acquisition, data analysis and data presentation. Each temperature was recorded by the data acquisition system with measurements taken every one second.

Data Analysis

For steady state testing, once steady state conditions were reached, the temperature data were used to calculate the heat rate from the hot water to the pipe's inner surface by applying Newton's law of cooling. The inlet and outlet hot water temperatures were employed for this calculation. The effective thermal conductivity was calculated from the heat rate and the measured temperature drop across the pipe insulation. The volume flow range for all experiments was 0.05 – 0.4 GPM and the Reynolds number was less than 2300 (i.e. laminar flow). With a constant heat flux condition, the Nusselt number was obtained,

$$Nu = \frac{h_i D_i}{k_w} = 4.36 \tag{49}$$

Therefore, the convection heat transfer coefficient for internal flow can be expressed as,

$$h_i = \frac{4.36 k_w}{D_i} \tag{50}$$

The heat rate for internal flow was computed as,

$$\dot{Q} = h_i A_{is} (T_i - T_o) \tag{51}$$

From an energy balance, the effective thermal conductivity was calculated with the use of the heat rate above,

$$k_{eff} = \frac{\dot{Q} t}{A_{is} \left(T_{is} - T_{os} \right)} \tag{52}$$

In transient testing, when the temperature data from one steady state condition to the desired steady condition were obtained, the free convection heat transfer coefficient, h_o, in the cooling bath was calculated from the temperature difference between the outer pipe surface and the cooling bath temperature. The Biot number was calculated with the use of the heat transfer coefficient. The Fourier number can be calculated with the use of the Biot number and an equation which contained a Bessel function. Finally, the thermal diffusivity was calculated from the Fourier number. The free convection heat transfer coefficient was then calculated from the Rayleigh number,

$$Ra_L = \frac{g\beta(T_{os} - T_{ss})t^3}{\nu\alpha_c} \tag{53}$$

For concentric cylinders, Raithby and Hollands[22] developed the following correlations for the effective thermal conductivity,

$$k_{ef} = 0.386k_c\left(\frac{\Pr}{0.861+\Pr}\right)^{1/4}\left(Ra_c^{*}\right)^{1/4} \tag{54}$$

Where

$$Ra_c^{*} = \frac{\left[\ln\left(D_s/D_o\right)\right]^4 Ra_L}{t^3\left(D_s^{-3/5} + D_o^{-3/5}\right)^5} \tag{55}$$

The heat transfer rate was expressed as,

$$\dot{Q} = \frac{2\pi k_{ef} L}{\ln(D_s/D_o)}\left(T_{os} - T_{ss}\right) \tag{56}$$

The free convection heat transfer coefficient was obtained as,

$$h_o = \frac{\dot{Q}}{A_{os}\left(T_{os} - T_{ss}\right)} \tag{57}$$

The Biot number can be expressed as,

$$Bi = \frac{h_o t}{k} \tag{58}$$

From the one dimensional form of the heat conduction equation with initial wall temperature and convective boundary conditions, the equations were developed by Schneider[23] as follows,

$$\theta^* = C_1 \exp(-\zeta_1^2 Fo) J_0(\zeta_1 r^*) = \frac{T_{os} - T_{ss}}{T_{osi} - T_{ss}} \tag{59}$$

Where $r^* = r / r_o$,

The discrete value for ζ_n (zeta, eigenvalue) can be calculated from the Biot number as,

$$Bi = \zeta_n \frac{J_1(\zeta_n)}{J_0(\zeta_n)} \tag{60}$$

The coefficient C_n can be calculated from the Bessel function,

$$C_n = \frac{2}{\zeta_n} \frac{J_1(\zeta_n)}{J_0^2(\zeta_n) + J_1^2(\zeta_n)} \tag{61}$$

From Eq. (59), the solution for the Fourier number can be obtained,

$$\alpha = \frac{Fot^2}{t_{ct}} \tag{62}$$

From the solution for Fourier number, the thermal diffusivity was calculated for a given elapsed cooling time as in Eq. (62).

Experimental Procedure

The experimental tests were conducted with a specific procedure developed for each case. For steady state tests, the hot water temperature had to be maintained with minimal variance. An A.O. Smith hot water heater was employed which had a large tank capacity and contained two heaters controlled by built-in temperature controllers with thermo stats (upper and lower reservoir part). Natural convection could exist in the reservoir which could cause temperature fluctuations during the heating operation. To obtain a constant flow rate, flow meter readings were frequently required. Even when the experiment reached steady state condition, the variance levels of the temperature measurements were confirmed by statistical tools.

For the transient test, initial steady state conditions were crucial factors, therefore, the same method for temperature variance level checking was performed prior to starting and ending of the experiment run.

RESULTS AND DISCUSSIONS

Part I. Analytical Model

In the analytical modeling study, both macro and micro plastic and elastic models were employed. The model includes constriction/spreading resistances for an elliptical contact area, the bulk resistance for the wire screen and an air space resistance for a contacting node. Plastic and elastic models for micro contacts and gap resistance models were employed.

To investigate the contribution of each resistance to the overall resistance in a node, total contact resistance and air resistance and the total resistance for a node is plotted as a function of applied pressure as shown in Fig. 11. This figure indicates that the contact resistance decreases as applied pressure increases while the air resistance decreases only slightly. The contact resistance sharply decreased due to increasing contact area. When the applied pressure reached roughly 283 kPa, the contact resistance was lower than the air resistance, and there-after the air resistance dominated the total resistance.

The contact resistances within a node can be classified into either contact resistance by the inner wall-to-wire, the wire-to-wire, or the wire-to-outer wall resistance. In the model, the inner wall-to-wire and wire-to-outer wall have similar properties; therefore, they were similar resistance components. Fig. 12 shows a plot of the total contact resistance and contact resistances for the inner wall-to-wire and wire-to-wire resistances. As shown in the figure, the inner wall-to-wire or wire-to-outer wall contact creates higher resistance than the wire-to- wire contact resistance thus controlling the overall resistance for the range of

applied pressures investigated. The resistance in the wire-to-wire contact has a relatively large decrease as 200 kPa is approached as indicated by the changing slope of the curve.

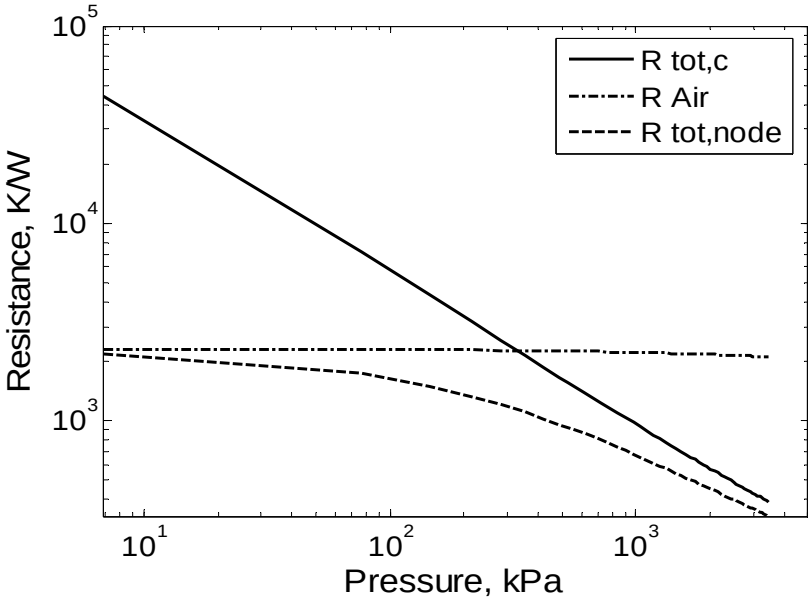

Fig. 11 Thermal resistance as a function of applied pressure in a node.

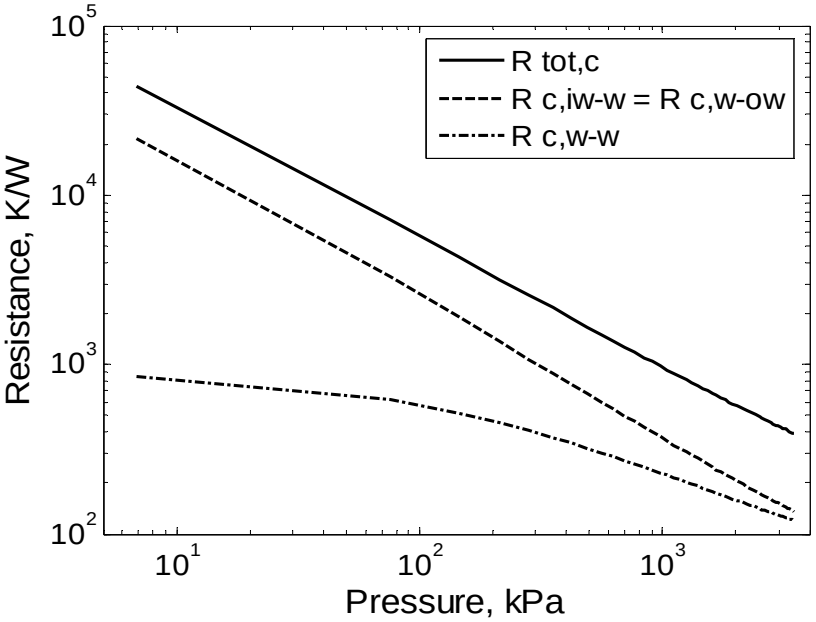

Fig. 12 Thermal resistance as a function of applied pressure in a node.

To obtain a better understanding of the contact resistance caused by the wall-to-wire interface, which seems to dominate the overall resistance in the node, a plot of multiple interface resistances is shown in Fig. 13. From Fig. 13, the dominant resistance component at the inner wall-to-wire interface was clearly the microcontact resistance (R_{tmc}: total microcontact) which is highly dependent on the applied interface pressure. The analysis also indicates that the macro constriction ($R_{c,iw}$) and spreading ($R_{c,w}$) resistances at the inner wall and wire are the least dominant resistances, and then this is followed by the microgap resistance ($R_{g,iw-w}$). All of these resistances are located at the inner wall-to-wire interface.

To highlight this same behavior within the wire-to-wire interface, Fig. 14 shows these same individual contact and gap resistances at this interface. Even in wire-to-wire contact, the total microcontact resistance ($R_{tmc,w-w}$) seems to be the dominant resistance parameter, similar to the inner wall-to-wire interface shown in Fig. 13. Again, the least influence at this interface comes from the macro constriction and spreading resistances. However, the addition of the bulk wire resistance does cause a lower overall total contact resistance when compared to the inner wall-to-wire interface which is indicated by the solid lines ($R_{c,iw-w}$ and $R_{c,w-w}$) in both Figs 13 and 14. This lower resistance is more prevalent between 230 and 600 kPa of applied pressure. The overall total contact resistance includes all of the resistances which comprise the thermal circuit network (see Fig. 4 for a single node).

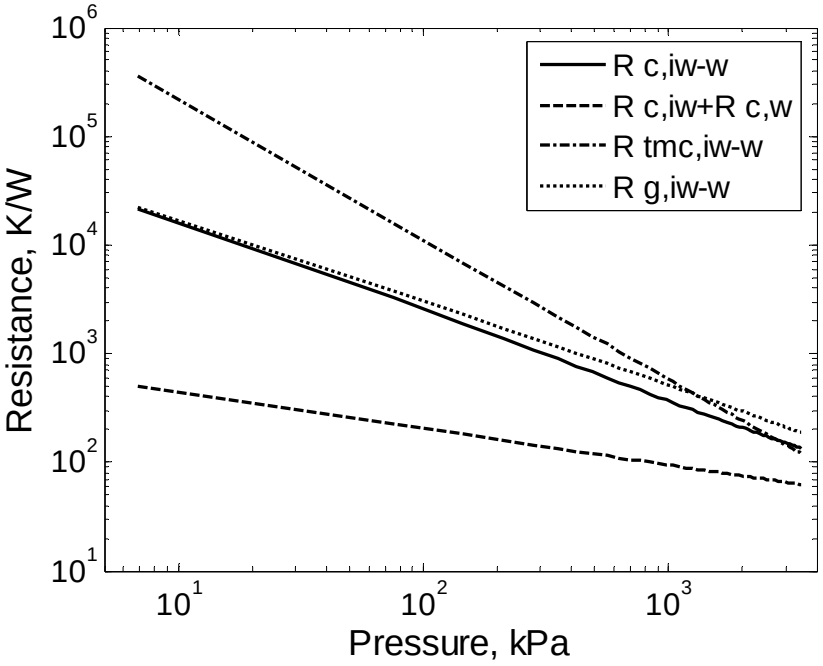

Fig. 13 Thermal resistance as a function of applied pressure within inner wall and wire of a node.

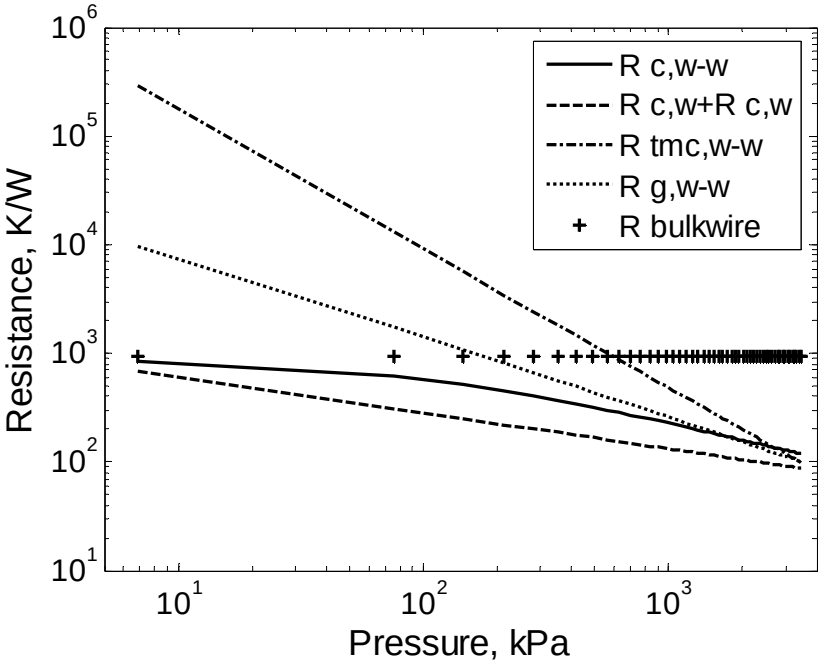

Fig. 14 Thermal resistance as a function of applied pressure within wire and wire of a node.

To investigate the effects of contact resistance as a function of applied pressure at a node, a nondimensionalized expression was developed which includes macrocontact, microcontact, micro gap, bulk wire and the air resistance in the space between inner and outer wall and within screen mesh, $R_{tot,c} / R_{tot,node}$,

$$\frac{R_{tot,c}}{R_{tot,node}} = 1 + \frac{R_{tot,c}}{R_{air}} \tag{63}$$

Eq.(63) is plotted in Fig. 15 as a function of applied nominal pressure over the range 1 kPa ≤ P ≤ 3500 kPa. It seems from this analysis that the interface contact resistances have a greater influence on the overall resistance over all pressure regions. Further, contact resistances sharply decreased as the applied pressure approaches 283 kPa which is mainly caused by the reduction in micro contact resistance.

For comparison, experimental data are also shown along with the model predictions in Fig. 15. The trend indicates a large reduction in contact resistance influence as the pressure is increased up to 690 kPa, then the air resistance begins to dominate for pressures greater than 1015 kPa. The comparison indicates that the inclusion of a plastic model for micro contacts was better at predicting the experimental data than the assumption of elastic micro contacts at these higher pressures (RMS errors have been computed).

As shown by Figs. 13 and 14, the resistance due to micro contacts and micro gaps is much larger than other resistances, and thus becomes the controlling factor for this system. This means that a wire screen can be a proper insulating medium for an interstitially insulated system if the applied pressure is controlled properly.

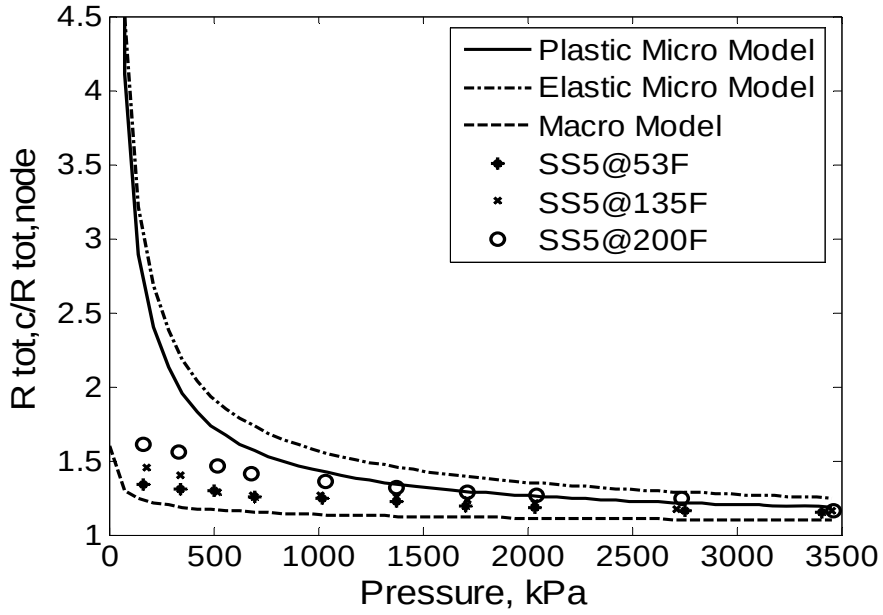

Fig. 15 Dimensionless thermal resistance as a function of applied pressure.

The total thermal resistance for three different deformation models is compared with experimental data as shown in Fig. 16. The comparison indicates that the trends for the total thermal resistance variation, which include the effect for plastic and elastic deformation are similar, but that the elastic model shows a higher resistance. The difference between two the contact models is mainly caused by the deformation mode of the contacting asperities in microcontact, and generally rough surfaces tend to follow the plastic model rather than elastic deformation model. However, the elastic macro model by itself has lower resistance and tends to under predict the experimental thermal resistance results.

Fig. 17 shows the thermal conductance for the various models employed in this study as a function of the experimental data. In this plot, a significant under prediction at light pressure range is observed, for micro models especially, for applied pressures under 1500 kPa. This is a similar trend as seem in Fig. 16 for low applied pressures.

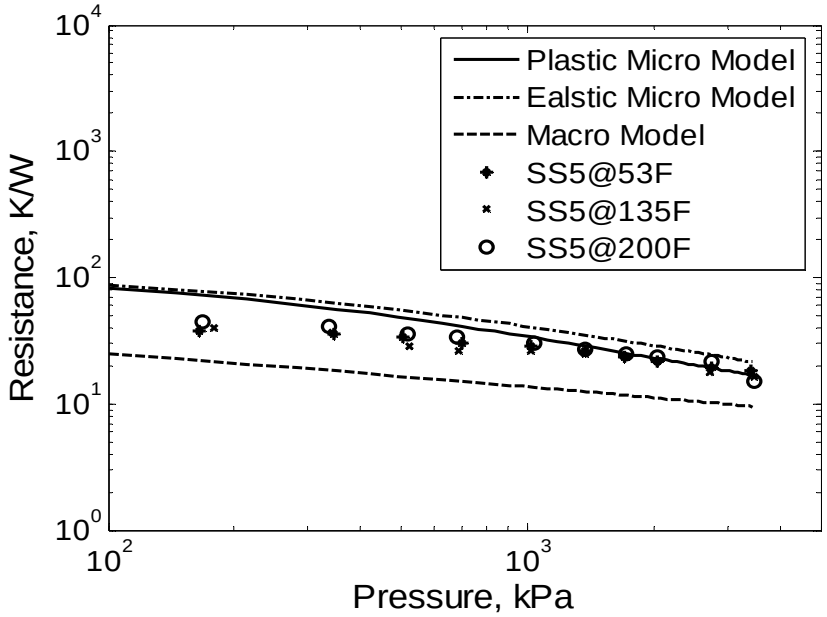

Fig. 16 Thermal resistance of each model and experimental data as a function of applied pressure.

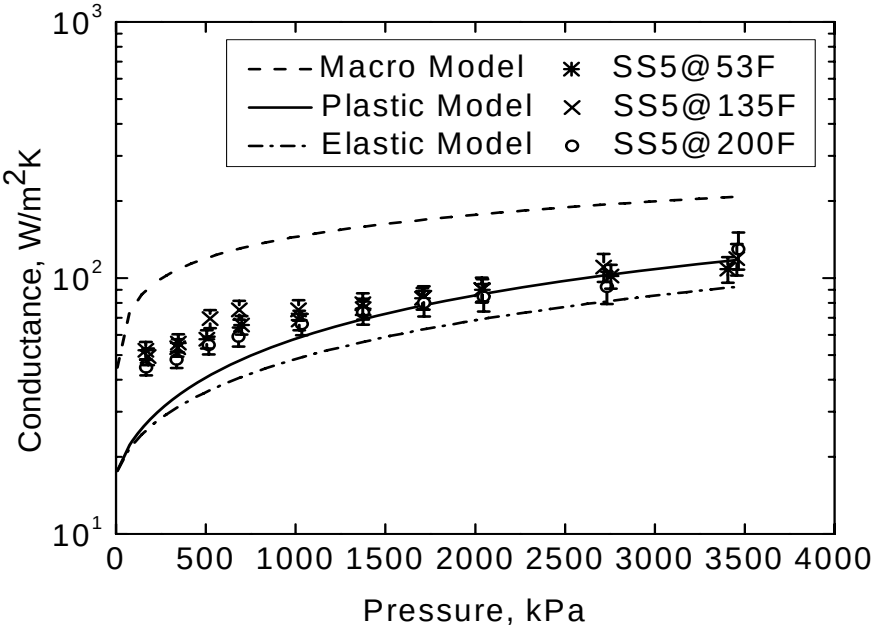

Fig. 17 Thermal conductance of each model and experimental data as a function of applied pressure.

Table 1: RMS Error between the Experimental Data and Models

Model	53°F	135°F	200°F	Average
Elastic Micro	29	29	19	26
Plastic Micro	19	19	10	16
Macro	68	69	78	72

As a quantitative comparison between model predictions and experimental data, Table 1 shows the RMS error between these results. For the plastic contact model, the error ranged from 10 to 19%, which happens to be the lowest values. With the assumption of elastic microcontact deformation, the RMS error ranged from 19 to 29%. While these values are higher than for the plastic deformation assumption, they are still lower than for the assumption of just macrocontact without inclusion of microcontact effects. In the macro model (does not include microcontact effects), the error ranged from 68 to 78% which is due to the assumption of perfect contact in the deformed area. Table 2 shows the geometrical and thermophysical properties of the metallic materials that were used for this analytical and experimental study.

In summary, the reason for higher conductance/lower resistance at lighter pressures (light applied load) as compared to the model predictions can be accounted for from visual inspection of the wire screen prior to any testing. In the untested state, pre-deformation was observable at each wire-to-wire interface for each node caused by the stresses of the fabrication process. The applied load due to fabrication formed an initial contact area which

results in lower resistance, or higher conductance, when compared to the model predictions. The model predictions do not take into account pre-deformation of any contacting surfaces.

Table 2 : Properties of materials

Material	Poison's Ratio	Modulus (GPa)	Roughness (μm)	Absolute Asperity Slope	Thermal Conductivity (W/mK)
Steel 4140 P110 (Inner or Outer Wall)	0.3	207	1.5	0.0938	42.7~46.7
Stainless Steel 316 (Mesh Screen)	0.3	190	0.4	0.0471	16.3~16.5
C(Length between nodes, mm)		25.4	D_w (Wire Diameter, mm)		0.925

Part II. Prototype Experiment

Steady State Test

Steady state experimental results compared the effective thermal conductivity of the insulation system to the flow fluid temperature or heat rate. The effective thermal conductivity, k_e , variation is shown in Fig. 18 as a function of incoming hot water temperature at five different volumetric fluxes (gallons per minute). At the lowest in-flow water temperature, 50°C, the effective thermal conductivity, k_e , had a relatively large variation which ranged from 0.084 W/m-K to 0.017 W/m-K as the volume flux was changed from 0.1 GPM to 0.4 GPM. The difference between 0.1 GPM and 0.4 GPM was 0.066 W/m-K. As the in-flow temperature was increased, the effective thermal conductivity difference between the lowest and highest volume flux decreased, for instance, at 80°C the difference was 0.024W/m-K. The effective thermal conductivity decreased as temperature increased. As the volume flux increased, the effective thermal conductivity changed as the temperature was reduced.

The effective thermal conductivity, k_e, as a function of heat rate (W) at five different in-flow hot water temperatures is shown in Fig. 19. At the lowest heat rate (10W), the effective thermal conductivity had relatively small differences among the five different temperatures. For a given heat rate condition, the thermal conductivity decreased as the in coming fluid temperature increased (e.g. at 10W), the lowest k_e was 0.011 W/m-K, while the highest value was 0.019 W/m-K with a difference of 0.008 W/m-K. The effective thermal conductivity increased as the heat rate was increased at the same temperature condition. For instance, at 80°C in-flow temperature, k_e increased from 0.011 to 0.05 W/m-K as the heat rate changed from 10 to 46W.

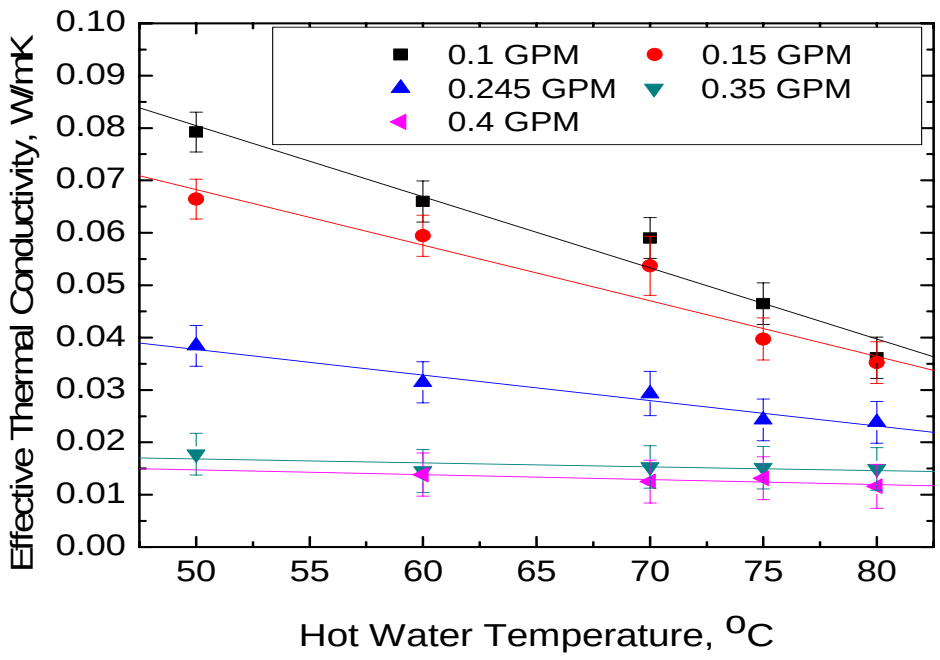

Fig. 18 Effective thermal conductivity at each volume flux as a function of starting hot water temperature

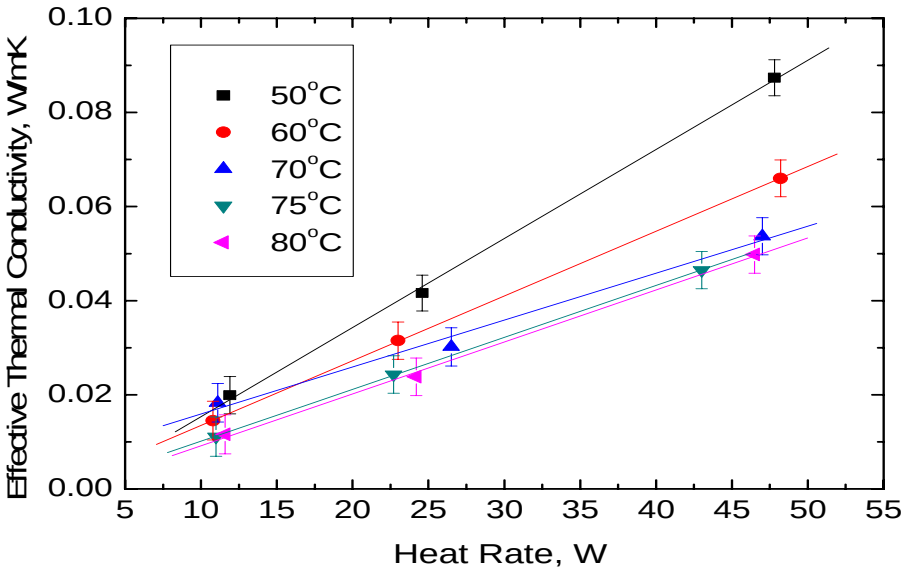

Fig. 19 Effective thermal conductivity at each starting hot water temperature as a function of heat rate

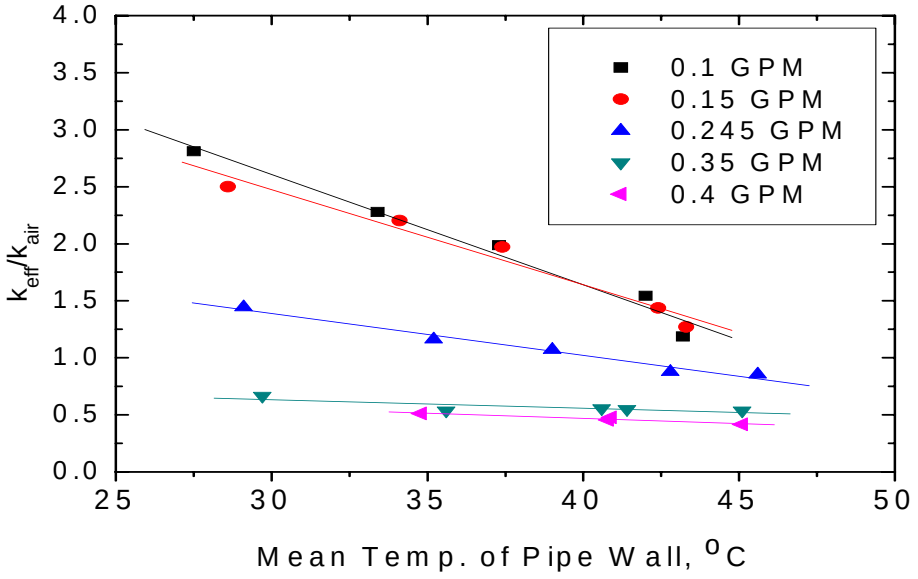

Fig. 20 Ratio of thermal conductivity at each volume flux as a function of mean temperature of pipe wall

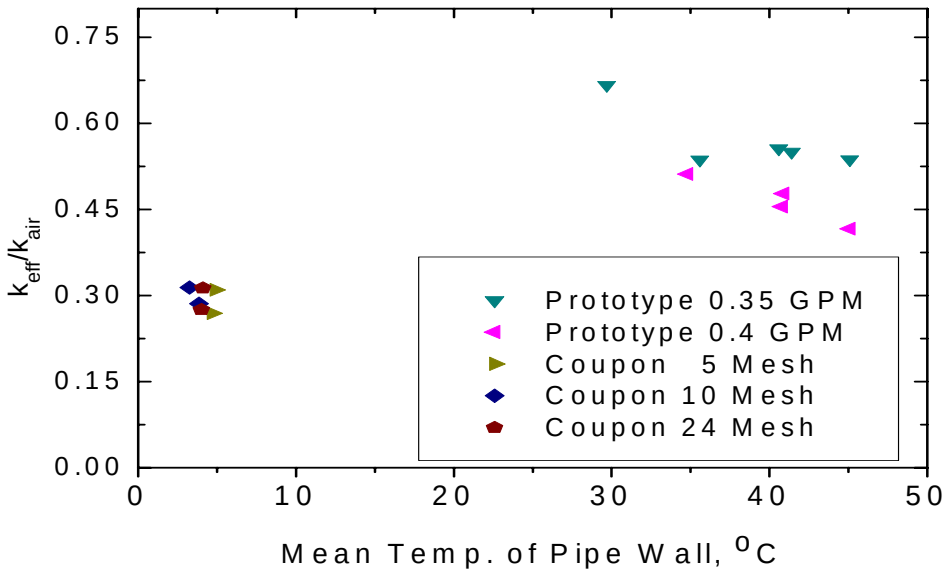

Fig. 21 Ratios of thermal conductivity for pipe prototype and coupon tests as a function of mean temperature of pipe wall

For comparison of effective thermal conductivity for IICP to air, the dimensionless thermal conductivity ratio, k_{eff}/k_{air}, is shown in Fig. 20 as a function of mean wall temperature of the pipe walls for five different volumetric fluxes. The effective thermal conductivity for the IICP had its highest values for volumetric fluxes equal to 0.1gpm and 0.15 gpm (275% and 150%, respectively). However, the effective thermal conductivity showed large decrease as the temperature was increased. As the inflow rate was increased, the dimensionless thermal conductivity ratio decreased. At lower inflow rates there was a significant decrease in the dimensionless thermal conductivity ratio while it was nearly constant as the volumetric flux was increased.

For comparison purposes, Fig. 21 shows the thermal conductivity ratio data, k_{eff}/k_{air}, for coupon tests previously conducted in phase I and the pipe prototype test data

for the current phase II investigation. The thermal conductivity values at pressures of 165 and 351 KPa and mean interface temperature of 5^{o}C were selected from the coupon tests for this comparison. These interface pressure values were closest to the experimental environmental conditions conducted in phase II. Under these values the calculated ratios for the coupons ranged from 0.27 to 0.32. The lowest ratio value computed from the pipe prototype tests was 0.38; this represents a ratio difference of 0.11 from the coupon tests. However, the estimated environmental pressure for the pipe prototype tests was approximately 1 atm (101KPa); this is approximately two times lower than the pressure value for the coupon tests. This difference in pressure was caused by the pipe's construction process. Therefore, this limits a direct one-to-one comparison between the values. But if one takes into consideration the experimental uncertainty in the experimentally measured thermal conductivity values the ratio difference becomes less significant. In conclusion, the values for the thermal conductivity ratio are very similar even though slight differences exist.

Transient Test

For the transient tests, the thermal diffusivity was calculated from the surface temperature measurements as a function of mean temperature for the pipe wall. The thermal diffusivity, α, is compared to five different starting temperatures during the cool down period as shown in Fig. 22. At the higher mean temperatures, the thermal diffusivity difference between 50°C and 80°C was relatively large, however, as the mean temperature decreased, the difference decreased. For instance, at 27°C mean temperature the difference

between 50°C and 80°C was $1.8\times10^{-6} m^2/s$ but at 4°C mean temperature, the difference decreased to $6.1\times10^{-9} m^2/s$, this difference is very small. For comparison purposes, the thermal diffusivity for this technology is shown with other conventional materials. Table 3 shows the comparison for these values.

The elapsed cooling times are shown in Fig. 23 for two (inner hot water temperatures of 50 and 80°C) cases. The cool down times were 16.6 and 18.1 hours, respectively, with similar cooling trends. For instance, when the starting temperature (the inner surface average temperature) was initially 72°C, the complete cool down period was 18.1 hours while at 47°C as the starting temperature it was 16.1 hours. However, the elapsed time difference was much smaller for the transient cool down period which started at 74°C and ended at 47°C, the measured time cycle was 1.4 hours. When the temperature trend for 47°C is shifted to approximately 74°C, the trends showed consistency.

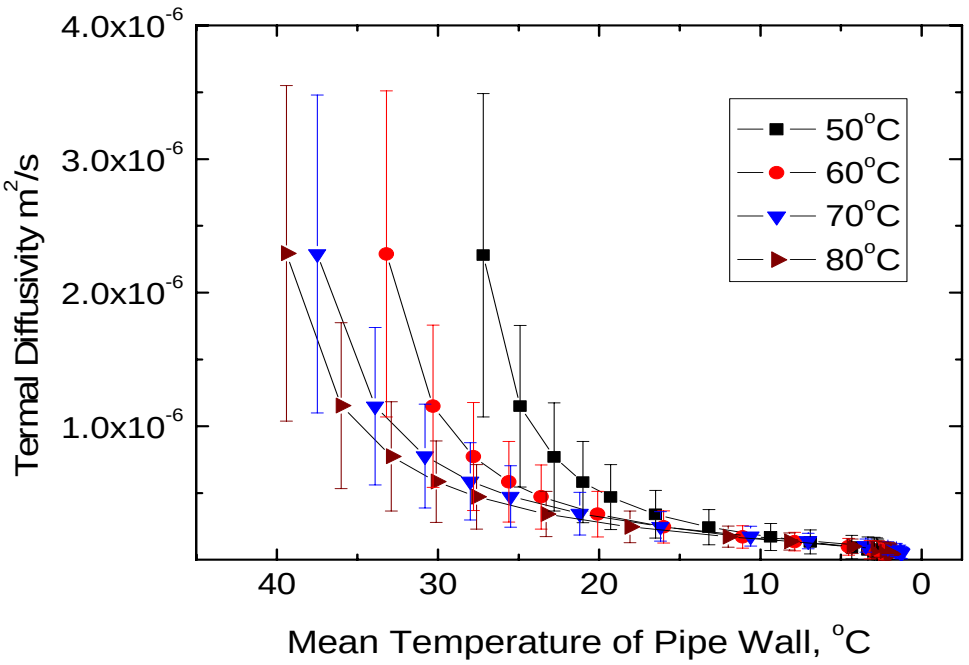

Fig. 22 Thermal diffusivity variations at each starting hot water temperature as a function of mean pipe wall temperature

Table 3: Thermal Diffusivity of Experiment and Conventional materials

Material	IICP	Carbon Steel 1010	Stainless Steel 304	Glass Fiber	Air
Thermal Diffusivity At 300K	6.10589E-07	1.88E-05	3.95E-06	1.42E-06	2.25E-05
Difference, %		2379	500	180	2848

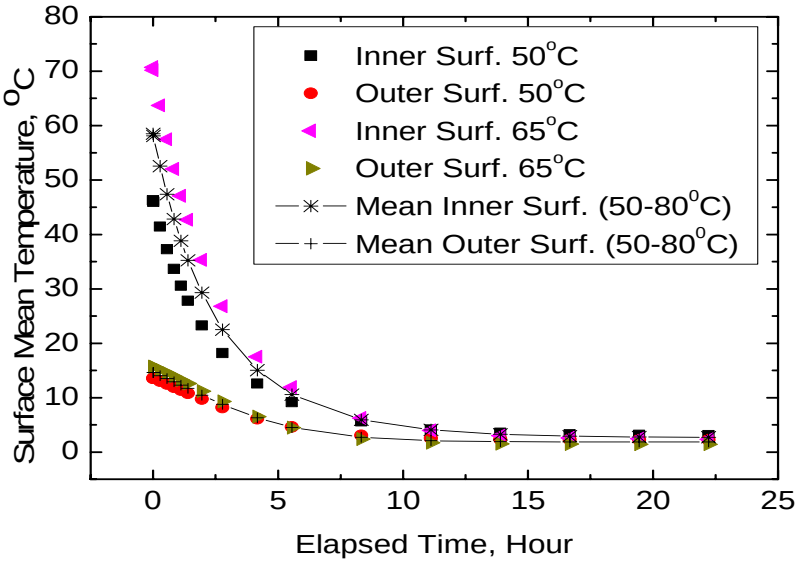

Fig. 23 Mean temperature of inner and outer surface temperature of each contained water temperature as a function of elapsed cooling time.

Figure 24 shows the ratio of the thermal diffusivities, α / α_{air}, for the IICP with respect to air as a function of mean temperature of pipe wall at each water temperature case. At low temperature (2.5°C), the IICP had a very low thermal diffusivity compare to air with a ratio values equal to 0.002, i.e. 0.2% of thermal diffusivity of air at same temperature. As the temperature was increased, the ratio for the thermal diffusivities increased up to 0.095 which represents 9.5% of the value for air. And as the temperature is increased further, the differences among the four different cases were observable but small enough to be within uncertainty range.

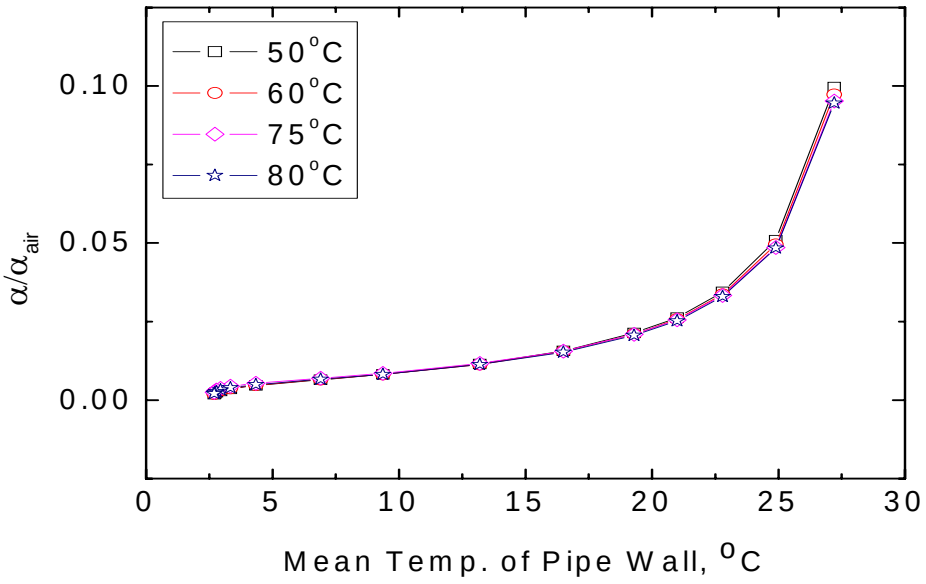

Fig. 24 Thermal diffusivity ratios at each starting hot water temperature as a function of the mean pipe wall temperature.

In summary, results from steady state and transient tests show the feasibility of the IICP technology. Visual investigation of the manufactured test pipe showed that the wire screen did not full come into contact with the pipe walls in every location. This may have affected the results for the effective thermal conductivity and the thermal diffusivity. However, as a prototype the pipe section was still very useful. For more realistic operating conditions, a full length pipe with more layers under more controlled manufacturing processes should be fabricated and evaluated for both thermal and mechanical performance.

CONCLUSIONS

Phase 3 of the IICP project investigated two major parts of the interstitially insulated coaxial pipe technology. It included analytical modeling for performance predictions and the testing of a prototype pipe for actual thermal performance characterization. By developing the analytical model for a single layer screen wire insulation, the thermal conductance or resistance could be predicted for any given contact pressure.

Macro and micro contact resistance models were used to predict the thermal performance of an interstitially insulated coaxial pipe system which contained a wire screen. The model developed showed very good agreement with the experimentally measured conductance, h, values over an applicable pressure range. This concept where a wire screen acts as the interstitial insulation dramatically increased the thermal resistance when compared with a bare pipe. As a result, the rate of heat loss from the inner hot wall to the outer cold wall dramatically decreased by more than two orders of magnitude. The thermal conductance ranged from roughly 2500 to 50 W/m²K for this configuration. In addition, the study modeled the influences of several contact parameters which encompassed both macrocontacts and microcontacts at the interface of contacting surfaces. For modeling purposes, the properties of P110-4140 pipe were used for the inner and outer wall material, and stainless steel 316 for the screen wire properties were employed for the interstitial insulation material. From the modeling results, the predicted thermal conductance ranged from 44.7 to 207 W/m²K with just macrocontacts evaluated, from 17 to 118 W/m²K with inclusion of the plastic deformation for microcontacts, and from 17 to 93 W/m²K with the

assumption of elastic deformation. The experimentally measured thermal conductance values ranged from 52 to 108 W/m²K at an interstitial mean temperature of 53°F(11.6°C), from 49 to 119 W/m²K for 135°F(57.2°C), and from 44 to 129 W/m²K for 200°F (93.3°C).

The average RMS errors were calculated for the various model predictions as compared to the experimentally measured values. Incorporating only the macrocontact model gave an upper limit of 72% for the RMS error, while the inclusion of the plastic deformation model for microcontacts gave an upper limit of 16%. The assumption of elastic microcontact deformation at the interfaces gave an upper limit of 26%.

Clearly, among the three deformation models, the inclusion of the plastic microcontacts with elastic macrocontact deformation showed very good results throughout the entire contact pressure range with especially excellent agreement at higher pressures. From the analytical model investigation, microcontact resistance was found to be the dominant resistance parameter. Therefore, by modifying the geometrical, mechanical and thermophysical parameters of the wire screen a pipe can be designed and fabricated that meets thermal performance specifications.

Experimental tests with a prototype pipe with two layers of stainless wire mesh separated by a thin aluminum layer was constructed which permitted preliminary calculation of the effective thermal conductivity k_e. Under various combinations, at steady state conditions, the effective thermal conductivity for in-flow hot water temperatures at different volume flow rates (0.1 to 0.4 GPM) was computed. The resulting values showed a low 0.011 W/m-K at 80°C; however, for the entire range of combinations, the value varied from 0.011 to 0.037 W/m-K. When the effect of heat rate on the effective thermal

conductivity was analyzed, the lowest values observed ranged from 0.011 to 0.02 W/m-K for a heat rate of 10W. These values occurred at inlet hot water temperatures between 50 to 80°C. It was observed that the effective thermal conductivity increased as the temperature and volume flow rate were decreased.

With seven different inlet hot water temperatures, transient tests were conducted so that the thermal diffusivity and the cooling times could be determined. The thermal diffusivity, α , was computed at different water temperatures. As the wall mean temperature was decreased, the thermal diffusivity decreased and among the temperature cases the thermal diffusivity variance also decreased. For comparison purposes, the thermal diffusivity values were compared with conventional insulation materials. The analysis showed a 228% reduction as compared to bare Carbon steel ANSI 1010, and a 80% reduction when compared to glass fiber insulation.

At an inlet hot water temperature of 80°C, the cooling time was 18.1 hours, and this value decreased to 16.6 hours for an inlet hot water temperature of 50°C. Using mean temperatures for the inner and outer walls, instead of inlet temperature, showed similar results. Therefore, it could be possible to predict cooling times for inlet hot water temperatures in the range between 50 to 80°C.

The results from both the modeling and experimental investigations seem to indicate superior insulating characteristics for the IICP when compared to current technologies, Thus, the present technology has shown promise for sub-sea piping and oil/gas applications and the viability of using a wire mesh as an insulating material has been proven in this investigation. However, to ensure the best performance in an actual pipe,

optimization of the IICP technology is required and further study is needed to account for the over-prediction at lighter pressures as indicated by the analytical contact model. Pre-deformation of the contact area within the wire-to-wire interface was clearly observed. This can be attributed to wire tension forces from the mesh fabrication process.

In summary, the contact model can be used to optimize the design for an actual product by conducting a parametric study of all the various parameters involved. Further, experimental investigations are needed to quantify the effects on thermal performance caused by a pressure differential between the inner and outer walls. This was clearly highlighted when the comparison between coupon and pipe prototypes thermal conductivity ratio values was performed and analyzed.

REFERENCES

[1]"Sub-sea Insulation." World Pipelines, May 2004 : pp. 49-54.

[2]Choqueuse, Dominique, Angele Chomard and Christian Bucherie. "Insulation Materials for Ultra Deep sea Flow Assurance: Evaluation of the Material Properties." OTC14115 (2002): pp. 1-8.

[3]Hallot, Raymond, Angele Chomard and Stephane Couprie. "Ils – A Passive Insulation Solution To Answer Cool Down Time Challenges On Deep Water Flowlines." OTC 14117 (2002): pp. 1-10.

[4]Marotta, E. E. and Fletcher, L. S., "Interstitially Insulated Coaxial Pipe" MMS/OTRC MEEN CHTL-05-509-35663 (2005): pp. 2-3, 24-25.

[5]Yovanovich, M. M. and Marotta, E. E., *Thermal Spreading and Contact Resistances*, Heat Transfer Handbook, Wiley, New York, 2003, Chap.4.

[6]Cividino, S., Yovanovich, M. M. and Fletcher, L. S., "A Model for Predicting the Joint Conductance pf a Woven Wire Screen Contacting Two Solids." *AIAA/ASME Thermophysics and Heat Transfer Conference 74-695*, 1974, pp.1-17.

[7]Johnson, K. L., *Contact Mechanics*, Cambridge University Press, Cambridge, 1985.

[8]Lambert, M. A. and Fletcher, L. S., "Review of Models for Thermal Contact Conductance of Metals", *AIAA Journal of Thermophysics and Heat Transfer*, Vol. 11, No. 2, 1997, pp. 129-140.

[9]Sridhar, M. R. and Yovanovich, M. M., "Review of Elastic and Plastic Contact Conductance Models" Comparison with Experiment", *Journal of Thermophysics and Heat transfer*, Vol. 8, No. 4, 1994, pp. 633-640.

[10]Savija, I., Culham, J. R., Yovanovich, M. M. and Marotta, E. E., "Review of Thermal Conductance Models for Joints Incorporating Enhancement Materials", *Journal of Thermophysics and Heat transfer*, Vol. 17, No. 1, 2003, pp. 43-52.

[11]Mills, A.F., *Heat Transfer*, 2nd ed., Prentice Hall, N.J, 1999.

[12]Yovanovich, M. M., "Thermal Constriction Resistance Between Contacting Metallic Paraboloids: Application to Instrument Bearings", *AIAA Thermophysics Conference 70-857*, 1970, pp.337-358.

[13]Cividino, s., 'Thermal Constriction Resistance of Woven Screen Between Parallel Plates in a Vacuum.", ME 751, Dec. 1972, Advanced Heat Conduction Project, Dept. of Mechanical Engineering, University of Waterloo, Waterloo, Ont.

[14]Rizzoni, G., *Principles and Applications of Electrical Engineering*, Irwin, 1993.

[15]Francis, H. A., "Application of Spherical Indentation Mechanics to Reversible and Irreversible Contact Between Rough Surfaces", *Wear*, 45, 1975, pp. 221-269.

[16]Cooper, M. G., Mikic, B. B., and Yovanovich, M. M., "Thermal Contact Conductance", *Int. J. Heat mass Transfer*, 12, 1969, 279-300.

[17]Yovanovich, M. M., "Thermal Contact Correlations, in Progress in Astronautics and Aeronautics: Spacecraft Radiative Transfer and Temperature Control", *AIAA*., Vol. 83, T. E. Horton, ed., AIAA, New York, 1982, pp. 83-95.

[18]Song, S., Yovanovich, M. M. and Nho, K., "Thermal Gap Conductance: Effects of Gas Pressure and Mechanical Load", *AIAA Journal of Thermophysics*, Vol. 6, No. 1, 1992, pp.62-68.

[19]Mikic, B. B., "Thermal Contact Conductance: Theoretical Considerations", *Int. J. Heat Mass Transfer*, 17, 1974, 205-214.

[20]Negus, K. J., and Yovanovich, M. M. "Correlation of Gap Conductance Integral for Conforming Rough Surfaces", *Journal of Thermophysics, Heat Transfer*, 12, 1988, 279-281.

[21]Yovanovich, M. M., Culham, J. R. and Teertstra, P. "Calculating Interface Resistance", *Electronic Cooling*, No. 3, 1997, pp. 1-7.

[22]Raithby, G. D. and Hollands, K. G. T. "A General Method of Obtaining Approximate Solutions to Laminar and Turbulent Free Convection Problems", *Advanced in Heat Transfer* , Vol. 11, Academic Press, New York, 1975, pp. 265-315.

[23]Schneider, P. J. *Conduction Heat Transfer*, Addison-Wesley, Reading, 1955.

APPENDICES

Appendix A- Experimental Data

Appendix B- Uncertainty

Appendix A – Experimental Data

Steady State Test

Effective Thermal Conductivity at Inflow hot water temperature and volume flux rate

	$50^{o}C$	$60^{o}C$	$70^{o}C$	$75^{o}C$	$80^{o}C$
0.1GPM	0.08406	0.065969	0.059016	0.046464	0.036143
0.15GPM	0.066428	0.059459	0.053689	0.039723	0.035211
0.245GPM	0.038436	0.03146	0.029328	0.024278	0.023846
0.35GPM	0.01776	0.014544	0.015296	0.015161	0.01495
0.4GPM		0.013841	0.012507	0.013142	0.011588

Effective Thermal Conductivity at Inflow hot water temperature and Heat rate

Heat Rate(W)	4.78E+01	2.46E+01	1.19E+01
$50^{o}C$	0.087371	0.041577	0.019901
Heat Rate(W)	4.82E+01	2.30E+01	1.11E+01
$60^{o}C$	0.065969	0.031461	0.014544
Heat Rate(W)	4.69E+01	2.65E+01	1.10E+01
$70^{o}C$	0.053689	0.030153	0.012475
Heat Rate(W)	4.30E+01	2.27E+01	1.10E+01
$75^{o}C$	0.046464	0.024278	0.011086
Heat Rate(W)	4.64E+01	2.42E+01	1.15 E+01
$80^{o}C$	0.050157	0.023846	0.011588

Transient Test

Thermal Diffusivity at given elapsed cooling time and mean surface temperature for initially contained Hot water

$60\,^{o}C$	α	$65\,^{o}C$	α	$73\,^{o}C$	α
33.17	2.288E-06	32.94	2.269E-06	37.46	2.286E-06
30.34	1.151E-06	29.94	1.143E-06	33.92	1.153E-06
27.83	7.729E-07	27.26	7.688E-07	30.79	7.756E-07
25.58	5.84E-07	24.86	5.819E-07	27.99	5.873E-07
23.57	4.708E-07	22.70	4.701E-07	25.48	4.745E-07
20.09	3.42E-07	18.97	3.429E-07	21.21	3.460E-07
15.95	2.46E-07	14.55	2.487E-07	16.23	2.505E-07
11.07	1.722E-07	9.45	1.770E-07	10.56	1.773E-07
7.89	1.356E-07	6.27	1.420E-07	7.03	1.414E-07
4.54	9.768E-08	3.16	1.065E-07	3.46	1.059E-07
3.20	7.629E-08	2.03	8.572E-08	2.09	8.714E-08
2.66	6.198E-08	1.61	7.054E-08	1.57	7.379E-08
2.44	5.191E-08	1.46	5.929E-08	1.36	6.313E-08
2.35	4.457E-08	1.40	5.093E-08	1.29	5.464E-08
2.32	3.901E-08	1.38	4.459E-08	1.25	4.797E-08

$75\,^{o}C$	α	$78\,^{o}C$	α	$80\,^{o}C$	α
37.74	2.285E-06	39.85	2.299E-06	39.41	2.293E-06
34.17	1.153E-06	36.23	1.158E-06	36.00	1.154E-06
30.98	7.756E-07	33.01	7.782E-07	32.93	7.749E-07
28.14	5.874E-07	30.14	5.886E-07	30.15	5.855E-07
25.58	4.748E-07	27.56	4.750E-07	27.63	4.721E-07
21.21	3.466E-07	23.14	3.457E-07	23.26	3.431E-07
16.10	2.515E-07	17.95	2.494E-07	18.06	2.472E-07
10.30	1.79E-07	11.96	1.755E-07	12.00	1.739E-07
6.74	1.437E-07	8.18	1.389E-07	8.18	1.379E-07
3.24	1.088E-07	4.33	1.012E-07	4.32	1.009E-07
1.95	8.992E-08	2.85	7.992E-08	2.84	7.974E-08
1.46	7.591E-08	2.28	6.530E-08	2.26	6.510E-08
1.28	6.462E-08	2.06	5.481E-08	2.03	5.459E-08
1.21	5.576E-08	1.98	4.708E-08	1.94	4.688E-08
1.18	4.889E-08	1.94	4.123E-08	1.89	4.104E-08

Inner and outer Surface Temperature at given elapsed cooling time for three different contained hot water temperatures.

	$50\,^{o}C$		$80\,^{o}C$	
Cooling Time (Sec.)	Inner(^{o}C)	Outer(^{o}C)	Inner(^{o}C)	Outer(^{o}C)
0.0001	46.29	13.57	70.69	15.71
60	45.98	13.54	70.25	15.67
1000	41.44	13.03	63.70	15.12
2000	37.27	12.47	57.49	14.51
3000	33.67	11.92	51.98	13.88
4000	30.55	11.36	47.06	13.23
5000	27.81	10.81	42.68	12.57
7000	23.27	9.72	35.27	11.25
10000	18.19	8.21	26.81	9.30
15000	12.61	6.11	17.51	6.49
20000	9.18	4.62	11.90	4.45
30000	5.63	3.06	6.26	2.37
40000	4.15	2.52	3.98	1.71
50000	3.54	2.34	3.02	1.51
60000	3.28	2.28	2.61	1.46
70000	3.18	2.27	2.43	1.44
80000	3.13	2.26	2.35	1.44

Appendix B – Uncertainty Analysis

Steady State Test

Uncertainty in inner surface Area

$$A_{is} = \pi D_i L$$

$$\Delta D_i = 0.00005\text{m},\ \Delta L = 0.0005\text{m}$$

$$\frac{dA_{is}}{dD_i} \cdot \Delta D_i = \pi L \cdot \Delta D_i \qquad \text{(A. 1)}$$

$$\frac{dA_{is}}{dL} \cdot \Delta L = \pi D_i \cdot \Delta L \qquad \text{(A. 2)}$$

$$\omega_A = \sqrt{\left(\frac{dA_{is}}{dD_i} \cdot \Delta D_i\right)^2 + \left(\frac{dA_{is}}{dL} \cdot \Delta L\right)^2} \qquad \text{(A. 3)}$$

Uncertainty in the heat transfer coefficient

$$h_i = \frac{4.36 k_w}{D_i}$$

$$\Delta k_w = 0.001 \text{ W/m-K}$$

$$\frac{dh_i}{dk_w} \cdot \Delta k_w = \frac{4.36}{D_i} \cdot \Delta k_w \qquad \text{(A. 4)}$$

$$\frac{dh_i}{dD_i} \cdot \Delta D_i = -\frac{4.36 k_w}{D_i^2} \cdot \Delta D_i \qquad \text{(A. 5)}$$

$$\omega_{h_i} = \sqrt{\left(\frac{dh_i}{dk_w} \cdot \Delta k_w\right)^2 + \left(\frac{dh_i}{dD_i} \cdot \Delta D_i\right)^2} \qquad \text{(A. 6)}$$

Uncertainty in heat rate

$$\dot{Q} = h_i A_{is} (T_i - T_o)$$

$$\Delta T = 0.0018\,^{o}C$$

$$\frac{d\dot{Q}}{dh_i} \cdot \Delta h = A_{is} (T_i - T_o) \cdot \Delta h_i \qquad \text{(A. 7)}$$

$$\frac{d\dot{Q}}{dA_{is}} \cdot \Delta A_{is} = h_i (T_i - T_o) \cdot \Delta A_{is} \qquad \text{(A. 8)}$$

$$\frac{d\dot{Q}}{dT_i} \cdot \Delta T_i = h_i A_{is} \cdot \Delta T_i \qquad \text{(A. 9)}$$

$$\frac{d\dot{Q}}{dT_o} \cdot \Delta T_o = -h_i A_{is} \cdot \Delta T_o \qquad \text{(A. 10)}$$

$$\omega_{\dot{Q}} = \sqrt{\left(\frac{d\dot{Q}}{dh_i} \cdot \Delta h\right)^2 + \left(\frac{d\dot{Q}}{dA_{is}} \cdot \Delta A_{is}\right)^2 + \left(\frac{d\dot{Q}}{dT_i} \cdot \Delta T_i\right)^2 + \left(\frac{d\dot{Q}}{dT_o} \cdot \Delta T_o\right)^2} \qquad \text{(A. 11)}$$

Uncertainty in the effective thermal conductivity

$$k_{eff} = \frac{\dot{Q}t}{A_{is}(T_i - T_o)}$$

$$\Delta t = 0.0001\text{m},\ t = 0.0127\text{m}$$

$$\frac{dk_{eff}}{d\dot{Q}} \cdot \Delta\dot{Q} = \frac{t}{A_{is}(T_i - T_o)} \cdot \Delta\dot{Q} \qquad \text{(A. 12)}$$

$$\frac{dk_{eff}}{dt} \cdot \Delta t = \frac{\dot{Q}}{A_{is}(T_i - T_o)} \cdot \Delta t \qquad \text{(A. 13)}$$

$$\frac{dk_{eff}}{dA_{is}} \cdot \Delta A_{is} = -\frac{\dot{Q}t}{A_{is}{}^2 (T_i - T_o)} \cdot \Delta A_{is} \tag{A. 14}$$

$$\frac{dk_{eff}}{dT_i} \cdot \Delta T_i = -\frac{\dot{Q}t}{A_{is} (T_i - T_o)^2} \cdot \Delta T_i \tag{A. 15}$$

$$\frac{dk_{eff}}{dT_o} \cdot \Delta T_o = \frac{\dot{Q}t}{A_{is} (T_i - T_o)^2} \cdot \Delta T_o \tag{A. 16}$$

$$\omega_{k_{eff}} = \sqrt{\left(\frac{dk_{eff}}{d\dot{Q}} \cdot \Delta\dot{Q}\right)^2 + \left(\frac{dk_{eff}}{dt} \cdot \Delta t\right)^2 + \left(\frac{dk_{eff}}{dA_{is}} \cdot \Delta A_{is}\right)^2 + \left(\frac{dk_{eff}}{dT_i} \cdot \Delta T_i\right)^2 + \left(\frac{dk_{eff}}{dT_o} \cdot \Delta T_o\right)^2} \tag{A. 17}$$

Inflow $50^{o}C$ hot water

	A.1	A.2			A.3		
	1.46E-04	1.20E-04			1.89E-04		
	A.4	A.5			A.6		
	5.72E-02	-2.44E-02			6.22E-02		
Inflow rate (GPM)	A.7	A.8	A.9	A.10	A.11		
1.00E-01	8.05E-02	4.08E-02	1.44E-02	-1.44E-02	9.25E-02		
1.50E-01	6.61E-02	3.35E-02	1.44E-02	-1.44E-02	7.69E-02		
2.45E-01	5.10E-02	1.45E-02	1.44E-02	-1.44E-02	6.47E-02		
3.50E-01	1.82E-02	9.25E-03	1.44E-02	-1.44E-02	2.89E-02		
Heat Rate (W)	A.7	A.8	A.9	A.10	A.11		
4.78E+01	8.12E-02	5.38E-02	1.44E-02	-1.44E-02	9.95E-02		
2.46E+01	4.18E-02	2.12E-02	1.44E-02	-1.44E-02	5.11E-02		
1.19E+01	2.02E-02	1.02E-02	1.44E-02	-1.44E-02	3.05E-02		

Inflow rate (GPM)	A.12	A.13	A.14	A.15	A.16	A.17($\omega_{k_{eff}}$)	$k_{eff}(W/m^2K)$	% Difference
1.00E-01	9.08E-04	3.66E-03	-4.01E-04	-1.42E-04	1.42E-04	3.80E-03	7.93E-02	4.79E+00
1.50E-01	9.19E-04	3.66E-03	-4.01E-04	-1.73E-04	1.73E-04	3.80E-03	6.64E-02	5.73E+00
2.45E-01	9.25E-04	3.66E-03	-4.01E-04	-3.32E-04	3.32E-04	3.88E-03	3.84E-02	1.01E+01
3.50E-01	1.25E-03	3.66E-03	-4.01E-04	-6.25E-04	6.25E-04	3.99E-03	1.78E-02	2.25E+01
Heat Rate (W)	A.12	A.13	A.14	A.15	A.16	A.17($\omega_{k_{eff}}$)	$k_{eff}(W/m^2K)$	% Difference
4.78E+01	9.68E-04	3.66E-03	-4.01E-04	-1.40E-04	1.40E-04	3.81E-03	8.74E-02	4.37E+00
2.46E+01	9.66E-04	3.66E-03	-4.01E-04	-2.73E-04	2.73E-04	3.83E-03	4.16E-02	9.21E+00
1.19E+01	1.19E-03	3.66E-03	-4.01E-04	-5.65E-04	5.65E-04	3.95E-03	1.99E-02	1.99E+01

Inflow $65^{o}C$ hot water

	A.1	A.2			A.3		
	1.46E-04	1.20E-04			1.89E-04		
	A.4	A.5			A.6		
	5.72E-02	-2.52E-02			6.25E-02		
Inflow rate (GPM)	A.7	A.8	A.9	A.10	A.11		
1.00E-01	7.99E-02	4.16E-02	1.49E-02	-1.49E-02	9.25E-02		
1.50E-01	7.13E-02	3.72E-02	1.49E-02	-1.49E-02	8.31E-02		
2.45E-01	3.81E-02	1.99E-02	1.49E-02	-1.49E-02	4.78E-02		
3.50E-01	1.84E-02	9.59E-03	1.49E-02	-1.49E-02	2.96E-02		
4.00E-01	1.79E-02	9.30E-03	1.49E-02	-1.49E-02	2.91E-02		
Heat rate (W)	A.7	A.8	A.9	A.10	A.11		
4.82E+01	7.99E-02	4.16E-02	1.49E-02	-1.49E-02	9.25E-02		
2.30E+01	3.81E-02	1.99E-02	1.49E-02	-1.49E-02	4.78E-02		
1.11E+01	1.79E-02	9.30E-03	1.49E-02	-1.49E-02	2.91E-02		

Inflow rate (GPM)	A.12	A.13	A.14	A.15	A.16	A.17($\omega_{k_{eff}}$)	$k_{eff}(W/m^2K)$	% Difference
1.00E-01	9.19E-04	3.78E-03	-4.14E-04	-1.48E-04	1.48E-04	3.91E-03	6.60E-02	5.93E+00
1.50E-01	9.25E-04	3.78E-03	-4.14E-04	-1.66E-04	1.66E-04	3.92E-03	5.95E-02	6.59E+00
2.45E-01	9.97E-04	3.78E-03	-4.14E-04	-3.10E-04	3.10E-04	3.95E-03	3.15E-02	1.26E+01
3.50E-01	1.27E-03	3.78E-03	-4.14E-04	-6.61E-04	6.61E-04	4.11E-03	1.45E-02	2.83E+01
4.00E-01	1.29E-03	3.78E-03	-4.14E-04	-6.42E-04	6.42E-04	4.11E-03	1.38E-02	2.97E+01
Heat rate (W)	A.12	A.13	A.14	A.15	A.16	A.17($\omega_{k_{eff}}$)	$k_{eff}(W/m^2K)$	% Difference
4.82E+01	9.19E-04	3.78E-03	-4.14E-04	-1.48E-04	1.48E-04	3.91E-03	6.60E-02	5.93E+00
2.30E+01	9.97E-04	3.78E-03	-4.14E-04	-3.10E-04	3.10E-04	3.95E-03	3.15E-02	1.26E+01
1.11E+01	1.29E-03	3.78E-03	-4.14E-04	-6.61E-04	6.61E-04	4.12E-03	1.45E-02	2.83E+01

Inflow $70^{o}C$ hot water

	A.1	A.2			A.3
	1.46E-04	1.20E-04			1.89E-04
	A.4	A.5			A.6
	5.72E-02	-2.52E-02			6.25E-02
Inflow rate (GPM)	A.7	A.8	A.9	A.10	A.11
1.00E-01	8.39E-02	4.05E-02	1.49E-02	-1.49E-02	9.55E-02
1.50E-01	7.78E-02	4.01E-01	1.49E-02	-1.49E-02	4.09E-01
2.45E-01	3.58E-02	2.15E-02	1.49E-03	-1.49E-02	3.60E-02
3.50E-01	2.37E-02	1.24E-02	1.49E-02	-1.49E-02	3.40E-02
4.00E-01	1.86E-02	9.64E-03	1.49E-02	-1.49E-02	2.97E-02
Heat rate (W)	A.7	A.8	A.9	A.10	A.11
4.69E+01	7.78E-02	5.87E-02	1.49E-02	-1.49E-02	9.97E-02
2.65E+01	2.52E-02	1.17E-02	1.49E-02	-1.49E-02	3.27E-02
1.10E+01	1.83E-02	9.67E-03	1.49E-02	-1.49E-02	2.95E-02

Inflow rate (GPM)	A.12	A.13	A.14	A.15	A.16	A.17($\omega_{k_{eff}}$)	$k_{eff}(W/m^2K)$	% Difference
1.00E-01	9.04E-04	3.78E-03	-4.14E-04	-1.41E-04	1.41E-04	3.91E-03	5.90E-02	6.63E+00
1.50E-01	4.18E-03	3.78E-03	-4.14E-04	-1.52E-04	1.52E-04	5.65E-03	5.37E-02	1.05E+01
2.45E-01	1.78E-03	3.78E-03	-4.14E-04	-4.35E-04	4.35E-04	4.25E-03	2.93E-02	1.45E+01
3.50E-01	1.14E-03	3.78E-03	-4.14E-04	-4.98E-04	4.98E-04	4.03E-03	1.53E-02	2.63E+01
4.00E-01	1.27E-03	3.78E-03	-4.14E-04	-6.36E-04	6.36E-04	4.11E-03	1.25E-02	3.28E+01
Heat rate (W)	A.12	A.13	A.14	A.15	A.16	A.17($\omega_{k_{eff}}$)	$k_{eff}(W/m^2K)$	% Difference
4.69E+01	1.02E-03	3.78E-03	-4.14E-04	-1.52E-04	1.52E-04	3.94E-03	5.37E-02	7.34E+00
2.65E+01	1.21E-03	3.78E-03	-4.14E-04	-5.99E-04	5.99E-04	4.07E-03	3.02E-02	1.35E+01
1.10E+01	1.28E-03	3.78E-03	-4.14E-04	-6.45E-04	6.45E-04	4.11E-03	1.83E-02	2.24E+01

Inflow 75 ^{o}C hot water

	A.1	A.2			A.3		
	1.46E-04	1.20E-04			1.89E-04		
	A.4	A.5			A.6		
	5.72E-02	-2.55E-02			6.26E-02		
Inflow rate (GPM)	A.7	A.8	A.9	A.10	A.11		
1.00E-01	7.05E-02	3.71E-02	1.51E-02	-1.51E-02	8.25E-02		
1.50E-01	7.18E-02	3.99E-02	1.51E-02	-1.51E-02	8.39E-02		
2.45E-01	3.72E-02	1.96E-02	1.51E-02	-1.51E-02	4.72E-02		
3.50E-01	2.42E-02	1.27E-02	1.51E-02	-1.51E-02	3.47E-02		
4.00E-01	2.05E-02	1.08E-02	1.51E-02	-1.51E-02	3.15E-02		
Heat rate (W)	A.7	A.8	A.9	A.10	A.11		
4.30E+01	7.05E-02	4.18E-02	1.51E-02	-1.51E-02	8.47E-02		
2.27E+01	3.72E-02	1.96E-02	1.51E-02	-1.51E-02	4.72E-02		
1.10E+01	1.81E-02	9.50E-03	1.51E-02	-1.51E-02	2.95E-02		

Inflow rate (GPM)	A.12	A.13	A.14	A.15	A.16	A.17($\omega_{k_{eff}}$)	$k_{eff}(W/m^2K)$	% Difference
1.00E-01	9.30E-04	3.82E-03	-4.19E-04	-1.70E-04	1.70E-04	3.96E-03	4.65E-02	8.53E+00
1.50E-01	9.83E-04	3.82E-03	-4.19E-04	-1.92E-04	1.92E-04	3.98E-03	3.97E-02	1.00E+01
2.45E-01	1.01E-03	3.82E-03	-4.19E-04	-3.22E-04	3.22E-04	4.00E-03	2.43E-02	1.65E+01
3.50E-01	1.14E-03	3.82E-03	-4.19E-04	-4.95E-04	4.95E-04	4.07E-03	1.52E-02	2.68E+01
4.00E-01	1.22E-03	3.82E-03	-4.19E-04	-5.84E-04	5.84E-04	4.12E-03	1.31E-02	3.13E+01
Heat rate (W)	A.12	A.13	A.14	A.15	A.16	A.17($\omega_{k_{eff}}$)	$k_{eff}(W/m^2K)$	% Difference
4.30E+01	9.55E-04	3.82E-03	-4.19E-04	-1.70E-04	1.70E-04	3.97E-03	4.65E-02	8.54E+00
2.27E+01	1.01E-03	3.82E-03	-4.19E-04	-3.22E-04	3.22E-04	4.00E-03	2.43E-02	1.65E+01
1.10E+01	1.30E-03	3.82E-03	-4.19E-04	-6.64E-04	6.64E-04	4.17E-03	1.11E-02	3.76E+01

Inflow 80 ^{o}C hot water

	A.1	A.2			A.3		
	1.46E-04	1.20E-04			1.89E-04		
	A.4	A.5			A.6		
	5.72E-02	-2.55E-02			6.26E-02		
Inflow rate (GPM)	A.7	A.8	A.9	A.10	A.11		
1.00E-01	5.68E-02	2.99E-02	1.51E-02	-1.51E-02	6.76E-02		
1.50E-01	5.48E-02	2.88E-02	1.51E-02	-1.51E-02	6.55E-02		
2.45E-01	3.97E-02	2.09E-02	1.51E-02	-1.51E-02	4.96E-02		
3.50E-01	2.44E-02	1.28E-02	1.51E-02	-1.51E-02	3.48E-02		
4.00E-01	1.89E-02	9.96E-03	1.51E-02	-1.51E-02	3.02E-02		
Heat rate (W)	A.7	A.8	A.9	A.10	A.11		
4.30E+01	7.62E-02	4.01E-02	1.51E-02	-1.51E-02	8.87E-02		
2.27E+01	3.97E-02	2.09E-02	1.51E-02	-1.51E-02	4.96E-02		
1.10E+01	1.89E-02	9.96E-03	1.51E-02	-1.51E-02	3.02E-02		

Inflow rate (GPM)	A.12	A.13	A.14	A.15	A.16	A.17($\omega_{k_{eff}}$)	$k_{eff}(W/m^2K)$	% Difference
1.00E-01	9.47E-04	3.82E-03	-4.19E-04	-2.11E-04	2.11E-04	3.97E-03	3.61E-02	1.10E+01
1.50E-01	9.50E-04	3.82E-03	-4.19E-04	-2.19E-04	2.19E-04	3.97E-03	3.52E-02	1.13E+01
2.45E-01	9.95E-04	3.82E-03	-4.19E-04	-3.02E-04	3.02E-04	3.99E-03	2.38E-02	1.68E+01
3.50E-01	1.14E-03	3.82E-03	-4.19E-04	-4.91E-04	4.91E-04	4.07E-03	1.50E-02	2.72E+01
4.00E-01	1.27E-03	3.82E-03	-4.19E-04	-8.16E-04	8.16E-04	4.21E-03	1.16E-02	3.63E+01
Heat rate (W)	A.12	A.13	A.14	A.15	A.16	A.17($\omega_{k_{eff}}$)	$k_{eff}(W/m^2K)$	% Difference
4.30E+01	9.26E-04	3.82E-03	-4.19E-04	-1.57E-04	1.57E-04	3.96E-03	4.98E-02	7.95E+00
2.27E+01	9.95E-04	3.82E-03	-4.19E-04	-3.02E-04	3.02E-04	3.99E-03	2.38E-02	1.68E+01
1.10E+01	1.27E-03	3.82E-03	-4.19E-04	-6.33E-04	6.33E-04	4.15E-03	1.16E-02	3.58E+01

Transient Test

Uncertainty in Rayleigh Number

$$Ra_L = \frac{g\beta(T_{os} - T_{ss})t^3}{\nu\alpha_c}$$

$\Delta g = 0.001\, m/s^2$, $\Delta\beta = 0.00001\, K^{-1}$, $\Delta T_{os} = 0.5\,^oC$, $\Delta T_{ss} = 0.05\,^oC$

$\Delta t = 0.002\text{m}$, $\Delta\nu = 0.1\, m^2/s$, $\Delta\alpha_c = 10^{-10}\, m^2/s$

$$\frac{dRa_L}{dg}\cdot\Delta g = \frac{\beta(T_{os} - T_{ss})t^3}{\nu\alpha_c}\cdot\Delta g \tag{A. 18}$$

$$\frac{dRa_L}{d\beta}\cdot\Delta\beta = \frac{g(T_{os} - T_{ss})t^3}{\nu\alpha_c}\cdot\Delta\beta \tag{A. 19}$$

$$\frac{dRa_L}{d\beta}\cdot\Delta T_{os} = \frac{g\beta t^3}{\nu\alpha_c}\cdot\Delta T_{os} \tag{A. 20}$$

$$\frac{dRa_L}{d\beta}\cdot\Delta T_{ss} = -\frac{g\beta t^3}{\nu\alpha_c}\cdot\Delta T_{ss} \tag{A. 21}$$

$$\frac{dRa_L}{d\beta}\cdot\Delta t = \frac{3g(T_{os} - T_{ss})t^2}{\nu\alpha_c}\cdot\Delta t \tag{A. 22}$$

$$\frac{dRa_L}{d\nu}\cdot\Delta\nu = -\frac{g\beta(T_{os} - T_{ss})t^3}{\nu^2\alpha_c}\cdot\Delta\nu \tag{A. 23}$$

$$\frac{dRa_L}{d\alpha_c}\cdot\Delta\alpha_c = -\frac{g\beta(T_{os} - T_{ss})t^3}{\nu{\alpha_c}^2}\cdot\Delta\alpha_c \tag{A. 24}$$

$$\omega_{Ra_L} = \sqrt{\left(\frac{dRa_L}{dg}\cdot\Delta g\right)^2 + \left(\frac{dRa_L}{d\beta}\cdot\Delta\beta\right)^2 + \left(\frac{dRa_L}{d\beta}\cdot\Delta T_{os}\right)^2 + \left(\frac{dRa_L}{d\beta}\cdot\Delta T_{ss}\right)^2 + \left(\frac{dRa_L}{d\beta}\cdot\Delta t\right)^2 + \left(\frac{dRa_L}{d\nu}\cdot\Delta\nu\right)^2 + \left(\frac{dRa_L}{d\alpha_c}\cdot\Delta\alpha_c\right)^2} \tag{A. 25}$$

Uncertainty in Concentric Cylinder Rayleigh Number

$$Ra_c^{\,*} = \frac{\left[\ln\left(D_s / D_o\right)\right]^4 Ra_L}{t^3\left(D_s^{\,-3/5} + D_o^{\,-3/5}\right)^5}$$

$\Delta D_s = 0.0000508\text{m}$

$\Delta D_o = 0.0004\text{m}$

$$\frac{dRa_c^{\,*}}{dD_s}\cdot\Delta D_s = \left\{\frac{3D_o^{\,18/5}D_s^{\,2}\left[\ln\left(D_s / D_o\right)\right]^4 Ra_L}{\left(D_s^{\,3/5} + D_o^{\,3/5}\right)^6 t^3} + \frac{4D_o^{\,3}D_s^{\,2}\left[\ln\left(D_s / D_o\right)\right]^3 Ra_L}{\left(D_s^{\,3/5} + D_o^{\,3/5}\right)^5 t^3}\right\}\cdot\Delta D_s \quad \text{(A. 26)}$$

$$\frac{dRa_c^{\,*}}{dD_o}\cdot\Delta D_o = \frac{-\left[\ln\left(D_s / D_o\right)\right]^3\cdot D_o^{\,2}\cdot\left\{4\cdot D_o^{\,3/5} - \left[3\cdot\ln\left(D_s / D_o\right) - 4\right]\cdot D_s^{\,3/5}\right\}\cdot D_s^{\,3}\cdot Ra_L}{\left(D_s^{\,3/5} + D_o^{\,3/5}\right)^6 t^3}\cdot\Delta D_o \quad \text{(A. 27)}$$

$$\frac{dRa_c^{\,*}}{dRa_L}\cdot\Delta Ra_L = \frac{\left[\ln\left(D_s / D_o\right)\right]^4}{t^3\left(D_s^{\,-3/5} + D_o^{\,-3/5}\right)^5}\cdot\Delta Ra_L \quad \text{(A. 28)}$$

$$\frac{dRa_c^{\,*}}{dRa_L}\cdot\Delta t = -\frac{3\left[\ln\left(D_s / D_o\right)\right]^4 Ra_L}{t^4\left(D_s^{\,-3/5} + D_o^{\,-3/5}\right)^5}\cdot\Delta t \quad \text{(A. 29)}$$

$$\omega_{Ra_c^{\,*}} = \sqrt{\left(\frac{dRa_c^{\,*}}{dD_s}\cdot\Delta D_s\right)^2 + \left(\frac{dRa_c^{\,*}}{dD_o}\cdot\Delta D_o\right)^2 + \left(\frac{dRa_c^{\,*}}{dRa_L}\cdot\Delta Ra_L\right)^2 + \left(\frac{dRa_c^{\,*}}{dRa_L}\cdot\Delta t\right)^2} \quad \text{(A. 30)}$$

Uncertainty in Effective thermal conductivity in Concentric Rayleigh Number

$$k_{ef} = 0.386k_c\left(\frac{\text{Pr}}{0.861 + \text{Pr}}\right)^{1/4}\left(Ra_c^{\,*}\right)^{1/4}$$

$\Delta k_c = 0.1\,W/m^2K$

$$\Delta \mathrm{Pr} = 0.1$$

$$\frac{dk_{ef}}{dk_c} \cdot \Delta k_c = 0.386 \left(\frac{\mathrm{Pr}}{0.861 + \mathrm{Pr}} \right)^{1/4} \left(Ra_c^{\,*} \right)^{1/4} \cdot \Delta k_c \tag{A. 31}$$

$$\frac{dk_{ef}}{d\,\mathrm{Pr}} \cdot \Delta \mathrm{Pr} = \frac{0.083087 k_c \left(Ra_c^{\,*} \right)^{1/4}}{\left(\mathrm{Pr} + 0.861 \right)^2 \cdot \left(\frac{\mathrm{Pr}}{0.861 + \mathrm{Pr}} \right)^{3/4}} \cdot \Delta \mathrm{Pr} \tag{A. 32}$$

$$\frac{dk_{ef}}{dRa_c^{\,*}} \cdot \Delta Ra_c^{\,*} = 0.386 k_c \left(\frac{\mathrm{Pr}}{0.861 + \mathrm{Pr}} \right)^{1/4} \cdot \frac{\left(Ra_c^{\,*} \right)^{-3/4}}{4} \cdot \Delta Ra_c^{\,*} \tag{A. 33}$$

$$\omega_{k_{ef}} = \sqrt{\left(\frac{dk_{ef}}{dk_c} \cdot \Delta k_c \right)^2 + \left(\frac{dk_{ef}}{d\,\mathrm{Pr}} \cdot \Delta \mathrm{Pr} \right)^2 + \left(\frac{dk_{ef}}{dRa_c^{\,*}} \cdot \Delta Ra_c^{\,*} \right)^2} \tag{A. 34}$$

Uncertainty in Heat rate

$$\dot{Q} = \frac{2\pi k_{ef} L}{\ln(D_s / D_o)} \left(T_{os} - T_{ss} \right)$$

$$\Delta L = 0.001 \mathrm{m}$$

$$\frac{d\dot{Q}}{dk_{ef}} \cdot \Delta k_{ef} = \frac{2\pi L}{\ln(D_s / D_o)} \left(T_{os} - T_{ss} \right) \cdot \Delta k_{ef} \tag{A. 35}$$

$$\frac{d\dot{Q}}{dL} \cdot \Delta L = \frac{2\pi k_{ef}}{\ln(D_s / D_o)} \left(T_{os} - T_{ss} \right) \cdot \Delta L \tag{A. 36}$$

$$\frac{d\dot{Q}}{dT_{os}} \cdot \Delta T_{os} = \frac{2\pi k_{ef} L}{\ln(D_s / D_o)} \cdot \Delta T_{os} \tag{A. 37}$$

$$\frac{d\dot{Q}}{dT_{ss}} \cdot \Delta T_{ss} = \frac{-2\pi k_{ef} L}{\ln(D_s / D_o)} \cdot \Delta T_{ss} \tag{A. 38}$$

$$\frac{d\dot{Q}}{dD_s}\cdot\Delta D_s=\frac{-2\pi k_{ef}L}{\left[\ln(D_s/D_o)\right]^2 D_s}\left(T_{os}-T_{ss}\right)\cdot\Delta D_s \tag{A. 39}$$

$$\frac{d\dot{Q}}{dD_o}\cdot\Delta D_o=\frac{2\pi k_{ef}L}{\left[\ln(D_s/D_o)\right]^2 D_o}\left(T_{os}-T_{ss}\right)\cdot\Delta D_o \tag{A. 40}$$

$$\omega_Q=\sqrt{\left(\frac{d\dot{Q}}{dk_{ef}}\cdot\Delta k_{ef}\right)^2+\left(\frac{d\dot{Q}}{dL}\cdot\Delta L\right)^2+\left(\frac{d\dot{Q}}{dT_{os}}\cdot\Delta T_{os}\right)^2+\left(\frac{d\dot{Q}}{dT_{ss}}\cdot\Delta T_{ss}\right)^2+\left(\frac{d\dot{Q}}{dD_s}\cdot\Delta D_s\right)^2+\left(\frac{d\dot{Q}}{dD_o}\cdot\Delta D_o\right)^2} \tag{A. 41}$$

Uncertainty in Free Convection heat transfer coefficient

$$h_o=\frac{\dot{Q}}{A_{os}\left(T_{os}-T_{ss}\right)}$$

$$\Delta A_{os}=0.00049163\,m^2$$

$$\frac{dh_o}{d\dot{Q}}\cdot\Delta\dot{Q}=\frac{1}{A_{os}\left(T_{os}-T_{ss}\right)}\cdot\Delta\dot{Q} \tag{A. 42}$$

$$\frac{dh_o}{dA_{os}}\cdot\Delta A_{os}=-\frac{\dot{Q}}{A_{os}{}^2\left(T_{os}-T_{ss}\right)}\cdot\Delta A_{os} \tag{A. 43}$$

$$\frac{dh_o}{dT_{os}}\cdot\Delta T_{os}=-\frac{\dot{Q}}{A_{os}\left(T_{os}-T_{ss}\right)^2}\cdot\Delta T_{os} \tag{A. 44}$$

$$\frac{dh_o}{dT_{ss}}\cdot\Delta T_{ss}=\frac{\dot{Q}}{A_{os}\left(T_{os}-T_{ss}\right)^2}\cdot\Delta T_{ss} \tag{A. 45}$$

$$\omega_{h_o}=\sqrt{\left(\frac{dh_o}{d\dot{Q}}\cdot\Delta\dot{Q}\right)^2+\left(\frac{dh_o}{dA_{os}}\cdot\Delta A_{os}\right)^2+\left(\frac{dh_o}{dT_{os}}\cdot\Delta T_{os}\right)^2+\left(\frac{dh_o}{dT_{ss}}\cdot\Delta T_{ss}\right)^2} \tag{A. 46}$$

Uncertainty in Biot Number

$$Bi = \frac{h_o t}{k}$$

$$\Delta k = 0.5 W / m^2 K$$

$$\frac{dBi}{dh_o} \cdot \Delta h_o = \frac{t}{k} \cdot \Delta h_o \quad \text{(A. 47)}$$

$$\frac{dBi}{dt} \cdot \Delta t = \frac{h_o}{k} \cdot \Delta t \quad \text{(A. 48)}$$

$$\frac{dBi}{dk} \cdot \Delta k = -\frac{h_o t}{k^2} \cdot \Delta k \quad \text{(A. 49)}$$

$$\omega_{h_o} = \sqrt{\left(\frac{dBi}{dh_o} \cdot \Delta h_o\right)^2 + \left(\frac{dBi}{dt} \cdot \Delta t\right)^2 + \left(\frac{dBi}{dk} \cdot \Delta k\right)^2} \quad \text{(A. 50)}$$

Uncertainty in Dimensionless Radius

$$r^* = r / r_o$$

$$\Delta r = 0.00005\text{m}$$

$$\Delta r_o = 0.00005\text{m}$$

$$\frac{dr^*}{dr} \cdot \Delta r = \frac{1}{r_o} \cdot \Delta r \quad \text{(A. 51)}$$

$$\frac{dr^*}{dr_o} \cdot \Delta r_o = -\frac{r}{r_o^2} \cdot \Delta r_o \quad \text{(A. 52)}$$

$$\omega_{r^*} = \sqrt{\left(\frac{dr^*}{dr} \cdot \Delta r\right)^2 + \left(\frac{dr^*}{dr_o} \cdot \Delta r_o\right)^2} \quad \text{(A. 53)}$$

Uncertainty in Coefficient

$$C_1 = \frac{2}{\zeta_1}\frac{J_1(\zeta_1)}{J_0{}^2(\zeta_1)+J_1{}^2(\zeta_1)}$$

$$\frac{dC_1}{d\zeta_1}\cdot\Delta\zeta_1 = \left\{-\frac{2}{\zeta_1{}^2}\frac{J_1(\zeta_1)}{J_0{}^2(\zeta_1)+J_1{}^2(\zeta_1)}+\frac{2}{\zeta_1}\left\{\frac{-J_2(\zeta_1)}{J_0{}^2(\zeta_1)+J_1{}^2(\zeta_1)}-\frac{J_1(\zeta_1)\cdot\left[2J_0(\zeta_1)+2J_1(\zeta_1)\right]}{\left[J_0{}^2(\zeta_1)+J_1{}^2(\zeta_1)\right]^2}\right\}\right\}\cdot\Delta\zeta_1 \quad \text{(A. 54)}$$

$$\omega_{C_1} = \sqrt{\left(\frac{dC_1}{d\zeta_1}\cdot\Delta\zeta_1\right)^2} \quad \text{(A. 55)}$$

Uncertainty in Dimensionless Temperature

$$\theta^* = \frac{T_{os}-T_{ss}}{T_{osi}-T_{ss}}$$

$$\Delta T_{osi} = 0.05\,^oC$$

$$\frac{d\theta^*}{dT_{os}}\cdot\Delta T_{os} = \frac{1}{T_{osi}-T_{ss}}\cdot\Delta T_{os} \quad \text{(A. 56)}$$

$$\frac{d\theta^*}{dT_{ss}}\cdot\Delta T_{ss} = \left[\frac{-1}{T_{osi}-T_{ss}}+\frac{T_{os}-T_{ss}}{\left(T_{osi}-T_{ss}\right)^2}\right]\cdot\Delta T_{ss} \quad \text{(A. 57)}$$

$$\frac{d\theta^*}{dT_{osi}}\cdot\Delta T_{osi} = \frac{-\left(T_{os}-T_{ss}\right)}{\left(T_{osi}-T_{ss}\right)^2}\cdot\Delta T_{osi} \quad \text{(A. 58)}$$

$$\omega_{\theta^*} = \sqrt{\left(\frac{d\theta^*}{dT_{os}}\cdot\Delta T_{os}\right)^2+\left(\frac{d\theta^*}{dT_{ss}}\cdot\Delta T_{ss}\right)^2+\left(\frac{d\theta^*}{dT_{osi}}\cdot\Delta T_{osi}\right)^2} \quad \text{(A. 59)}$$

Uncertainty in Fourier Number

$$Fo = \frac{\ln\left(\frac{\theta^*}{C_1 J_0(\zeta_1 r^*)}\right)}{-\zeta_1^{\,2}}$$

$$\frac{dFo}{d\theta^*}\cdot\Delta\theta^* = \frac{\frac{1}{\theta^*}}{-\zeta_1^{\,2}}\cdot\Delta\theta^* \tag{A. 60}$$

$$\frac{dFo}{dC_1}\cdot\Delta C_1 = \frac{-\frac{1}{C_1}}{-\zeta_1^{\,2}}\cdot\Delta C_1 \tag{A. 61}$$

$$\frac{dFo}{d\zeta_1}\cdot\Delta\zeta_1 = \left[\frac{2\ln\left(\frac{\theta^*}{C_1 J_0(\zeta_1 r^*)}\right)}{\zeta_1^{\,3}} + \frac{\left(-\frac{1}{r^* J_1(\zeta_1)}\right)}{-\zeta_1^{\,2}}\right]\cdot\Delta\zeta_1 \tag{A. 62}$$

$$\frac{dFo}{dr^*}\cdot\Delta r^* = \frac{-\frac{1}{\zeta_1 J_1(r^*)}}{-\zeta_1^{\,2}}\cdot\Delta r^* \tag{A. 63}$$

$$\omega_{Fo} = \sqrt{\left(\frac{dFo}{d\theta^*}\cdot\Delta\theta^*\right)^2 + \left(\frac{dFo}{dC_1}\cdot\Delta C_1\right)^2 + \left(\frac{dFo}{d\zeta_1}\cdot\Delta\zeta_1\right)^2 + \left(\frac{dFo}{dr^*}\cdot\Delta r^*\right)^2} \tag{A. 64}$$

Uncertainty in Thermal Diffusivity

$$\alpha = \frac{Fot^2}{t_{ct}}$$

$$\frac{d\alpha}{dFo}\cdot\Delta Fo = \frac{t^2}{t_{ct}}\cdot\Delta Fo \tag{A. 65}$$

$$\frac{d\alpha}{dt}\cdot\Delta t=\frac{2Fot}{t_{ct}}\cdot\Delta t \tag{A. 66}$$

$$\frac{d\alpha}{dt_{ct}}\cdot\Delta t_{ct}=-\frac{Fot}{t_{ct}^{\ 2}}\cdot\Delta t_{tc} \tag{A. 67}$$

$$\omega_{\alpha}=\sqrt{\left(\frac{d\alpha}{dFo}\cdot\Delta Fo\right)^{2}+\left(\frac{d\alpha}{dt}\cdot\Delta t\right)^{2}+\left(\frac{d\alpha}{dt_{ct}}\cdot\Delta t_{ct}\right)^{2}} \tag{A. 68}$$

Cooling from $50\,^{o}C$

Time (Hour)	A.18	A.19	A.20	A.21	A.22	A.23	A.24	A.25
1.67E-02	8.12E-06	1.23E-03	1.23E-03	-1.23E-04	3.76E-02	-1.40E-04	-7.97E-12	3.77E-02
2.78E-01	7.11E-06	1.07E-03	1.23E-03	-1.23E-04	3.30E-02	-1.22E-04	-6.98E-12	3.30E-02
5.56E-01	6.21E-06	9.37E-04	1.23E-03	-1.23E-04	2.88E-02	-1.07E-04	-6.09E-12	2.88E-02
8.33E-01	5.45E-06	8.22E-04	1.23E-03	-1.23E-04	2.52E-02	-9.37E-05	-5.34E-12	2.53E-02
1.11E+00	4.80E-06	7.25E-04	1.23E-03	-1.23E-04	2.23E-02	-8.27E-05	-4.71E-12	2.23E-02
1.39E+00	4.26E-06	6.42E-04	1.23E-03	-1.23E-04	1.97E-02	-7.33E-05	-4.18E-12	1.98E-02
1.94E+00	3.39E-06	5.12E-04	1.23E-03	-1.23E-04	1.57E-02	-5.84E-05	-3.33E-12	1.58E-02
2.78E+00	2.50E-06	3.77E-04	1.23E-03	-1.23E-04	1.16E-02	-4.30E-05	-2.45E-12	1.17E-02
4.17E+00	1.63E-06	2.46E-04	1.23E-03	-1.23E-04	7.54E-03	-2.80E-05	-1.60E-12	7.64E-03
5.56E+00	1.14E-06	1.72E-04	1.23E-03	-1.23E-04	5.29E-03	-1.96E-05	-1.12E-12	5.44E-03
8.33E+00	6.41E-07	9.68E-05	1.23E-03	-1.23E-04	2.97E-03	-1.10E-05	-6.29E-13	3.22E-03
1.11E+01	4.10E-07	6.19E-05	1.23E-03	-1.23E-04	1.90E-03	-7.05E-06	-4.02E-13	2.27E-03
1.39E+01	3.01E-07	4.54E-05	1.23E-03	-1.23E-04	1.39E-03	-5.17E-06	-2.95E-13	1.86E-03
1.67E+01	2.51E-07	3.78E-05	1.23E-03	-1.23E-04	1.16E-03	-4.31E-06	-2.46E-13	1.69E-03
1.94E+01	2.28E-07	3.44E-05	1.23E-03	-1.23E-04	1.06E-03	-3.93E-06	-2.24E-13	1.63E-03
2.22E+01	2.18E-07	3.29E-05	1.23E-03	-1.23E-04	1.01E-03	-3.76E-06	-2.14E-13	1.60E-03
Time (Hour)	A.26	A.27	A.28	A.29				A.30
1.67E-02	6.99E-06	-1.81E-05	1.03E-03	-4.12E-04				1.11E-03
2.78E-01	6.71E-06	-1.73E-05	8.99E-04	-3.96E-04				9.83E-04
5.56E-01	6.42E-06	-1.66E-05	7.85E-04	-3.78E-04				8.72E-04
0.00E+00	6.12E-06	-1.58E-05	6.89E-04	-3.61E-04				7.78E-04
1.11E+00	5.82E-06	-1.50E-05	6.08E-04	-3.43E-04				6.98E-04
1.39E+00	5.52E-06	-1.43E-05	5.39E-04	-3.26E-04				6.30E-04
1.94E+00	4.94E-06	-1.28E-05	4.30E-04	-2.92E-04				5.19E-04
2.78E+00	4.13E-06	-1.07E-05	3.17E-04	-2.44E-04				4.00E-04
4.17E+00	3.01E-06	-7.77E-06	2.08E-04	-1.77E-04				2.74E-04
5.56E+00	2.21E-06	-5.71E-06	1.48E-04	-1.30E-04				1.97E-04
8.33E+00	1.37E-06	-3.55E-06	8.77E-05	-8.10E-05				1.19E-04
1.11E+01	1.08E-06	-2.79E-06	6.17E-05	-6.38E-05				8.88E-05
1.39E+01	9.86E-07	-2.55E-06	5.07E-05	-5.82E-05				7.72E-05
1.67E+01	9.56E-07	-2.47E-06	4.62E-05	-5.64E-05				7.29E-05
1.94E+01	9.47E-07	-2.45E-06	4.43E-05	-5.58E-05				7.13E-05
2.22E+01	9.44E-07	-2.44E-06	4.35E-05	-5.57E-05				7.07E-05

Time (Hour)	A.31	A.32	A.33				A.34
1.67E-02	1.53E-02	2.13E-06	4.17E-01				4.17E-01
2.78E-01	1.51E-02	2.11E-06	3.82E-01				3.82E-01
5.56E-01	1.49E-02	2.09E-06	3.50E-01				3.50E-01
0.00E+00	1.48E-02	2.06E-06	3.24E-01				3.24E-01
1.11E+00	1.46E-02	2.04E-06	3.02E-01				3.02E-01
1.39E+00	1.44E-02	2.01E-06	2.83E-01				2.83E-01
1.94E+00	1.40E-02	1.96E-06	2.54E-01				2.54E-01
2.78E+00	1.34E-02	1.87E-06	2.24E-01				2.24E-01
4.17E+00	1.24E-02	1.73E-06	1.94E-01				1.94E-01
5.56E+00	1.14E-02	1.60E-06	1.76E-01				1.77E-01
8.33E+00	1.02E-02	1.42E-06	1.52E-01				1.53E-01
1.11E+01	9.58E-03	1.34E-06	1.36E-01				1.36E-01
1.39E+01	9.36E-03	1.31E-06	1.26E-01				1.27E-01
1.67E+01	9.29E-03	1.30E-06	1.22E-01				1.22E-01
1.94E+01	9.26E-03	1.30E-06	1.20E-01				1.21E-01
2.22E+01	9.26E-03	1.29E-06	1.20E-01				1.20E-01
Time (Hour)	A.35	A.36	A.37	A.38	A.39	A.40	A.41
1.67E-02	4.41E+02	4.28E+01	6.03E+02	-6.03E+01	-7.40E+01	2.19E+02	7.85E+02
2.78E-01	3.54E+02	3.75E+01	5.97E+02	-5.97E+01	-6.42E+01	1.90E+02	7.26E+02
5.56E-01	2.83E+02	3.27E+01	5.90E+02	-5.90E+01	-5.54E+01	1.64E+02	6.80E+02
0.00E+00	2.30E+02	2.87E+01	5.83E+02	-5.83E+01	-4.80E+01	1.42E+02	6.48E+02
1.11E+00	1.89E+02	2.53E+01	5.76E+02	-5.76E+01	-4.18E+01	1.24E+02	6.23E+02
1.39E+00	1.57E+02	2.24E+01	5.68E+02	-5.68E+01	-3.66E+01	1.08E+02	6.04E+02
1.94E+00	1.12E+02	1.79E+01	5.53E+02	-5.53E+01	-2.84E+01	8.37E+01	5.74E+02
2.78E+00	7.30E+01	1.32E+01	5.29E+02	-5.29E+01	-2.00E+01	5.90E+01	5.40E+02
4.17E+00	4.12E+01	8.57E+00	4.88E+02	-4.88E+01	-1.20E+01	3.55E+01	4.94E+02
5.56E+00	2.63E+01	6.01E+00	4.52E+02	-4.52E+01	-7.80E+00	2.30E+01	4.56E+02
8.33E+00	1.28E+01	3.38E+00	4.01E+02	-4.01E+01	-3.89E+00	1.15E+01	4.04E+02
1.11E+01	7.26E+00	2.16E+00	3.78E+02	-3.78E+01	-2.34E+00	6.92E+00	3.80E+02
1.39E+01	4.96E+00	1.58E+00	3.69E+02	-3.69E+01	-1.68E+00	4.96E+00	3.71E+02
1.67E+01	4.00E+00	1.32E+00	3.67E+02	-3.67E+01	-1.39E+00	4.10E+00	3.69E+02
1.94E+01	3.59E+00	1.20E+00	3.66E+02	-3.66E+01	-1.26E+00	3.72E+00	3.68E+02
2.22E+01	3.41E+00	1.15E+00	3.65E+02	-3.65E+01	-1.21E+00	3.56E+00	3.67E+02

Time (Hour)	A.42	A.43	A.44	A.45	A.46
1.67E-02	8.30E+01	-1.21E+00	-1.11E+01	1.11E+00	8.37E+01
2.78E-01	8.75E+01	-1.32E+00	-1.38E+01	1.38E+00	8.86E+01
5.56E-01	9.40E+01	-1.43E+00	-1.71E+01	1.71E+00	9.56E+01
0.00E+00	1.02E+02	-1.53E+00	-2.09E+01	2.09E+00	1.04E+02
1.11E+00	1.11E+02	-1.63E+00	-2.53E+01	2.53E+00	1.14E+02
1.39E+00	1.22E+02	-1.73E+00	-3.02E+01	3.02E+00	1.25E+02
1.94E+00	1.45E+02	-1.89E+00	-4.13E+01	4.13E+00	1.51E+02
2.78E+00	1.85E+02	-2.05E+00	-6.09E+01	6.09E+00	1.95E+02
4.17E+00	2.60E+02	-2.11E+00	-9.65E+01	9.65E+00	2.78E+02
5.56E+00	3.42E+02	-2.05E+00	-1.33E+02	1.33E+01	3.68E+02
8.33E+00	5.40E+02	-2.02E+00	-2.34E+02	2.34E+01	5.89E+02
1.11E+01	7.96E+02	-2.34E+00	-4.24E+02	4.24E+01	9.02E+02
1.39E+01	1.06E+03	-2.84E+00	-7.02E+02	7.02E+01	1.27E+03
1.67E+01	1.26E+03	-3.28E+00	-9.72E+02	9.72E+01	1.60E+03
1.94E+01	1.38E+03	-3.56E+00	-1.16E+03	1.16E+02	1.81E+03
2.22E+01	1.44E+03	-3.70E+00	-1.26E+03	1.26E+02	1.92E+03

Time (Hour)	A.47	A.48	A.49	A.50
1.67E-02	5.32E+00	1.79E+01	-5.70E-01	1.87E+01
2.78E-01	5.63E+00	1.78E+01	-5.64E-01	1.86E+01
5.56E-01	6.07E+00	1.76E+01	-5.58E-01	1.86E+01
0.00E+00	6.61E+00	1.74E+01	-5.51E-01	1.86E+01
1.11E+00	7.25E+00	1.71E+01	-5.44E-01	1.86E+01
1.39E+00	7.96E+00	1.69E+01	-5.37E-01	1.87E+01
1.94E+00	9.59E+00	1.65E+01	-5.22E-01	1.90E+01
2.78E+00	1.24E+01	1.57E+01	-4.99E-01	2.00E+01
4.17E+00	1.76E+01	1.45E+01	-4.61E-01	2.29E+01
5.56E+00	2.33E+01	1.35E+01	-4.27E-01	2.69E+01
8.33E+00	3.74E+01	1.19E+01	-3.79E-01	3.93E+01
1.11E+01	5.73E+01	1.13E+01	-3.57E-01	5.84E+01
1.39E+01	8.08E+01	1.10E+01	-3.49E-01	8.16E+01
1.67E+01	1.01E+02	1.09E+01	-3.46E-01	1.02E+02
1.94E+01	1.15E+02	1.09E+01	-3.46E-01	1.15E+02
2.22E+01	1.22E+02	1.09E+01	-3.45E-01	1.22E+02

A.51	A.52	A.53
1.64E-04	-4.37E-04	4.67E-04

Time (Hour)	A.54			A.55
1.67E-02	-6.92E+01			6.92E+01
2.78E-01	-6.89E+01			6.89E+01
5.56E-01	-6.87E+01			6.87E+01
0.00E+00	-6.87E+01			6.87E+01
1.11E+00	-6.88E+01			6.88E+01
1.39E+00	-6.91E+01			6.91E+01
1.94E+00	-7.04E+01			7.04E+01
2.78E+00	-7.41E+01			7.41E+01
4.17E+00	-8.46E+01			8.46E+01
5.56E+00	-9.98E+01			9.98E+01
8.33E+00	-1.46E+02			1.46E+02
1.11E+01	-2.17E+02			2.17E+02
1.39E+01	-3.03E+02			3.03E+02
1.67E+01	-3.79E+02			3.79E+02
1.94E+01	-4.28E+02			4.28E+02
2.22E+01	-4.55E+02			4.55E+02
Time (Hour)	A.56	A.57	A.58	A.59
1.67E-02	3.83E-02	-9.47E-06	-3.82E-03	3.84E-02
2.78E-01	3.83E-02	-1.59E-04	-3.67E-03	3.84E-02
5.56E-01	3.83E-02	-3.21E-04	-3.50E-03	3.84E-02
0.00E+00	3.83E-02	-4.84E-04	-3.34E-03	3.84E-02
1.11E+00	3.83E-02	-6.47E-04	-3.18E-03	3.84E-02
1.39E+00	3.83E-02	-8.09E-04	-3.02E-03	3.84E-02
1.94E+00	3.83E-02	-1.13E-03	-2.70E-03	3.84E-02
2.78E+00	3.83E-02	-1.57E-03	-2.26E-03	3.84E-02
4.17E+00	3.83E-02	-2.18E-03	-1.64E-03	3.84E-02
5.56E+00	3.83E-02	-2.62E-03	-1.21E-03	3.84E-02
8.33E+00	3.83E-02	-3.08E-03	-7.51E-04	3.84E-02
1.11E+01	3.83E-02	-3.24E-03	-5.91E-04	3.84E-02
1.39E+01	3.83E-02	-3.29E-03	-5.39E-04	3.84E-02
1.67E+01	3.83E-02	-3.30E-03	-5.22E-04	3.84E-02
1.94E+01	3.83E-02	-3.31E-03	-5.17E-04	3.84E-02
2.22E+01	3.83E-02	-3.31E-03	-5.16E-04	3.84E-02

Time (Hour)	A.60	A.61	A.62	A.63	A.64
1.67E-02	-6.78E-03	7.60E+00	3.05E-01	7.84E-05	7.60E+00
2.78E-01	-7.06E-03	7.57E+00	2.67E-01	7.84E-05	7.57E+00
5.56E-01	-7.38E-03	7.55E+00	2.25E-01	7.84E-05	7.55E+00
0.00E+00	-7.74E-03	7.55E+00	1.81E-01	7.84E-05	7.55E+00
1.11E+00	-8.14E-03	7.57E+00	1.35E-01	7.85E-05	7.57E+00
1.39E+00	-8.57E-03	7.60E+00	8.66E-02	7.85E-05	7.61E+00
1.94E+00	-9.58E-03	7.75E+00	-1.72E-02	7.86E-05	7.75E+00
2.78E+00	-1.15E-02	8.16E+00	-1.97E-01	7.87E-05	8.16E+00
4.17E+00	-1.58E-02	9.34E+00	-5.88E-01	7.89E-05	9.36E+00
5.56E+00	-2.15E-02	1.10E+01	-1.11E+00	7.91E-05	1.11E+01
8.33E+00	-3.47E-02	1.62E+01	-2.58E+00	7.94E-05	1.64E+01
1.11E+01	-4.42E-02	2.41E+01	-4.57E+00	7.96E-05	2.45E+01
1.39E+01	-4.85E-02	3.37E+01	-6.79E+00	7.97E-05	3.43E+01
1.67E+01	-5.01E-02	4.21E+01	-8.65E+00	7.97E-05	4.30E+01
1.94E+01	-5.06E-02	4.76E+01	-9.85E+00	7.97E-05	4.86E+01
2.22E+01	-5.07E-02	5.06E+01	-1.04E+01	7.97E-05	5.16E+01

Time (Hour)	A.65	A.66	A.67	A.68(ω_α)	α	% Difference
1.67E-02	2.04E-05	7.43E-07	-1.97E-08	2.05E-05	3.77E-05	5.42E+01
2.78E-01	1.22E-06	4.49E-08	-7.12E-11	1.22E-06	2.28E-06	5.36E+01
5.56E-01	6.09E-07	2.26E-08	-1.79E-11	6.10E-07	1.15E-06	5.31E+01
0.00E+00	4.06E-07	1.52E-08	-8.03E-12	4.06E-07	7.70E-07	5.27E+01
1.11E+00	3.05E-07	1.15E-08	-4.55E-12	3.05E-07	5.82E-07	5.24E+01
1.39E+00	2.45E-07	9.24E-09	-2.93E-12	2.45E-07	4.70E-07	5.23E+01
1.94E+00	1.79E-07	6.71E-09	-1.52E-12	1.79E-07	3.41E-07	5.24E+01
2.78E+00	1.32E-07	4.82E-09	-7.66E-13	1.32E-07	2.45E-07	5.38E+01
4.17E+00	1.01E-07	3.36E-09	-3.56E-13	1.01E-07	1.71E-07	5.89E+01
5.56E+00	8.95E-08	2.63E-09	-2.09E-13	8.95E-08	1.34E-07	6.70E+01
8.33E+00	8.80E-08	1.87E-09	-9.87E-14	8.80E-08	9.48E-08	9.28E+01
1.11E+01	9.88E-08	1.44E-09	-5.73E-14	9.88E-08	7.33E-08	1.35E+02
1.39E+01	1.11E-07	1.17E-09	-3.71E-14	1.11E-07	5.93E-08	1.87E+02
1.67E+01	1.15E-07	9.77E-10	-2.59E-14	1.15E-07	4.97E-08	2.33E+02
1.94E+01	1.12E-07	8.39E-10	-1.90E-14	1.12E-07	4.26E-08	2.63E+02
2.22E+01	1.04E-07	7.33E-10	-1.46E-14	1.04E-07	3.73E-08	2.79E+02

Cooling from $60\,^{o}C$

Time (Hour)	A.18	A.19	A.20	A.21	A.22	A.23	A.24	A.25
1.67E-02	1.07E-05	1.62E-03	1.23E-03	-1.23E-04	4.96E-02	-1.84E-04	-1.05E-11	4.97E-02
2.78E-01	9.46E-06	1.43E-03	1.23E-03	-1.23E-04	4.39E-02	-1.63E-04	-9.28E-12	4.39E-02
5.56E-01	8.34E-06	1.26E-03	1.23E-03	-1.23E-04	3.86E-02	-1.43E-04	-8.18E-12	3.87E-02
8.33E-01	7.38E-06	1.11E-03	1.23E-03	-1.23E-04	3.42E-02	-1.27E-04	-7.24E-12	3.42E-02
1.11E+00	6.55E-06	9.89E-04	1.23E-03	-1.23E-04	3.04E-02	-1.13E-04	-6.43E-12	3.04E-02
1.39E+00	5.85E-06	8.82E-04	1.23E-03	-1.23E-04	2.71E-02	-1.01E-04	-5.73E-12	2.71E-02
1.94E+00	4.71E-06	7.11E-04	1.23E-03	-1.23E-04	2.18E-02	-8.11E-05	-4.62E-12	2.19E-02
2.78E+00	3.51E-06	5.30E-04	1.23E-03	-1.23E-04	1.63E-02	-6.04E-05	-3.44E-12	1.63E-02
4.17E+00	2.31E-06	3.48E-04	1.23E-03	-1.23E-04	1.07E-02	-3.97E-05	-2.27E-12	1.08E-02
5.56E+00	1.62E-06	2.44E-04	1.23E-03	-1.23E-04	7.51E-03	-2.79E-05	-1.59E-12	7.61E-03
8.33E+00	8.85E-07	1.34E-04	1.23E-03	-1.23E-04	4.10E-03	-1.52E-05	-8.68E-13	4.29E-03
1.11E+01	5.34E-07	8.06E-05	1.23E-03	-1.23E-04	2.47E-03	-9.19E-06	-5.24E-13	2.77E-03
1.39E+01	3.65E-07	5.50E-05	1.23E-03	-1.23E-04	1.69E-03	-6.28E-06	-3.58E-13	2.09E-03
1.67E+01	2.86E-07	4.31E-05	1.23E-03	-1.23E-04	1.32E-03	-4.92E-06	-2.80E-13	1.81E-03
1.94E+01	2.50E-07	3.78E-05	1.23E-03	-1.23E-04	1.16E-03	-4.30E-06	-2.45E-13	1.69E-03
2.22E+01	2.34E-07	3.53E-05	1.23E-03	-1.23E-04	1.09E-03	-4.03E-06	-2.30E-13	1.64E-03

Time (Hour)	A.26	A.27	A.28	A.29	A.30
1.67E-02	7.66E-06	-1.98E-05	1.35E-03	-4.52E-04	1.43E-03
2.78E-01	7.38E-06	-1.91E-05	1.20E-03	-4.35E-04	1.27E-03
5.56E-01	7.07E-06	-1.83E-05	1.05E-03	-4.17E-04	1.13E-03
0.00E+00	6.75E-06	-1.75E-05	9.32E-04	-3.98E-04	1.01E-03
1.11E+00	6.43E-06	-1.66E-05	8.28E-04	-3.79E-04	9.11E-04
1.39E+00	6.11E-06	-1.58E-05	7.39E-04	-3.60E-04	8.22E-04
1.94E+00	5.46E-06	-1.41E-05	5.96E-04	-3.22E-04	6.77E-04
2.78E+00	4.52E-06	-1.17E-05	4.45E-04	-2.67E-04	5.19E-04
4.17E+00	3.19E-06	-8.25E-06	2.94E-04	-1.88E-04	3.49E-04
5.56E+00	2.22E-06	-5.75E-06	2.07E-04	-1.31E-04	2.45E-04
8.33E+00	1.22E-06	-3.14E-06	1.17E-04	-7.17E-05	1.37E-04
1.11E+01	8.73E-07	-2.26E-06	7.54E-05	-5.15E-05	9.13E-05
1.39E+01	7.67E-07	-1.98E-06	5.70E-05	-4.52E-05	7.28E-05
1.67E+01	7.35E-07	-1.90E-06	4.93E-05	-4.33E-05	6.57E-05
1.94E+01	7.26E-07	-1.87E-06	4.61E-05	-4.28E-05	6.30E-05
2.22E+01	7.23E-07	-1.87E-06	4.48E-05	-4.26E-05	6.19E-05

Time (Hour)	A.31	A.32	A.33				A.34
1.67E-02	1.56E-02	2.18E-06	5.01E-01				5.02E-01
2.78E-01	1.55E-02	2.16E-06	4.60E-01				4.61E-01
5.56E-01	1.53E-02	2.14E-06	4.23E-01				4.23E-01
0.00E+00	1.51E-02	2.12E-06	3.92E-01				3.92E-01
1.11E+00	1.50E-02	2.09E-06	3.65E-01				3.66E-01
1.39E+00	1.48E-02	2.06E-06	3.43E-01				3.43E-01
1.94E+00	1.44E-02	2.01E-06	3.07E-01				3.08E-01
2.78E+00	1.37E-02	1.91E-06	2.71E-01				2.71E-01
4.17E+00	1.26E-02	1.75E-06	2.37E-01				2.37E-01
5.56E+00	1.15E-02	1.60E-06	2.18E-01				2.18E-01
8.33E+00	9.86E-03	1.38E-06	1.92E-01				1.92E-01
1.11E+01	9.08E-03	1.27E-06	1.64E-01				1.64E-01
1.39E+01	8.79E-03	1.23E-06	1.44E-01				1.44E-01
1.67E+01	8.70E-03	1.22E-06	1.34E-01				1.34E-01
1.94E+01	8.67E-03	1.21E-06	1.30E-01				1.30E-01
2.22E+01	8.66E-03	1.21E-06	1.28E-01				1.28E-01
Time (Hour)	A.35	A.36	A.37	A.38	A.39	A.40	A.41
1.67E-02	7.00E+02	5.77E+01	6.17E+02	-6.17E+01	-9.99E+01	2.95E+02	9.87E+02
2.78E-01	5.68E+02	5.10E+01	6.11E+02	-6.11E+01	-8.75E+01	2.58E+02	8.81E+02
5.56E-01	4.60E+02	4.49E+01	6.05E+02	-6.05E+01	-7.62E+01	2.25E+02	8.00E+02
0.00E+00	3.77E+02	3.97E+01	5.98E+02	-5.98E+01	-6.67E+01	1.97E+02	7.40E+02
1.11E+00	3.12E+02	3.53E+01	5.90E+02	-5.90E+01	-5.85E+01	1.73E+02	6.96E+02
1.39E+00	2.61E+02	3.15E+01	5.83E+02	-5.83E+01	-5.15E+01	1.52E+02	6.62E+02
1.94E+00	1.89E+02	2.54E+01	5.67E+02	-5.67E+01	-4.04E+01	1.19E+02	6.14E+02
2.78E+00	1.24E+02	1.89E+01	5.41E+02	-5.41E+01	-2.87E+01	8.48E+01	5.65E+02
4.17E+00	7.13E+01	1.24E+01	4.96E+02	-4.96E+01	-1.73E+01	5.11E+01	5.06E+02
5.56E+00	4.61E+01	8.73E+00	4.53E+02	-4.53E+01	-1.11E+01	3.27E+01	4.59E+02
8.33E+00	2.21E+01	4.77E+00	3.89E+02	-3.89E+01	-5.21E+00	1.54E+01	3.92E+02
1.11E+01	1.14E+01	2.88E+00	3.58E+02	-3.58E+01	-2.89E+00	8.54E+00	3.60E+02
1.39E+01	6.85E+00	1.97E+00	3.47E+02	-3.47E+01	-1.91E+00	5.65E+00	3.49E+02
1.67E+01	5.00E+00	1.54E+00	3.43E+02	-3.43E+01	-1.48E+00	4.38E+00	3.45E+02
1.94E+01	4.24E+00	1.35E+00	3.42E+02	-3.42E+01	-1.29E+00	3.82E+00	3.44E+02
2.22E+01	3.91E+00	1.26E+00	3.42E+02	-3.42E+01	-1.21E+00	3.58E+00	3.44E+02

Time (Hour)	A.42	A.43	A.44	A.45	A.46
1.67E-02	7.91E+01	-1.03E+00	-7.18E+00	7.18E-01	7.94E+01
2.78E-01	7.99E+01	-1.12E+00	-8.76E+00	8.76E-01	8.04E+01
5.56E-01	8.23E+01	-1.20E+00	-1.07E+01	1.07E+00	8.30E+01
0.00E+00	8.61E+01	-1.28E+00	-1.29E+01	1.29E+00	8.71E+01
1.11E+00	9.11E+01	-1.36E+00	-1.54E+01	1.54E+00	9.24E+01
1.39E+00	9.71E+01	-1.43E+00	-1.81E+01	1.81E+00	9.88E+01
1.94E+00	1.12E+02	-1.54E+00	-2.43E+01	2.43E+00	1.14E+02
2.78E+00	1.38E+02	-1.63E+00	-3.45E+01	3.45E+00	1.42E+02
4.17E+00	1.88E+02	-1.60E+00	-5.16E+01	5.16E+00	1.95E+02
5.56E+00	2.43E+02	-1.46E+00	-6.68E+01	6.68E+00	2.52E+02
8.33E+00	3.80E+02	-1.25E+00	-1.05E+02	1.05E+01	3.95E+02
1.11E+01	5.79E+02	-1.37E+00	-1.91E+02	1.91E+01	6.10E+02
1.39E+01	8.20E+02	-1.71E+00	-3.48E+02	3.48E+01	8.92E+02
1.67E+01	1.04E+03	-2.07E+00	-5.37E+02	5.37E+01	1.17E+03
1.94E+01	1.18E+03	-2.32E+00	-6.91E+02	6.91E+01	1.37E+03
2.22E+01	1.26E+03	-2.47E+00	-7.84E+02	7.84E+01	1.48E+03

Time (Hour)	A.47	A.48	A.49	A.50
1.67E-02	5.04E+00	1.84E+01	-5.83E-01	1.90E+01
2.78E-01	5.10E+00	1.82E+01	-5.77E-01	1.89E+01
5.56E-01	5.27E+00	1.80E+01	-5.71E-01	1.88E+01
0.00E+00	5.53E+00	1.78E+01	-5.65E-01	1.86E+01
1.11E+00	5.87E+00	1.76E+01	-5.58E-01	1.85E+01
1.39E+00	6.28E+00	1.73E+01	-5.51E-01	1.85E+01
1.94E+00	7.26E+00	1.69E+01	-5.35E-01	1.84E+01
2.78E+00	9.04E+00	1.61E+01	-5.11E-01	1.85E+01
4.17E+00	1.24E+01	1.47E+01	-4.68E-01	1.93E+01
5.56E+00	1.60E+01	1.35E+01	-4.28E-01	2.09E+01
8.33E+00	2.51E+01	1.16E+01	-3.68E-01	2.76E+01
1.11E+01	3.87E+01	1.07E+01	-3.39E-01	4.02E+01
1.39E+01	5.66E+01	1.03E+01	-3.28E-01	5.76E+01
1.67E+01	7.42E+01	1.02E+01	-3.24E-01	7.49E+01
1.94E+01	8.69E+01	1.02E+01	-3.23E-01	8.75E+01
2.22E+01	9.43E+01	1.02E+01	-3.23E-01	9.48E+01

A.51	A.52	A.53
1.64E-04	-4.37E-04	4.67E-04

Time (Hour)	A.54			A.55
1.67E-02	-7.04E+01			7.04E+01
2.78E-01	-6.98E+01			6.98E+01
5.56E-01	-6.93E+01			6.93E+01
0.00E+00	-6.88E+01			6.88E+01
1.11E+00	-6.85E+01			6.85E+01
1.39E+00	-6.82E+01			6.82E+01
1.94E+00	-6.79E+01			6.79E+01
2.78E+00	-6.83E+01			6.83E+01
4.17E+00	-7.13E+01			7.13E+01
5.56E+00	-7.75E+01			7.75E+01
8.33E+00	-1.02E+02			1.02E+02
1.11E+01	-1.49E+02			1.49E+02
1.39E+01	-2.14E+02			2.14E+02
1.67E+01	-2.78E+02			2.78E+02
1.94E+01	-3.25E+02			3.25E+02
2.22E+01	-3.53E+02			3.53E+02
Time (Hour)	A.56	A.57	A.58	A.59
1.67E-02	3.49E-02	-8.08E-06	-3.48E-03	3.51E-02
2.78E-01	3.49E-02	-1.37E-04	-3.35E-03	3.50E-02
5.56E-01	3.49E-02	-2.78E-04	-3.21E-03	3.50E-02
0.00E+00	3.49E-02	-4.22E-04	-3.07E-03	3.50E-02
1.11E+00	3.49E-02	-5.68E-04	-2.92E-03	3.50E-02
1.39E+00	3.49E-02	-7.16E-04	-2.77E-03	3.50E-02
1.94E+00	3.49E-02	-1.01E-03	-2.48E-03	3.50E-02
2.78E+00	3.49E-02	-1.43E-03	-2.05E-03	3.50E-02
4.17E+00	3.49E-02	-2.04E-03	-1.45E-03	3.50E-02
5.56E+00	3.49E-02	-2.48E-03	-1.01E-03	3.50E-02
8.33E+00	3.49E-02	-2.94E-03	-5.52E-04	3.50E-02
1.11E+01	3.49E-02	-3.09E-03	-3.96E-04	3.50E-02
1.39E+01	3.49E-02	-3.14E-03	-3.48E-04	3.50E-02
1.67E+01	3.49E-02	-3.15E-03	-3.34E-04	3.50E-02
1.94E+01	3.49E-02	-3.16E-03	-3.29E-04	3.50E-02
2.22E+01	3.49E-02	-3.16E-03	-3.28E-04	3.50E-02

Time (Hour)	A.60	A.61	A.62	A.63	A.64
1.67E-02	-6.18E-03	7.73E+00	2.85E-01	7.83E-05	7.73E+00
2.78E-01	-6.42E-03	7.67E+00	2.47E-01	7.83E-05	7.67E+00
5.56E-01	-6.70E-03	7.61E+00	2.06E-01	7.84E-05	7.62E+00
0.00E+00	-7.01E-03	7.57E+00	1.62E-01	7.84E-05	7.57E+00
1.11E+00	-7.36E-03	7.53E+00	1.16E-01	7.84E-05	7.53E+00
1.39E+00	-7.75E-03	7.50E+00	6.82E-02	7.84E-05	7.50E+00
1.94E+00	-8.68E-03	7.47E+00	-3.44E-02	7.85E-05	7.47E+00
2.78E+00	-1.05E-02	7.52E+00	-2.07E-01	7.86E-05	7.52E+00
4.17E+00	-1.49E-02	7.87E+00	-5.53E-01	7.88E-05	7.88E+00
5.56E+00	-2.14E-02	8.57E+00	-9.83E-01	7.91E-05	8.63E+00
8.33E+00	-3.93E-02	1.14E+01	-2.15E+00	7.95E-05	1.16E+01
1.11E+01	-5.49E-02	1.66E+01	-3.83E+00	7.98E-05	1.70E+01
1.39E+01	-6.25E-02	2.38E+01	-5.87E+00	7.99E-05	2.45E+01
1.67E+01	-6.53E-02	3.10E+01	-7.80E+00	7.99E-05	3.20E+01
1.94E+01	-6.61E-02	3.62E+01	-9.18E+00	8.00E-05	3.74E+01
2.22E+01	-6.64E-02	3.93E+01	-9.97E+00	8.00E-05	4.05E+01

Time (Hour)	A.65	A.66	A.67	A.68(ω_α)	α	% Difference
1.67E-02	2.08E-05	7.46E-07	-1.97E-08	2.08E-05	3.79E-05	5.49E+01
2.78E-01	1.24E-06	4.50E-08	-7.15E-11	1.24E-06	2.29E-06	5.41E+01
5.56E-01	6.14E-07	2.27E-08	-1.80E-11	6.15E-07	1.15E-06	5.34E+01
0.00E+00	4.07E-07	1.52E-08	-8.05E-12	4.07E-07	7.73E-07	5.27E+01
1.11E+00	3.04E-07	1.15E-08	-4.56E-12	3.04E-07	5.84E-07	5.20E+01
1.39E+00	2.42E-07	9.27E-09	-2.94E-12	2.42E-07	4.71E-07	5.14E+01
1.94E+00	1.72E-07	6.73E-09	-1.53E-12	1.72E-07	3.42E-07	5.04E+01
2.78E+00	1.21E-07	4.84E-09	-7.69E-13	1.21E-07	2.46E-07	4.93E+01
4.17E+00	8.48E-08	3.39E-09	-3.59E-13	8.49E-08	1.72E-07	4.93E+01
5.56E+00	6.96E-08	2.67E-09	-2.12E-13	6.96E-08	1.36E-07	5.13E+01
8.33E+00	6.22E-08	1.92E-09	-1.02E-13	6.22E-08	9.77E-08	6.37E+01
1.11E+01	6.87E-08	1.50E-09	-5.96E-14	6.87E-08	7.63E-08	9.01E+01
1.39E+01	7.92E-08	1.22E-09	-3.87E-14	7.92E-08	6.20E-08	1.28E+02
1.67E+01	8.59E-08	1.02E-09	-2.70E-14	8.59E-08	5.19E-08	1.66E+02
1.94E+01	8.62E-08	8.77E-10	-1.99E-14	8.62E-08	4.46E-08	1.93E+02
2.22E+01	8.17E-08	7.68E-10	-1.52E-14	8.17E-08	3.90E-08	2.09E+02

Cooling from $65\,^{o}C$

Time (Hour)	A.18	A.19	A.20	A.21	A.22	A.23	A.24	A.25
1.67E-02	1.20E-05	1.82E-03	1.23E-03	-1.23E-04	5.57E-02	-2.07E-04	-1.18E-11	5.58E-02
2.78E-01	1.07E-05	1.61E-03	1.23E-03	-1.23E-04	4.96E-02	-1.84E-04	-1.05E-11	4.96E-02
5.56E-01	9.47E-06	1.43E-03	1.23E-03	-1.23E-04	4.39E-02	-1.63E-04	-9.29E-12	4.39E-02
8.33E-01	8.42E-06	1.27E-03	1.23E-03	-1.23E-04	3.90E-02	-1.45E-04	-8.26E-12	3.90E-02
1.11E+00	7.51E-06	1.13E-03	1.23E-03	-1.23E-04	3.48E-02	-1.29E-04	-7.36E-12	3.48E-02
1.39E+00	6.72E-06	1.01E-03	1.23E-03	-1.23E-04	3.11E-02	-1.16E-04	-6.59E-12	3.12E-02
1.94E+00	5.43E-06	8.20E-04	1.23E-03	-1.23E-04	2.52E-02	-9.35E-05	-5.33E-12	2.52E-02
2.78E+00	4.05E-06	6.11E-04	1.23E-03	-1.23E-04	1.87E-02	-6.96E-05	-3.97E-12	1.88E-02
4.17E+00	2.61E-06	3.94E-04	1.23E-03	-1.23E-04	1.21E-02	-4.50E-05	-2.56E-12	1.22E-02
5.56E+00	1.77E-06	2.68E-04	1.23E-03	-1.23E-04	8.22E-03	-3.05E-05	-1.74E-12	8.32E-03
8.33E+00	9.05E-07	1.37E-04	1.23E-03	-1.23E-04	4.19E-03	-1.56E-05	-8.88E-13	4.37E-03
1.11E+01	5.35E-07	8.07E-05	1.23E-03	-1.23E-04	2.48E-03	-9.20E-06	-5.25E-13	2.77E-03
1.39E+01	3.79E-07	5.72E-05	1.23E-03	-1.23E-04	1.76E-03	-6.53E-06	-3.72E-13	2.15E-03
1.67E+01	3.16E-07	4.76E-05	1.23E-03	-1.23E-04	1.46E-03	-5.43E-06	-3.10E-13	1.91E-03
1.94E+01	2.90E-07	4.38E-05	1.23E-03	-1.23E-04	1.34E-03	-4.99E-06	-2.85E-13	1.83E-03
2.22E+01	2.80E-07	4.23E-05	1.23E-03	-1.23E-04	1.30E-03	-4.82E-06	-2.75E-13	1.79E-03

Time (Hour)	A.26	A.27	A.28	A.29	A.30
1.67E-02	6.21E-06	-1.61E-05	1.52E-03	-3.66E-04	1.56E-03
2.78E-01	5.94E-06	-1.54E-05	1.35E-03	-3.50E-04	1.40E-03
5.56E-01	5.64E-06	-1.46E-05	1.20E-03	-3.33E-04	1.24E-03
0.00E+00	5.34E-06	-1.38E-05	1.06E-03	-3.15E-04	1.11E-03
1.11E+00	5.02E-06	-1.30E-05	9.49E-04	-2.96E-04	9.94E-04
1.39E+00	4.71E-06	-1.22E-05	8.49E-04	-2.78E-04	8.93E-04
1.94E+00	4.08E-06	-1.06E-05	6.87E-04	-2.41E-04	7.28E-04
2.78E+00	3.20E-06	-8.27E-06	5.12E-04	-1.89E-04	5.46E-04
4.17E+00	2.00E-06	-5.17E-06	3.32E-04	-1.18E-04	3.52E-04
5.56E+00	1.20E-06	-3.09E-06	2.27E-04	-7.05E-05	2.37E-04
8.33E+00	4.57E-07	-1.18E-06	1.19E-04	-2.69E-05	1.22E-04
1.11E+01	2.46E-07	-6.36E-07	7.54E-05	-1.45E-05	7.68E-05
1.39E+01	1.91E-07	-4.93E-07	5.85E-05	-1.13E-05	5.96E-05
1.67E+01	1.77E-07	-4.56E-07	5.21E-05	-1.04E-05	5.32E-05
1.94E+01	1.73E-07	-4.47E-07	4.97E-05	-1.02E-05	5.08E-05
2.22E+01	1.72E-07	-4.45E-07	4.88E-05	-1.01E-05	4.98E-05

Time (Hour)	A.31	A.32	A.33				A.34
1.67E-02	1.48E-02	2.07E-06	6.43E-01				6.43E-01
2.78E-01	1.47E-02	2.05E-06	5.94E-01				5.94E-01
5.56E-01	1.45E-02	2.02E-06	5.49E-01				5.50E-01
0.00E+00	1.43E-02	2.00E-06	5.12E-01				5.12E-01
1.11E+00	1.41E-02	1.97E-06	4.80E-01				4.80E-01
1.39E+00	1.38E-02	1.93E-06	4.53E-01				4.53E-01
1.94E+00	1.34E-02	1.87E-06	4.10E-01				4.11E-01
2.78E+00	1.26E-02	1.76E-06	3.69E-01				3.69E-01
4.17E+00	1.12E-02	1.56E-06	3.39E-01				3.39E-01
5.56E+00	9.82E-03	1.37E-06	3.36E-01				3.36E-01
8.33E+00	7.72E-03	1.08E-06	3.56E-01				3.56E-01
1.11E+01	6.62E-03	9.25E-07	3.56E-01				3.56E-01
1.39E+01	6.21E-03	8.68E-07	3.34E-01				3.34E-01
1.67E+01	6.09E-03	8.51E-07	3.16E-01				3.16E-01
1.94E+01	6.06E-03	8.47E-07	3.06E-01				3.07E-01
2.22E+01	6.05E-03	8.46E-07	3.02E-01				3.02E-01
Time (Hour)	A.35	A.36	A.37	A.38	A.39	A.40	A.41
1.67E-02	1.01E+03	6.15E+01	5.85E+02	-5.85E+01	-1.06E+02	3.14E+02	1.22E+03
2.78E-01	8.28E+02	5.47E+01	5.79E+02	-5.79E+01	-9.36E+01	2.76E+02	1.05E+03
5.56E-01	6.78E+02	4.84E+01	5.71E+02	-5.71E+01	-8.18E+01	2.42E+02	9.26E+02
0.00E+00	5.61E+02	4.30E+01	5.63E+02	-5.63E+01	-7.17E+01	2.12E+02	8.29E+02
1.11E+00	4.69E+02	3.84E+01	5.55E+02	-5.55E+01	-6.30E+01	1.86E+02	7.56E+02
1.39E+00	3.96E+02	3.43E+01	5.46E+02	-5.46E+01	-5.55E+01	1.64E+02	7.00E+02
1.94E+00	2.91E+02	2.78E+01	5.27E+02	-5.27E+01	-4.33E+01	1.28E+02	6.20E+02
2.78E+00	1.95E+02	2.07E+01	4.96E+02	-4.96E+01	-3.03E+01	8.96E+01	5.44E+02
4.17E+00	1.15E+02	1.34E+01	4.41E+02	-4.41E+01	-1.74E+01	5.14E+01	4.61E+02
5.56E+00	7.77E+01	9.07E+00	3.88E+02	-3.88E+01	-1.04E+01	3.07E+01	3.99E+02
8.33E+00	4.20E+01	4.63E+00	3.05E+02	-3.05E+01	-4.17E+00	1.23E+01	3.10E+02
1.11E+01	2.48E+01	2.73E+00	2.61E+02	-2.61E+01	-2.11E+00	6.24E+00	2.64E+02
1.39E+01	1.65E+01	1.94E+00	2.45E+02	-2.45E+01	-1.41E+00	4.15E+00	2.47E+02
1.67E+01	1.30E+01	1.61E+00	2.40E+02	-2.40E+01	-1.15E+00	3.39E+00	2.42E+02
1.94E+01	1.16E+01	1.48E+00	2.39E+02	-2.39E+01	-1.05E+00	3.10E+00	2.41E+02
2.22E+01	1.10E+01	1.43E+00	2.39E+02	-2.39E+01	-1.01E+00	2.99E+00	2.40E+02

Time (Hour)	A.42	A.43	A.44	A.45	A.46
1.67E-02	8.67E+01	-7.08E-01	-4.38E+00	4.38E-01	8.68E+01
2.78E-01	8.46E+01	-7.53E-01	-5.23E+00	5.23E-01	8.48E+01
5.56E-01	8.39E+01	-7.97E-01	-6.26E+00	6.26E-01	8.41E+01
0.00E+00	8.45E+01	-8.37E-01	-7.39E+00	7.39E-01	8.49E+01
1.11E+00	8.64E+01	-8.70E-01	-8.61E+00	8.61E-01	8.68E+01
1.39E+00	8.93E+01	-8.97E-01	-9.92E+00	9.92E-01	8.99E+01
1.94E+00	9.79E+01	-9.28E-01	-1.27E+01	1.27E+00	9.87E+01
2.78E+00	1.15E+02	-9.19E-01	-1.69E+01	1.69E+00	1.17E+02
4.17E+00	1.51E+02	-7.90E-01	-2.25E+01	2.25E+00	1.53E+02
5.56E+00	1.93E+02	-6.12E-01	-2.57E+01	2.57E+00	1.95E+02
8.33E+00	2.93E+02	-3.60E-01	-2.96E+01	2.96E+00	2.95E+02
1.11E+01	4.23E+02	-2.82E-01	-3.91E+01	3.91E+00	4.25E+02
1.39E+01	5.58E+02	-2.89E-01	-5.66E+01	5.66E+00	5.61E+02
1.67E+01	6.58E+02	-3.15E-01	-7.42E+01	7.42E+00	6.62E+02
1.94E+01	7.11E+02	-3.34E-01	-8.55E+01	8.55E+00	7.17E+02
2.22E+01	7.36E+02	-3.44E-01	-9.12E+01	9.12E+00	7.42E+02
Time (Hour)	A.47	A.48	A.49		A.50
1.67E-02	5.51E+00	1.74E+01	-5.53E-01		1.83E+01
2.78E-01	5.38E+00	1.72E+01	-5.47E-01		1.81E+01
5.56E-01	5.34E+00	1.70E+01	-5.40E-01		1.78E+01
0.00E+00	5.39E+00	1.68E+01	-5.32E-01		1.76E+01
1.11E+00	5.51E+00	1.65E+01	-5.24E-01		1.74E+01
1.39E+00	5.71E+00	1.63E+01	-5.16E-01		1.72E+01
1.94E+00	6.27E+00	1.57E+01	-4.98E-01		1.69E+01
2.78E+00	7.40E+00	1.48E+01	-4.69E-01		1.65E+01
4.17E+00	9.72E+00	1.31E+01	-4.17E-01		1.63E+01
5.56E+00	1.24E+01	1.15E+01	-3.66E-01		1.69E+01
8.33E+00	1.87E+01	9.07E+00	-2.88E-01		2.08E+01
1.11E+01	2.70E+01	7.77E+00	-2.47E-01		2.81E+01
1.39E+01	3.56E+01	7.29E+00	-2.32E-01		3.64E+01
1.67E+01	4.20E+01	7.15E+00	-2.27E-01		4.26E+01
1.94E+01	4.55E+01	7.12E+00	-2.26E-01		4.61E+01
2.22E+01	4.71E+01	7.11E+00	-2.26E-01		4.76E+01
	A.51	A.52			A.53
	1.64E-04	-4.37E-04			4.67E-04

Time (Hour)	A.54			A.55
1.67E-02	-6.76E+01			6.76E+01
2.78E-01	-6.67E+01			6.67E+01
5.56E-01	-6.59E+01			6.59E+01
0.00E+00	-6.51E+01			6.51E+01
1.11E+00	-6.44E+01			6.44E+01
1.39E+00	-6.37E+01			6.37E+01
1.94E+00	-6.25E+01			6.25E+01
2.78E+00	-6.11E+01			6.11E+01
4.17E+00	-6.05E+01			6.05E+01
5.56E+00	-6.28E+01			6.28E+01
8.33E+00	-7.75E+01			7.75E+01
1.11E+01	-1.05E+02			1.05E+02
1.39E+01	-1.36E+02			1.36E+02
1.67E+01	-1.59E+02			1.59E+02
1.94E+01	-1.72E+02			1.72E+02
2.22E+01	-1.78E+02			1.78E+02
Time (Hour)	A.56	A.57	A.58	A.59
1.67E-02	4.30E-02	-1.18E-05	-4.29E-03	4.32E-02
2.78E-01	4.30E-02	-2.00E-04	-4.10E-03	4.32E-02
5.56E-01	4.30E-02	-4.06E-04	-3.89E-03	4.32E-02
0.00E+00	4.30E-02	-6.18E-04	-3.68E-03	4.32E-02
1.11E+00	4.30E-02	-8.34E-04	-3.47E-03	4.32E-02
1.39E+00	4.30E-02	-1.05E-03	-3.25E-03	4.31E-02
1.94E+00	4.30E-02	-1.48E-03	-2.82E-03	4.31E-02
2.78E+00	4.30E-02	-2.09E-03	-2.21E-03	4.31E-02
4.17E+00	4.30E-02	-2.92E-03	-1.38E-03	4.31E-02
5.56E+00	4.30E-02	-3.48E-03	-8.26E-04	4.32E-02
8.33E+00	4.30E-02	-3.99E-03	-3.15E-04	4.32E-02
1.11E+01	4.30E-02	-4.13E-03	-1.70E-04	4.32E-02
1.39E+01	4.30E-02	-4.17E-03	-1.32E-04	4.32E-02
1.67E+01	4.30E-02	-4.18E-03	-1.22E-04	4.32E-02
1.94E+01	4.30E-02	-4.18E-03	-1.19E-04	4.32E-02
2.22E+01	4.30E-02	-4.18E-03	-1.19E-04	4.32E-02

Time (Hour)	A.60	A.61	A.62	A.63	A.64		
1.67E-02	-7.63E-03	7.43E+00	3.29E-01	7.84E-05	7.43E+00		
2.78E-01	-7.98E-03	7.34E+00	2.85E-01	7.85E-05	7.34E+00		
5.56E-01	-8.40E-03	7.25E+00	2.36E-01	7.85E-05	7.25E+00		
0.00E+00	-8.88E-03	7.17E+00	1.84E-01	7.85E-05	7.17E+00		
1.11E+00	-9.43E-03	7.09E+00	1.30E-01	7.86E-05	7.09E+00		
1.39E+00	-1.01E-02	7.02E+00	7.31E-02	7.86E-05	7.02E+00		
1.94E+00	-1.16E-02	6.89E+00	-4.81E-02	7.87E-05	6.89E+00		
2.78E+00	-1.48E-02	6.74E+00	-2.48E-01	7.88E-05	6.75E+00		
4.17E+00	-2.38E-02	6.70E+00	-6.34E-01	7.91E-05	6.73E+00		
5.56E+00	-3.99E-02	6.97E+00	-1.10E+00	7.95E-05	7.05E+00		
8.33E+00	-1.05E-01	8.67E+00	-2.41E+00	8.04E-05	9.00E+00		
1.11E+01	-1.97E-01	1.18E+01	-4.20E+00	8.11E-05	1.25E+01		
1.39E+01	-2.55E-01	1.54E+01	-5.95E+00	8.14E-05	1.65E+01		
1.67E+01	-2.75E-01	1.80E+01	-7.16E+00	8.15E-05	1.94E+01		
1.94E+01	-2.81E-01	1.95E+01	-7.79E+00	8.16E-05	2.10E+01		
2.22E+01	-2.83E-01	2.01E+01	-8.07E+00	8.16E-05	2.17E+01		
Time (Hour)	A.65	A.66	A.67		A.68(ω_α)	α	% Difference
1.67E-02	2.00E-05	7.39E-07	-1.96E-08		2.00E-05	3.75E-05	5.33E+01
2.78E-01	1.18E-06	4.47E-08	-7.09E-11		1.19E-06	2.27E-06	5.22E+01
5.56E-01	5.85E-07	2.25E-08	-1.79E-11		5.85E-07	1.14E-06	5.12E+01
0.00E+00	3.85E-07	1.51E-08	-8.01E-12		3.86E-07	7.69E-07	5.02E+01
1.11E+00	2.86E-07	1.15E-08	-4.55E-12		2.86E-07	5.82E-07	4.92E+01
1.39E+00	2.26E-07	9.25E-09	-2.94E-12		2.27E-07	4.70E-07	4.82E+01
1.94E+00	1.59E-07	6.75E-09	-1.53E-12		1.59E-07	3.43E-07	4.63E+01
2.78E+00	1.09E-07	4.90E-09	-7.77E-13		1.09E-07	2.49E-07	4.38E+01
4.17E+00	7.23E-08	3.48E-09	-3.69E-13		7.24E-08	1.77E-07	4.09E+01
5.56E+00	5.69E-08	2.80E-09	-2.22E-13		5.69E-08	1.42E-07	4.01E+01
8.33E+00	4.84E-08	2.10E-09	-1.11E-13		4.84E-08	1.07E-07	4.55E+01
1.11E+01	5.05E-08	1.69E-09	-6.70E-14		5.05E-08	8.57E-08	5.90E+01
1.39E+01	5.31E-08	1.39E-09	-4.41E-14		5.31E-08	7.05E-08	7.53E+01
1.67E+01	5.21E-08	1.17E-09	-3.09E-14		5.21E-08	5.93E-08	8.79E+01
1.94E+01	4.83E-08	1.00E-09	-2.27E-14		4.83E-08	5.09E-08	9.49E+01
2.22E+01	4.37E-08	8.78E-10	-1.74E-14		4.37E-08	4.46E-08	9.81E+01

Cooling from $73\,^{o}C$

Time (Hour)	A.18	A.19	A.20	A.21	A.22	A.23	A.24	A.25
1.67E-02	1.36E-05	2.06E-03	1.23E-03	-1.23E-04	6.32E-02	-2.35E-04	-1.34E-11	6.33E-02
2.78E-01	1.21E-05	1.83E-03	1.23E-03	-1.23E-04	5.61E-02	-2.08E-04	-1.19E-11	5.61E-02
5.56E-01	1.07E-05	1.61E-03	1.23E-03	-1.23E-04	4.95E-02	-1.84E-04	-1.05E-11	4.95E-02
8.33E-01	9.46E-06	1.43E-03	1.23E-03	-1.23E-04	4.38E-02	-1.63E-04	-9.28E-12	4.39E-02
1.11E+00	8.40E-06	1.27E-03	1.23E-03	-1.23E-04	3.90E-02	-1.45E-04	-8.25E-12	3.90E-02
1.39E+00	7.49E-06	1.13E-03	1.23E-03	-1.23E-04	3.47E-02	-1.29E-04	-7.35E-12	3.48E-02
1.94E+00	6.02E-06	9.08E-04	1.23E-03	-1.23E-04	2.79E-02	-1.04E-04	-5.90E-12	2.79E-02
2.78E+00	4.43E-06	6.68E-04	1.23E-03	-1.23E-04	2.05E-02	-7.62E-05	-4.34E-12	2.06E-02
4.17E+00	2.80E-06	4.23E-04	1.23E-03	-1.23E-04	1.30E-02	-4.82E-05	-2.75E-12	1.31E-02
5.56E+00	1.87E-06	2.83E-04	1.23E-03	-1.23E-04	8.68E-03	-3.22E-05	-1.84E-12	8.77E-03
8.33E+00	9.47E-07	1.43E-04	1.23E-03	-1.23E-04	4.39E-03	-1.63E-05	-9.29E-13	4.56E-03
1.11E+01	5.60E-07	8.45E-05	1.23E-03	-1.23E-04	2.59E-03	-9.63E-06	-5.49E-13	2.87E-03
1.39E+01	3.94E-07	5.94E-05	1.23E-03	-1.23E-04	1.82E-03	-6.77E-06	-3.86E-13	2.20E-03
1.67E+01	3.23E-07	4.87E-05	1.23E-03	-1.23E-04	1.50E-03	-5.56E-06	-3.17E-13	1.94E-03
1.94E+01	2.93E-07	4.43E-05	1.23E-03	-1.23E-04	1.36E-03	-5.05E-06	-2.88E-13	1.84E-03
2.22E+01	2.81E-07	4.24E-05	1.23E-03	-1.23E-04	1.30E-03	-4.83E-06	-2.76E-13	1.79E-03
Time (Hour)	A.26	A.27	A.28	A.29				A.30
1.67E-02	7.22E-06	-1.86E-05	1.72E-03	-4.25E-04				1.78E-03
2.78E-01	6.86E-06	-1.77E-05	1.53E-03	-4.05E-04				1.58E-03
5.56E-01	6.48E-06	-1.68E-05	1.35E-03	-3.82E-04				1.40E-03
0.00E+00	6.11E-06	-1.58E-05	1.20E-03	-3.60E-04				1.25E-03
1.11E+00	5.74E-06	-1.48E-05	1.06E-03	-3.38E-04				1.11E-03
1.39E+00	5.37E-06	-1.39E-05	9.47E-04	-3.17E-04				9.99E-04
1.94E+00	4.66E-06	-1.20E-05	7.61E-04	-2.75E-04				8.09E-04
2.78E+00	3.69E-06	-9.54E-06	5.60E-04	-2.18E-04				6.01E-04
4.17E+00	2.39E-06	-6.18E-06	3.56E-04	-1.41E-04				3.83E-04
5.56E+00	1.49E-06	-3.86E-06	2.39E-04	-8.81E-05				2.55E-04
8.33E+00	5.75E-07	-1.49E-06	1.24E-04	-3.39E-05				1.29E-04
1.11E+01	2.55E-07	-6.58E-07	7.83E-05	-1.50E-05				7.97E-05
1.39E+01	1.51E-07	-3.89E-07	6.00E-05	-8.88E-06				6.07E-05
1.67E+01	1.17E-07	-3.03E-07	5.29E-05	-6.92E-06				5.33E-05
1.94E+01	1.07E-07	-2.76E-07	5.00E-05	-6.30E-06				5.04E-05
2.22E+01	1.04E-07	-2.68E-07	4.89E-05	-6.11E-06				4.93E-05

Time (Hour)	A.31	A.32	A.33				A.34
1.67E-02	1.54E-02	2.15E-06	6.53E-01				6.53E-01
2.78E-01	1.52E-02	2.12E-06	6.04E-01				6.04E-01
5.56E-01	1.50E-02	2.10E-06	5.59E-01				5.59E-01
0.00E+00	1.48E-02	2.06E-06	5.20E-01				5.20E-01
1.11E+00	1.45E-02	2.03E-06	4.87E-01				4.87E-01
1.39E+00	1.43E-02	2.00E-06	4.59E-01				4.59E-01
1.94E+00	1.38E-02	1.93E-06	4.13E-01				4.13E-01
2.78E+00	1.30E-02	1.82E-06	3.65E-01				3.66E-01
4.17E+00	1.17E-02	1.63E-06	3.22E-01				3.22E-01
5.56E+00	1.04E-02	1.45E-06	3.05E-01				3.05E-01
8.33E+00	8.18E-03	1.14E-06	3.16E-01				3.16E-01
1.11E+01	6.67E-03	9.33E-07	3.60E-01				3.60E-01
1.39E+01	5.85E-03	8.18E-07	4.06E-01				4.07E-01
1.67E+01	5.50E-03	7.68E-07	4.30E-01				4.30E-01
1.94E+01	5.37E-03	7.51E-07	4.37E-01				4.37E-01
2.22E+01	5.33E-03	7.45E-07	4.37E-01				4.37E-01
Time (Hour)	A.35	A.36	A.37	A.38	A.39	A.40	A.41
1.67E-02	1.16E+03	7.24E+01	6.08E+02	-6.08E+01	-1.25E+02	3.70E+02	1.37E+03
2.78E-01	9.52E+02	6.42E+01	6.00E+02	-6.00E+01	-1.10E+02	3.24E+02	1.18E+03
5.56E-01	7.78E+02	5.67E+01	5.92E+02	-5.92E+01	-9.55E+01	2.82E+02	1.03E+03
0.00E+00	6.41E+02	5.02E+01	5.83E+02	-5.83E+01	-8.34E+01	2.46E+02	9.08E+02
1.11E+00	5.34E+02	4.46E+01	5.74E+02	-5.74E+01	-7.29E+01	2.15E+02	8.19E+02
1.39E+00	4.48E+02	3.98E+01	5.64E+02	-5.64E+01	-6.40E+01	1.89E+02	7.51E+02
1.94E+00	3.24E+02	3.19E+01	5.45E+02	-5.45E+01	-4.96E+01	1.46E+02	6.55E+02
2.78E+00	2.11E+02	2.35E+01	5.14E+02	-5.14E+01	-3.44E+01	1.02E+02	5.69E+02
4.17E+00	1.18E+02	1.49E+01	4.61E+02	-4.61E+01	-1.95E+01	5.77E+01	4.82E+02
5.56E+00	7.45E+01	9.94E+00	4.10E+02	-4.10E+01	-1.16E+01	3.43E+01	4.20E+02
8.33E+00	3.90E+01	5.02E+00	3.23E+02	-3.23E+01	-4.62E+00	1.36E+01	3.27E+02
1.11E+01	2.63E+01	2.97E+00	2.63E+02	-2.63E+01	-2.23E+00	6.58E+00	2.66E+02
1.39E+01	2.09E+01	2.09E+00	2.31E+02	-2.31E+01	-1.37E+00	4.06E+00	2.33E+02
1.67E+01	1.81E+01	1.71E+00	2.17E+02	-2.17E+01	-1.06E+00	3.13E+00	2.19E+02
1.94E+01	1.67E+01	1.56E+00	2.12E+02	-2.12E+01	-9.40E-01	2.78E+00	2.14E+02
2.22E+01	1.60E+01	1.49E+00	2.10E+02	-2.10E+01	-8.93E-01	2.64E+00	2.12E+02

Time (Hour)	A.42	A.43	A.44	A.45	A.46
1.67E-02	8.62E+01	-7.52E-01	-4.10E+00	4.10E-01	8.63E+01
2.78E-01	8.37E+01	-7.97E-01	-4.90E+00	4.90E-01	8.38E+01
5.56E-01	8.23E+01	-8.41E-01	-5.86E+00	5.86E-01	8.26E+01
0.00E+00	8.24E+01	-8.82E-01	-6.93E+00	6.93E-01	8.27E+01
1.11E+00	8.36E+01	-9.17E-01	-8.11E+00	8.11E-01	8.40E+01
1.39E+00	8.59E+01	-9.47E-01	-9.39E+00	9.39E-01	8.65E+01
1.94E+00	9.35E+01	-9.89E-01	-1.22E+01	1.22E+00	9.43E+01
2.78E+00	1.10E+02	-1.00E+00	-1.69E+01	1.69E+00	1.11E+02
4.17E+00	1.48E+02	-9.22E-01	-2.45E+01	2.45E+00	1.50E+02
5.56E+00	1.93E+02	-7.66E-01	-3.04E+01	3.04E+00	1.95E+02
8.33E+00	2.96E+02	-4.59E-01	-3.61E+01	3.61E+00	2.99E+02
1.11E+01	4.08E+02	-2.81E-01	-3.73E+01	3.73E+00	4.10E+02
1.39E+01	5.08E+02	-2.07E-01	-3.91E+01	3.91E+00	5.10E+02
1.67E+01	5.81E+02	-1.85E-01	-4.25E+01	4.25E+00	5.83E+02
1.94E+01	6.25E+02	-1.81E-01	-4.59E+01	4.59E+00	6.27E+02
2.22E+01	6.47E+02	-1.82E-01	-4.81E+01	4.81E+00	6.49E+02

Time (Hour)	A.47	A.48	A.49	A.50
1.67E-02	5.48E+00	1.81E+01	-5.74E-01	1.89E+01
2.78E-01	5.32E+00	1.79E+01	-5.67E-01	1.86E+01
5.56E-01	5.24E+00	1.76E+01	-5.59E-01	1.84E+01
0.00E+00	5.25E+00	1.73E+01	-5.51E-01	1.81E+01
1.11E+00	5.33E+00	1.71E+01	-5.42E-01	1.79E+01
1.39E+00	5.49E+00	1.68E+01	-5.33E-01	1.77E+01
1.94E+00	5.99E+00	1.62E+01	-5.15E-01	1.73E+01
2.78E+00	7.08E+00	1.53E+01	-4.86E-01	1.69E+01
4.17E+00	9.50E+00	1.37E+01	-4.36E-01	1.67E+01
5.56E+00	1.24E+01	1.22E+01	-3.87E-01	1.74E+01
8.33E+00	1.90E+01	9.61E+00	-3.05E-01	2.13E+01
1.11E+01	2.60E+01	7.84E+00	-2.49E-01	2.72E+01
1.39E+01	3.24E+01	6.87E+00	-2.18E-01	3.31E+01
1.67E+01	3.70E+01	6.46E+00	-2.05E-01	3.76E+01
1.94E+01	3.98E+01	6.31E+00	-2.00E-01	4.03E+01
2.22E+01	4.12E+01	6.26E+00	-1.99E-01	4.17E+01

A.51	A.52	A.53
1.64E-04	-4.37E-04	4.67E-04

Time (Hour)	A.54			A.55
1.67E-02	-6.98E+01			6.98E+01
2.78E-01	-6.89E+01			6.89E+01
5.56E-01	-6.79E+01			6.79E+01
0.00E+00	-6.70E+01			6.70E+01
1.11E+00	-6.61E+01			6.61E+01
1.39E+00	-6.53E+01			6.53E+01
1.94E+00	-6.39E+01			6.39E+01
2.78E+00	-6.24E+01			6.24E+01
4.17E+00	-6.19E+01			6.19E+01
5.56E+00	-6.45E+01			6.45E+01
8.33E+00	-7.91E+01			7.91E+01
1.11E+01	-1.01E+02			1.01E+02
1.39E+01	-1.24E+02			1.24E+02
1.67E+01	-1.41E+02			1.41E+02
1.94E+01	-1.51E+02			1.51E+02
2.22E+01	-1.56E+02			1.56E+02
Time (Hour)	A.56	A.57	A.58	A.59
1.67E-02	3.70E-02	-1.15E-05	-3.69E-03	3.72E-02
2.78E-01	3.70E-02	-1.92E-04	-3.51E-03	3.72E-02
5.56E-01	3.70E-02	-3.85E-04	-3.32E-03	3.72E-02
0.00E+00	3.70E-02	-5.78E-04	-3.12E-03	3.72E-02
1.11E+00	3.70E-02	-7.68E-04	-2.93E-03	3.71E-02
1.39E+00	3.70E-02	-9.56E-04	-2.75E-03	3.71E-02
1.94E+00	3.70E-02	-1.32E-03	-2.38E-03	3.71E-02
2.78E+00	3.70E-02	-1.81E-03	-1.89E-03	3.71E-02
4.17E+00	3.70E-02	-2.48E-03	-1.22E-03	3.71E-02
5.56E+00	3.70E-02	-2.94E-03	-7.65E-04	3.71E-02
8.33E+00	3.70E-02	-3.41E-03	-2.94E-04	3.72E-02
1.11E+01	3.70E-02	-3.57E-03	-1.30E-04	3.72E-02
1.39E+01	3.70E-02	-3.63E-03	-7.70E-05	3.72E-02
1.67E+01	3.70E-02	-3.64E-03	-6.00E-05	3.72E-02
1.94E+01	3.70E-02	-3.65E-03	-5.47E-05	3.72E-02
2.22E+01	3.70E-02	-3.65E-03	-5.30E-05	3.72E-02

Time (Hour)	A.60	A.61	A.62	A.63	A.64
1.67E-02	-6.57E-03	7.67E+00	2.98E-01	7.84E-05	7.68E+00
2.78E-01	-6.90E-03	7.57E+00	2.48E-01	7.84E-05	7.57E+00
5.56E-01	-7.30E-03	7.46E+00	1.93E-01	7.84E-05	7.47E+00
0.00E+00	-7.75E-03	7.37E+00	1.37E-01	7.84E-05	7.37E+00
1.11E+00	-8.26E-03	7.27E+00	7.92E-02	7.85E-05	7.28E+00
1.39E+00	-8.82E-03	7.19E+00	2.02E-02	7.85E-05	7.19E+00
1.94E+00	-1.02E-02	7.04E+00	-1.02E-01	7.86E-05	7.04E+00
2.78E+00	-1.28E-02	6.88E+00	-2.96E-01	7.87E-05	6.88E+00
4.17E+00	-1.99E-02	6.83E+00	-6.58E-01	7.90E-05	6.87E+00
5.56E+00	-3.19E-02	7.15E+00	-1.10E+00	7.94E-05	7.23E+00
8.33E+00	-8.36E-02	8.83E+00	-2.41E+00	8.02E-05	9.16E+00
1.11E+01	-1.90E-01	1.14E+01	-4.28E+00	8.11E-05	1.22E+01
1.39E+01	-3.24E-01	1.40E+01	-6.19E+00	8.18E-05	1.53E+01
1.67E+01	-4.16E-01	1.60E+01	-7.57E+00	8.21E-05	1.77E+01
1.94E+01	-4.58E-01	1.72E+01	-8.34E+00	8.23E-05	1.91E+01
2.22E+01	-4.73E-01	1.78E+01	-8.70E+00	8.23E-05	1.98E+01

Time (Hour)	A.65	A.66	A.67	A.68(ω_α)	α	% Difference
1.67E-02	2.06E-05	7.44E-07	-1.97E-08	2.07E-05	3.78E-05	5.46E+01
2.78E-01	1.22E-06	4.50E-08	-7.14E-11	1.22E-06	2.29E-06	5.35E+01
5.56E-01	6.02E-07	2.27E-08	-1.80E-11	6.03E-07	1.15E-06	5.23E+01
0.00E+00	3.96E-07	1.53E-08	-8.08E-12	3.96E-07	7.76E-07	5.11E+01
1.11E+00	2.93E-07	1.16E-08	-4.59E-12	2.94E-07	5.87E-07	5.00E+01
1.39E+00	2.32E-07	9.34E-09	-2.97E-12	2.32E-07	4.74E-07	4.89E+01
1.94E+00	1.62E-07	6.81E-09	-1.54E-12	1.62E-07	3.46E-07	4.69E+01
2.78E+00	1.11E-07	4.93E-09	-7.83E-13	1.11E-07	2.50E-07	4.44E+01
4.17E+00	7.38E-08	3.49E-09	-3.69E-13	7.39E-08	1.77E-07	4.17E+01
5.56E+00	5.83E-08	2.78E-09	-2.21E-13	5.84E-08	1.41E-07	4.13E+01
8.33E+00	4.92E-08	2.09E-09	-1.10E-13	4.93E-08	1.06E-07	4.65E+01
1.11E+01	4.92E-08	1.72E-09	-6.81E-14	4.92E-08	8.71E-08	5.64E+01
1.39E+01	4.94E-08	1.45E-09	-4.61E-14	4.94E-08	7.38E-08	6.70E+01
1.67E+01	4.76E-08	1.24E-09	-3.29E-14	4.76E-08	6.31E-08	7.54E+01
1.94E+01	4.40E-08	1.08E-09	-2.44E-14	4.40E-08	5.46E-08	8.06E+01
2.22E+01	3.99E-08	9.44E-10	-1.87E-14	3.99E-08	4.80E-08	8.33E+01

Cooling from $75^{o}C$

Time (Hour)	A.18	A.19	A.20	A.21	A.22	A.23	A.24	A.25
1.67E-02	1.38E-05	2.09E-03	1.23E-03	-1.23E-04	6.42E-02	-2.38E-04	-1.36E-11	6.42E-02
2.78E-01	1.23E-05	1.85E-03	1.23E-03	-1.23E-04	5.69E-02	-2.11E-04	-1.21E-11	5.70E-02
5.56E-01	1.08E-05	1.64E-03	1.23E-03	-1.23E-04	5.03E-02	-1.87E-04	-1.06E-11	5.03E-02
8.33E-01	9.61E-06	1.45E-03	1.23E-03	-1.23E-04	4.45E-02	-1.65E-04	-9.43E-12	4.46E-02
1.11E+00	8.54E-06	1.29E-03	1.23E-03	-1.23E-04	3.96E-02	-1.47E-04	-8.38E-12	3.96E-02
1.39E+00	7.61E-06	1.15E-03	1.23E-03	-1.23E-04	3.53E-02	-1.31E-04	-7.47E-12	3.53E-02
1.94E+00	6.11E-06	9.22E-04	1.23E-03	-1.23E-04	2.83E-02	-1.05E-04	-5.99E-12	2.84E-02
2.78E+00	4.50E-06	6.79E-04	1.23E-03	-1.23E-04	2.08E-02	-7.74E-05	-4.41E-12	2.09E-02
4.17E+00	2.85E-06	4.30E-04	1.23E-03	-1.23E-04	1.32E-02	-4.91E-05	-2.80E-12	1.33E-02
5.56E+00	1.91E-06	2.88E-04	1.23E-03	-1.23E-04	8.84E-03	-3.28E-05	-1.87E-12	8.93E-03
8.33E+00	9.52E-07	1.44E-04	1.23E-03	-1.23E-04	4.41E-03	-1.64E-05	-9.34E-13	4.58E-03
1.11E+01	5.48E-07	8.27E-05	1.23E-03	-1.23E-04	2.54E-03	-9.43E-06	-5.37E-13	2.82E-03
1.39E+01	3.75E-07	5.67E-05	1.23E-03	-1.23E-04	1.74E-03	-6.46E-06	-3.68E-13	2.13E-03
1.67E+01	3.03E-07	4.58E-05	1.23E-03	-1.23E-04	1.41E-03	-5.22E-06	-2.98E-13	1.87E-03
1.94E+01	2.74E-07	4.13E-05	1.23E-03	-1.23E-04	1.27E-03	-4.71E-06	-2.68E-13	1.77E-03
2.22E+01	2.62E-07	3.95E-05	1.23E-03	-1.23E-04	1.21E-03	-4.50E-06	-2.57E-13	1.73E-03

Time (Hour)	A.26	A.27	A.28	A.29	A.30
1.67E-02	7.16E-06	-1.85E-05	1.75E-03	-4.22E-04	1.80E-03
2.78E-01	6.81E-06	-1.76E-05	1.55E-03	-4.02E-04	1.60E-03
5.56E-01	6.43E-06	-1.66E-05	1.37E-03	-3.79E-04	1.42E-03
0.00E+00	6.05E-06	-1.56E-05	1.21E-03	-3.57E-04	1.27E-03
1.11E+00	5.67E-06	-1.47E-05	1.08E-03	-3.34E-04	1.13E-03
1.39E+00	5.29E-06	-1.37E-05	9.62E-04	-3.12E-04	1.01E-03
1.94E+00	4.56E-06	-1.18E-05	7.72E-04	-2.69E-04	8.18E-04
2.78E+00	3.55E-06	-9.16E-06	5.69E-04	-2.09E-04	6.06E-04
4.17E+00	2.20E-06	-5.69E-06	3.62E-04	-1.30E-04	3.84E-04
5.56E+00	1.30E-06	-3.37E-06	2.43E-04	-7.69E-05	2.55E-04
8.33E+00	4.51E-07	-1.17E-06	1.25E-04	-2.66E-05	1.28E-04
1.11E+01	1.89E-07	-4.89E-07	7.69E-05	-1.12E-05	7.77E-05
1.39E+01	1.14E-07	-2.95E-07	5.81E-05	-6.73E-06	5.85E-05
1.67E+01	9.30E-08	-2.40E-07	5.10E-05	-5.49E-06	5.13E-05
1.94E+01	8.71E-08	-2.25E-07	4.82E-05	-5.14E-06	4.85E-05
2.22E+01	8.55E-08	-2.21E-07	4.71E-05	-5.04E-06	4.74E-05

Time (Hour)	A.31	A.32	A.33				A.34
1.67E-02	1.54E-02	2.15E-06	6.66E-01				6.66E-01
2.78E-01	1.52E-02	2.12E-06	6.16E-01				6.16E-01
5.56E-01	1.50E-02	2.09E-06	5.70E-01				5.70E-01
0.00E+00	1.47E-02	2.06E-06	5.31E-01				5.31E-01
1.11E+00	1.45E-02	2.03E-06	4.98E-01				4.98E-01
1.39E+00	1.42E-02	1.99E-06	4.70E-01				4.70E-01
1.94E+00	1.37E-02	1.92E-06	4.25E-01				4.25E-01
2.78E+00	1.29E-02	1.80E-06	3.80E-01				3.80E-01
4.17E+00	1.14E-02	1.60E-06	3.44E-01				3.45E-01
5.56E+00	1.00E-02	1.40E-06	3.39E-01				3.39E-01
8.33E+00	7.70E-03	1.08E-06	3.75E-01				3.76E-01
1.11E+01	6.19E-03	8.66E-07	4.39E-01				4.39E-01
1.39E+01	5.46E-03	7.63E-07	4.83E-01				4.83E-01
1.67E+01	5.19E-03	7.25E-07	4.93E-01				4.93E-01
1.94E+01	5.10E-03	7.13E-07	4.89E-01				4.89E-01
2.22E+01	5.08E-03	7.10E-07	4.85E-01				4.85E-01
Time (Hour)	A.35	A.36	A.37	A.38	A.39	A.40	A.41
1.67E-02	1.20E+03	7.33E+01	6.06E+02	-6.06E+01	-1.27E+02	3.75E+02	1.41E+03
2.78E-01	9.86E+02	6.51E+01	5.99E+02	-5.99E+01	-1.11E+02	3.28E+02	1.21E+03
5.56E-01	8.06E+02	5.75E+01	5.90E+02	-5.90E+01	-9.69E+01	2.86E+02	1.05E+03
0.00E+00	6.66E+02	5.09E+01	5.81E+02	-5.81E+01	-8.45E+01	2.50E+02	9.25E+02
1.11E+00	5.54E+02	4.52E+01	5.72E+02	-5.72E+01	-7.39E+01	2.18E+02	8.33E+02
1.39E+00	4.66E+02	4.03E+01	5.62E+02	-5.62E+01	-6.47E+01	1.91E+02	7.61E+02
1.94E+00	3.38E+02	3.24E+01	5.42E+02	-5.42E+01	-5.00E+01	1.48E+02	6.60E+02
2.78E+00	2.23E+02	2.38E+01	5.09E+02	-5.09E+01	-3.46E+01	1.02E+02	5.69E+02
4.17E+00	1.28E+02	1.51E+01	4.52E+02	-4.52E+01	-1.95E+01	5.75E+01	4.76E+02
5.56E+00	8.42E+01	1.01E+01	3.96E+02	-3.96E+01	-1.14E+01	3.37E+01	4.09E+02
8.33E+00	4.66E+01	5.04E+00	3.04E+02	-3.04E+01	-4.37E+00	1.29E+01	3.09E+02
1.11E+01	3.13E+01	2.90E+00	2.45E+02	-2.45E+01	-2.03E+00	5.98E+00	2.48E+02
1.39E+01	2.36E+01	1.99E+00	2.15E+02	-2.15E+01	-1.22E+00	3.61E+00	2.18E+02
1.67E+01	1.95E+01	1.61E+00	2.05E+02	-2.05E+01	-9.39E-01	2.77E+00	2.07E+02
1.94E+01	1.75E+01	1.45E+00	2.01E+02	-2.01E+01	-8.33E-01	2.46E+00	2.03E+02
2.22E+01	1.65E+01	1.39E+00	2.00E+02	-2.00E+01	-7.93E-01	2.34E+00	2.02E+02

Time (Hour)	A.42	A.43	A.44	A.45	A.46
1.67E-02	8.71E+01	-7.34E-01	-3.94E+00	3.94E-01	8.72E+01
2.78E-01	8.44E+01	-7.78E-01	-4.70E+00	4.70E-01	8.45E+01
5.56E-01	8.28E+01	-8.20E-01	-5.62E+00	5.62E-01	8.30E+01
0.00E+00	8.26E+01	-8.57E-01	-6.63E+00	6.63E-01	8.29E+01
1.11E+00	8.36E+01	-8.90E-01	-7.74E+00	7.74E-01	8.40E+01
1.39E+00	8.57E+01	-9.15E-01	-8.93E+00	8.93E-01	8.62E+01
1.94E+00	9.27E+01	-9.46E-01	-1.15E+01	1.15E+00	9.35E+01
2.78E+00	1.08E+02	-9.40E-01	-1.55E+01	1.55E+00	1.10E+02
4.17E+00	1.43E+02	-8.16E-01	-2.13E+01	2.13E+00	1.45E+02
5.56E+00	1.84E+02	-6.34E-01	-2.47E+01	2.47E+00	1.85E+02
8.33E+00	2.79E+02	-3.37E-01	-2.63E+01	2.63E+00	2.80E+02
1.11E+01	3.88E+02	-1.98E-01	-2.68E+01	2.68E+00	3.89E+02
1.39E+01	4.98E+02	-1.53E-01	-3.04E+01	3.04E+00	4.99E+02
1.67E+01	5.85E+02	-1.47E-01	-3.60E+01	3.60E+00	5.86E+02
1.94E+01	6.37E+02	-1.50E-01	-4.08E+01	4.08E+00	6.38E+02
2.22E+01	6.63E+02	-1.54E-01	-4.36E+01	4.36E+00	6.65E+02

Time (Hour)	A.47	A.48	A.49	A.50
1.67E-02	5.54E+00	1.80E+01	-5.73E-01	1.89E+01
2.78E-01	5.37E+00	1.78E+01	-5.66E-01	1.86E+01
5.56E-01	5.27E+00	1.76E+01	-5.58E-01	1.84E+01
0.00E+00	5.26E+00	1.73E+01	-5.49E-01	1.81E+01
1.11E+00	5.33E+00	1.70E+01	-5.41E-01	1.79E+01
1.39E+00	5.47E+00	1.67E+01	-5.31E-01	1.76E+01
1.94E+00	5.93E+00	1.61E+01	-5.12E-01	1.72E+01
2.78E+00	6.96E+00	1.51E+01	-4.81E-01	1.67E+01
4.17E+00	9.19E+00	1.34E+01	-4.27E-01	1.63E+01
5.56E+00	1.18E+01	1.18E+01	-3.74E-01	1.67E+01
8.33E+00	1.78E+01	9.04E+00	-2.87E-01	1.99E+01
1.11E+01	2.47E+01	7.28E+00	-2.31E-01	2.58E+01
1.39E+01	3.17E+01	6.41E+00	-2.04E-01	3.23E+01
1.67E+01	3.72E+01	6.09E+00	-1.93E-01	3.77E+01
1.94E+01	4.05E+01	5.99E+00	-1.90E-01	4.10E+01
2.22E+01	4.22E+01	5.97E+00	-1.89E-01	4.26E+01

A.51	A.52	A.53
1.64E-04	-4.37E-04	4.67E-04

Time (Hour)	A.54			A.55
1.67E-02	-6.98E+01			6.98E+01
2.78E-01	-6.88E+01			6.88E+01
5.56E-01	-6.78E+01			6.78E+01
0.00E+00	-6.69E+01			6.69E+01
1.11E+00	-6.60E+01			6.60E+01
1.39E+00	-6.51E+01			6.51E+01
1.94E+00	-6.36E+01			6.36E+01
2.78E+00	-6.17E+01			6.17E+01
4.17E+00	-6.03E+01			6.03E+01
5.56E+00	-6.19E+01			6.19E+01
8.33E+00	-7.43E+01			7.43E+01
1.11E+01	-9.63E+01			9.63E+01
1.39E+01	-1.21E+02			1.21E+02
1.67E+01	-1.42E+02			1.42E+02
1.94E+01	-1.54E+02			1.54E+02
2.22E+01	-1.60E+02			1.60E+02
Time (Hour)	A.56	A.57	A.58	A.59
1.67E-02	3.73E-02	-1.15E-05	-3.72E-03	3.75E-02
2.78E-01	3.73E-02	-1.93E-04	-3.54E-03	3.75E-02
5.56E-01	3.73E-02	-3.89E-04	-3.34E-03	3.75E-02
0.00E+00	3.73E-02	-5.87E-04	-3.14E-03	3.75E-02
1.11E+00	3.73E-02	-7.85E-04	-2.95E-03	3.74E-02
1.39E+00	3.73E-02	-9.82E-04	-2.75E-03	3.74E-02
1.94E+00	3.73E-02	-1.36E-03	-2.37E-03	3.74E-02
2.78E+00	3.73E-02	-1.89E-03	-1.84E-03	3.74E-02
4.17E+00	3.73E-02	-2.59E-03	-1.14E-03	3.74E-02
5.56E+00	3.73E-02	-3.05E-03	-6.77E-04	3.74E-02
8.33E+00	3.73E-02	-3.50E-03	-2.34E-04	3.75E-02
1.11E+01	3.73E-02	-3.63E-03	-9.83E-05	3.75E-02
1.39E+01	3.73E-02	-3.67E-03	-5.93E-05	3.75E-02
1.67E+01	3.73E-02	-3.68E-03	-4.83E-05	3.75E-02
1.94E+01	3.73E-02	-3.69E-03	-4.53E-05	3.75E-02
2.22E+01	3.73E-02	-3.69E-03	-4.44E-05	3.75E-02

Time (Hour)	A.60	A.61	A.62	A.63	A.64
1.67E-02	-6.62E-03	7.67E+00	3.00E-01	7.84E-05	7.67E+00
2.78E-01	-6.96E-03	7.56E+00	2.50E-01	7.84E-05	7.56E+00
5.56E-01	-7.36E-03	7.45E+00	1.95E-01	7.84E-05	7.46E+00
0.00E+00	-7.83E-03	7.35E+00	1.37E-01	7.85E-05	7.35E+00
1.11E+00	-8.35E-03	7.26E+00	7.77E-02	7.85E-05	7.26E+00
1.39E+00	-8.95E-03	7.16E+00	1.64E-02	7.85E-05	7.16E+00
1.94E+00	-1.04E-02	7.00E+00	-1.12E-01	7.86E-05	7.00E+00
2.78E+00	-1.34E-02	6.80E+00	-3.18E-01	7.88E-05	6.81E+00
4.17E+00	-2.16E-02	6.67E+00	-7.03E-01	7.91E-05	6.71E+00
5.56E+00	-3.66E-02	6.86E+00	-1.17E+00	7.95E-05	6.96E+00
8.33E+00	-1.07E-01	8.31E+00	-2.51E+00	8.04E-05	8.68E+00
1.11E+01	-2.57E-01	1.09E+01	-4.47E+00	8.15E-05	1.18E+01
1.39E+01	-4.29E-01	1.38E+01	-6.54E+00	8.22E-05	1.52E+01
1.67E+01	-5.27E-01	1.61E+01	-8.08E+00	8.25E-05	1.80E+01
1.94E+01	-5.63E-01	1.75E+01	-8.95E+00	8.26E-05	1.97E+01
2.22E+01	-5.74E-01	1.82E+01	-9.35E+00	8.26E-05	2.05E+01

Time (Hour)	A.65	A.66	A.67	A.68(ω_α)	α	% Difference
1.67E-02	2.06E-05	7.44E-07	-1.97E-08	2.06E-05	3.78E-05	5.46E+01
2.78E-01	1.22E-06	4.50E-08	-7.14E-11	1.22E-06	2.29E-06	5.34E+01
5.56E-01	6.01E-07	2.27E-08	-1.80E-11	6.02E-07	1.15E-06	5.22E+01
0.00E+00	3.95E-07	1.53E-08	-8.08E-12	3.96E-07	7.76E-07	5.10E+01
1.11E+00	2.93E-07	1.16E-08	-4.59E-12	2.93E-07	5.87E-07	4.99E+01
1.39E+00	2.31E-07	9.35E-09	-2.97E-12	2.31E-07	4.75E-07	4.87E+01
1.94E+00	1.61E-07	6.82E-09	-1.55E-12	1.61E-07	3.47E-07	4.66E+01
2.78E+00	1.10E-07	4.95E-09	-7.86E-13	1.10E-07	2.52E-07	4.37E+01
4.17E+00	7.21E-08	3.52E-09	-3.73E-13	7.22E-08	1.79E-07	4.03E+01
5.56E+00	5.61E-08	2.83E-09	-2.25E-13	5.62E-08	1.44E-07	3.91E+01
8.33E+00	4.67E-08	2.14E-09	-1.13E-13	4.67E-08	1.09E-07	4.29E+01
1.11E+01	4.74E-08	1.77E-09	-7.02E-14	4.74E-08	8.99E-08	5.28E+01
1.39E+01	4.92E-08	1.49E-09	-4.74E-14	4.92E-08	7.59E-08	6.48E+01
1.67E+01	4.85E-08	1.27E-09	-3.37E-14	4.85E-08	6.46E-08	7.50E+01
1.94E+01	4.54E-08	1.10E-09	-2.49E-14	4.54E-08	5.58E-08	8.14E+01
2.22E+01	4.14E-08	9.62E-10	-1.91E-14	4.14E-08	4.89E-08	8.46E+01

Cooling from $78\,^{o}C$

Time (Hour)	A.18	A.19	A.20	A.21	A.22	A.23	A.24	A.25
1.67E-02	1.38E-05	2.09E-03	1.23E-03	-1.23E-04	6.41E-02	-2.38E-04	-1.36E-11	6.41E-02
2.78E-01	1.22E-05	1.85E-03	1.23E-03	-1.23E-04	5.67E-02	-2.11E-04	-1.20E-11	5.67E-02
5.56E-01	1.08E-05	1.63E-03	1.23E-03	-1.23E-04	5.00E-02	-1.86E-04	-1.06E-11	5.00E-02
8.33E-01	9.53E-06	1.44E-03	1.23E-03	-1.23E-04	4.42E-02	-1.64E-04	-9.35E-12	4.42E-02
1.11E+00	8.46E-06	1.28E-03	1.23E-03	-1.23E-04	3.92E-02	-1.46E-04	-8.30E-12	3.93E-02
1.39E+00	7.54E-06	1.14E-03	1.23E-03	-1.23E-04	3.49E-02	-1.30E-04	-7.40E-12	3.50E-02
1.94E+00	6.05E-06	9.12E-04	1.23E-03	-1.23E-04	2.80E-02	-1.04E-04	-5.93E-12	2.81E-02
2.78E+00	4.45E-06	6.72E-04	1.23E-03	-1.23E-04	2.06E-02	-7.66E-05	-4.37E-12	2.07E-02
4.17E+00	2.84E-06	4.28E-04	1.23E-03	-1.23E-04	1.31E-02	-4.88E-05	-2.78E-12	1.32E-02
5.56E+00	1.91E-06	2.89E-04	1.23E-03	-1.23E-04	8.86E-03	-3.29E-05	-1.88E-12	8.95E-03
8.33E+00	9.73E-07	1.47E-04	1.23E-03	-1.23E-04	4.51E-03	-1.67E-05	-9.54E-13	4.68E-03
1.11E+01	5.64E-07	8.51E-05	1.23E-03	-1.23E-04	2.61E-03	-9.70E-06	-5.53E-13	2.89E-03
1.39E+01	3.82E-07	5.77E-05	1.23E-03	-1.23E-04	1.77E-03	-6.58E-06	-3.75E-13	2.16E-03
1.67E+01	3.04E-07	4.58E-05	1.23E-03	-1.23E-04	1.41E-03	-5.23E-06	-2.98E-13	1.87E-03
1.94E+01	2.70E-07	4.08E-05	1.23E-03	-1.23E-04	1.25E-03	-4.65E-06	-2.65E-13	1.76E-03
2.22E+01	2.56E-07	3.86E-05	1.23E-03	-1.23E-04	1.19E-03	-4.40E-06	-2.51E-13	1.71E-03
Time (Hour)	A.26	A.27	A.28	A.29				A.30
1.67E-02	8.35E-06	-2.16E-05	1.75E-03	-4.93E-04				1.81E-03
2.78E-01	8.00E-06	-2.07E-05	1.55E-03	-4.72E-04				1.62E-03
5.56E-01	7.61E-06	-1.97E-05	1.36E-03	-4.49E-04				1.43E-03
0.00E+00	7.22E-06	-1.87E-05	1.20E-03	-4.26E-04				1.28E-03
1.11E+00	6.82E-06	-1.76E-05	1.07E-03	-4.02E-04				1.14E-03
1.39E+00	6.43E-06	-1.66E-05	9.53E-04	-3.79E-04				1.03E-03
1.94E+00	5.67E-06	-1.46E-05	7.64E-04	-3.34E-04				8.34E-04
2.78E+00	4.59E-06	-1.19E-05	5.63E-04	-2.71E-04				6.25E-04
4.17E+00	3.11E-06	-8.03E-06	3.60E-04	-1.83E-04				4.04E-04
5.56E+00	2.07E-06	-5.34E-06	2.44E-04	-1.22E-04				2.73E-04
8.33E+00	1.01E-06	-2.61E-06	1.27E-04	-5.96E-05				1.41E-04
1.11E+01	6.56E-07	-1.70E-06	7.87E-05	-3.87E-05				8.77E-05
1.39E+01	5.46E-07	-1.41E-06	5.88E-05	-3.22E-05				6.71E-05
1.67E+01	5.13E-07	-1.33E-06	5.10E-05	-3.02E-05				5.93E-05
1.94E+01	5.03E-07	-1.30E-06	4.79E-05	-2.96E-05				5.63E-05
2.22E+01	5.00E-07	-1.29E-06	4.66E-05	-2.95E-05				5.52E-05

Time (Hour)	A.31	A.32	A.33				A.34
1.67E-02	1.60E-02	2.23E-06	5.98E-01				5.98E-01
2.78E-01	1.58E-02	2.21E-06	5.50E-01				5.51E-01
5.56E-01	1.56E-02	2.18E-06	5.07E-01				5.07E-01
0.00E+00	1.54E-02	2.15E-06	4.70E-01				4.70E-01
1.11E+00	1.52E-02	2.12E-06	4.38E-01				4.39E-01
1.39E+00	1.50E-02	2.09E-06	4.11E-01				4.11E-01
1.94E+00	1.45E-02	2.03E-06	3.68E-01				3.68E-01
2.78E+00	1.37E-02	1.92E-06	3.23E-01				3.23E-01
4.17E+00	1.25E-02	1.74E-06	2.79E-01				2.80E-01
5.56E+00	1.13E-02	1.57E-06	2.56E-01				2.56E-01
8.33E+00	9.42E-03	1.32E-06	2.26E-01				2.26E-01
1.11E+01	8.45E-03	1.18E-06	1.95E-01				1.95E-01
1.39E+01	8.07E-03	1.13E-06	1.71E-01				1.71E-01
1.67E+01	7.95E-03	1.11E-06	1.58E-01				1.59E-01
1.94E+01	7.91E-03	1.11E-06	1.53E-01				1.53E-01
2.22E+01	7.90E-03	1.10E-06	1.50E-01				1.51E-01
Time (Hour)	A.35	A.36	A.37	A.38	A.39	A.40	A.41
1.67E-02	1.08E+03	7.61E+01	6.30E+02	-6.30E+01	-1.32E+02	3.89E+02	1.32E+03
2.78E-01	8.78E+02	6.74E+01	6.23E+02	-6.23E+01	-1.15E+02	3.41E+02	1.14E+03
5.56E-01	7.13E+02	5.94E+01	6.16E+02	-6.16E+01	-1.00E+02	2.96E+02	9.96E+02
0.00E+00	5.84E+02	5.25E+01	6.08E+02	-6.08E+01	-8.76E+01	2.59E+02	8.90E+02
1.11E+00	4.84E+02	4.66E+01	5.99E+02	-5.99E+01	-7.67E+01	2.26E+02	8.10E+02
1.39E+00	4.04E+02	4.15E+01	5.90E+02	-5.90E+01	-6.73E+01	1.99E+02	7.49E+02
1.94E+00	2.90E+02	3.33E+01	5.72E+02	-5.72E+01	-5.23E+01	1.54E+02	6.65E+02
2.78E+00	1.87E+02	2.45E+01	5.43E+02	-5.43E+01	-3.65E+01	1.08E+02	5.88E+02
4.17E+00	1.03E+02	1.56E+01	4.92E+02	-4.92E+01	-2.11E+01	6.23E+01	5.10E+02
5.56E+00	6.39E+01	1.05E+01	4.45E+02	-4.45E+01	-1.29E+01	3.80E+01	4.53E+02
8.33E+00	2.87E+01	5.36E+00	3.72E+02	-3.72E+01	-5.47E+00	1.61E+01	3.75E+02
1.11E+01	1.43E+01	3.10E+00	3.34E+02	-3.34E+01	-2.84E+00	8.40E+00	3.36E+02
1.39E+01	8.53E+00	2.11E+00	3.19E+02	-3.19E+01	-1.84E+00	5.44E+00	3.20E+02
1.67E+01	6.28E+00	1.67E+00	3.14E+02	-3.14E+01	-1.44E+00	4.25E+00	3.15E+02
1.94E+01	5.39E+00	1.49E+00	3.12E+02	-3.12E+01	-1.27E+00	3.76E+00	3.14E+02
2.22E+01	5.02E+00	1.41E+00	3.12E+02	-3.12E+01	-1.21E+00	3.56E+00	3.13E+02

Time (Hour)	A.42	A.43	A.44	A.45	A.46
1.67E-02	8.18E+01	-8.92E-01	-4.80E+00	4.80E-01	8.19E+01
2.78E-01	7.98E+01	-9.54E-01	-5.80E+00	5.80E-01	8.01E+01
5.56E-01	7.93E+01	-1.02E+00	-7.02E+00	7.02E-01	7.96E+01
0.00E+00	8.00E+01	-1.08E+00	-8.40E+00	8.40E-01	8.05E+01
1.11E+00	8.21E+01	-1.13E+00	-9.94E+00	9.94E-01	8.27E+01
1.39E+00	8.52E+01	-1.18E+00	-1.16E+01	1.16E+00	8.61E+01
1.94E+00	9.44E+01	-1.26E+00	-1.54E+01	1.54E+00	9.56E+01
2.78E+00	1.13E+02	-1.31E+00	-2.19E+01	2.19E+00	1.15E+02
4.17E+00	1.54E+02	-1.26E+00	-3.31E+01	3.31E+00	1.58E+02
5.56E+00	2.03E+02	-1.13E+00	-4.37E+01	4.37E+00	2.08E+02
8.33E+00	3.31E+02	-9.05E-01	-6.91E+01	6.91E+00	3.38E+02
1.11E+01	5.11E+02	-9.10E-01	-1.20E+02	1.20E+01	5.25E+02
1.39E+01	7.19E+02	-1.07E+00	-2.07E+02	2.07E+01	7.48E+02
1.67E+01	8.91E+02	-1.24E+00	-3.04E+02	3.04E+01	9.42E+02
1.94E+01	9.97E+02	-1.36E+00	-3.75E+02	3.75E+01	1.07E+03
2.22E+01	1.05E+03	-1.43E+00	-4.14E+02	4.14E+01	1.13E+03

Time (Hour)	A.47	A.48	A.49	A.50
1.67E-02	5.20E+00	1.88E+01	-5.96E-01	1.95E+01
2.78E-01	5.08E+00	1.86E+01	-5.89E-01	1.92E+01
5.56E-01	5.05E+00	1.83E+01	-5.82E-01	1.90E+01
0.00E+00	5.11E+00	1.81E+01	-5.74E-01	1.88E+01
1.11E+00	5.25E+00	1.78E+01	-5.66E-01	1.86E+01
1.39E+00	5.46E+00	1.76E+01	-5.58E-01	1.84E+01
1.94E+00	6.07E+00	1.70E+01	-5.40E-01	1.81E+01
2.78E+00	7.33E+00	1.61E+01	-5.13E-01	1.77E+01
4.17E+00	1.00E+01	1.46E+01	-4.65E-01	1.78E+01
5.56E+00	1.32E+01	1.32E+01	-4.20E-01	1.87E+01
8.33E+00	2.15E+01	1.11E+01	-3.51E-01	2.42E+01
1.11E+01	3.33E+01	9.93E+00	-3.15E-01	3.48E+01
1.39E+01	4.75E+01	9.49E+00	-3.01E-01	4.85E+01
1.67E+01	5.98E+01	9.34E+00	-2.96E-01	6.05E+01
1.94E+01	6.77E+01	9.29E+00	-2.95E-01	6.83E+01
2.22E+01	7.17E+01	9.28E+00	-2.95E-01	7.23E+01

A.51	A.52	A.53
1.64E-04	-4.37E-04	4.67E-04

Time (Hour)	A.54			A.55
1.67E-02	-7.19E+01			7.19E+01
2.78E-01	-7.11E+01			7.11E+01
5.56E-01	-7.02E+01			7.02E+01
0.00E+00	-6.95E+01			6.95E+01
1.11E+00	-6.87E+01			6.87E+01
1.39E+00	-6.80E+01			6.80E+01
1.94E+00	-6.68E+01			6.68E+01
2.78E+00	-6.56E+01			6.56E+01
4.17E+00	-6.57E+01			6.57E+01
5.56E+00	-6.93E+01			6.93E+01
8.33E+00	-8.97E+01			8.97E+01
1.11E+01	-1.29E+02			1.29E+02
1.39E+01	-1.80E+02			1.80E+02
1.67E+01	-2.25E+02			2.25E+02
1.94E+01	-2.54E+02			2.54E+02
2.22E+01	-2.69E+02			2.69E+02
Time (Hour)	A.56	A.57	A.58	A.59
1.67E-02	3.20E-02	-8.62E-06	-3.19E-03	3.21E-02
2.78E-01	3.20E-02	-1.45E-04	-3.05E-03	3.21E-02
5.56E-01	3.20E-02	-2.93E-04	-2.91E-03	3.21E-02
0.00E+00	3.20E-02	-4.43E-04	-2.76E-03	3.21E-02
1.11E+00	3.20E-02	-5.93E-04	-2.61E-03	3.21E-02
1.39E+00	3.20E-02	-7.42E-04	-2.46E-03	3.21E-02
1.94E+00	3.20E-02	-1.04E-03	-2.16E-03	3.21E-02
2.78E+00	3.20E-02	-1.45E-03	-1.75E-03	3.21E-02
4.17E+00	3.20E-02	-2.01E-03	-1.19E-03	3.21E-02
5.56E+00	3.20E-02	-2.41E-03	-7.90E-04	3.21E-02
8.33E+00	3.20E-02	-2.81E-03	-3.86E-04	3.21E-02
1.11E+01	3.20E-02	-2.95E-03	-2.51E-04	3.21E-02
1.39E+01	3.20E-02	-2.99E-03	-2.09E-04	3.21E-02
1.67E+01	3.20E-02	-3.00E-03	-1.96E-04	3.21E-02
1.94E+01	3.20E-02	-3.01E-03	-1.92E-04	3.21E-02
2.22E+01	3.20E-02	-3.01E-03	-1.91E-04	3.21E-02

Time (Hour)	A.60	A.61	A.62	A.63	A.64
1.67E-02	-5.67E-03	7.90E+00	2.66E-01	7.83E-05	7.90E+00
2.78E-01	-5.92E-03	7.81E+00	2.21E-01	7.83E-05	7.81E+00
5.56E-01	-6.22E-03	7.72E+00	1.72E-01	7.83E-05	7.72E+00
0.00E+00	-6.56E-03	7.63E+00	1.21E-01	7.84E-05	7.63E+00
1.11E+00	-6.93E-03	7.55E+00	6.81E-02	7.84E-05	7.55E+00
1.39E+00	-7.36E-03	7.48E+00	1.35E-02	7.84E-05	7.48E+00
1.94E+00	-8.36E-03	7.35E+00	-1.01E-01	7.85E-05	7.35E+00
2.78E+00	-1.03E-02	7.22E+00	-2.85E-01	7.86E-05	7.23E+00
4.17E+00	-1.53E-02	7.25E+00	-6.33E-01	7.88E-05	7.28E+00
5.56E+00	-2.30E-02	7.66E+00	-1.05E+00	7.91E-05	7.73E+00
8.33E+00	-4.73E-02	9.97E+00	-2.25E+00	7.97E-05	1.02E+01
1.11E+01	-7.32E-02	1.44E+01	-4.03E+00	8.01E-05	1.50E+01
1.39E+01	-8.81E-02	2.01E+01	-6.09E+00	8.02E-05	2.10E+01
1.67E+01	-9.39E-02	2.52E+01	-7.81E+00	8.03E-05	2.64E+01
1.94E+01	-9.58E-02	2.84E+01	-8.89E+00	8.03E-05	2.98E+01
2.22E+01	-9.63E-02	3.01E+01	-9.44E+00	8.03E-05	3.15E+01

Time (Hour)	A.65	A.66	A.67	A.68(ω_α)	α	% Difference
1.67E-02	2.12E-05	7.49E-07	-1.98E-08	2.13E-05	3.81E-05	5.58E+01
2.78E-01	1.26E-06	4.53E-08	-7.18E-11	1.26E-06	2.30E-06	5.48E+01
5.56E-01	6.22E-07	2.28E-08	-1.81E-11	6.23E-07	1.16E-06	5.38E+01
0.00E+00	4.10E-07	1.53E-08	-8.11E-12	4.11E-07	7.78E-07	5.28E+01
1.11E+00	3.04E-07	1.16E-08	-4.60E-12	3.05E-07	5.89E-07	5.18E+01
1.39E+00	2.41E-07	9.35E-09	-2.97E-12	2.41E-07	4.75E-07	5.08E+01
1.94E+00	1.69E-07	6.80E-09	-1.54E-12	1.70E-07	3.46E-07	4.90E+01
2.78E+00	1.17E-07	4.91E-09	-7.79E-13	1.17E-07	2.49E-07	4.68E+01
4.17E+00	7.82E-08	3.45E-09	-3.66E-13	7.83E-08	1.76E-07	4.46E+01
5.56E+00	6.24E-08	2.73E-09	-2.17E-13	6.24E-08	1.39E-07	4.49E+01
8.33E+00	5.49E-08	1.99E-09	-1.05E-13	5.50E-08	1.01E-07	5.43E+01
1.11E+01	6.04E-08	1.57E-09	-6.24E-14	6.04E-08	7.99E-08	7.56E+01
1.39E+01	6.79E-08	1.29E-09	-4.08E-14	6.79E-08	6.53E-08	1.04E+02
1.67E+01	7.09E-08	1.08E-09	-2.85E-14	7.09E-08	5.48E-08	1.29E+02
1.94E+01	6.86E-08	9.27E-10	-2.10E-14	6.86E-08	4.71E-08	1.46E+02
2.22E+01	6.36E-08	8.12E-10	-1.61E-14	6.36E-08	4.12E-08	1.54E+02

Cooling from $80\,^{o}C$

Time (Hour)	A.18	A.19	A.20	A.21	A.22	A.23	A.24	A.25
1.67E-02	1.37E-05	2.06E-03	1.23E-03	-1.23E-04	6.33E-02	-2.35E-04	-1.34E-11	6.34E-02
2.78E-01	1.22E-05	1.84E-03	1.23E-03	-1.23E-04	5.64E-02	-2.09E-04	-1.19E-11	5.64E-02
5.56E-01	1.08E-05	1.62E-03	1.23E-03	-1.23E-04	4.99E-02	-1.85E-04	-1.06E-11	4.99E-02
8.33E-01	9.54E-06	1.44E-03	1.23E-03	-1.23E-04	4.42E-02	-1.64E-04	-9.36E-12	4.42E-02
1.11E+00	8.47E-06	1.28E-03	1.23E-03	-1.23E-04	3.93E-02	-1.46E-04	-8.31E-12	3.93E-02
1.39E+00	7.54E-06	1.14E-03	1.23E-03	-1.23E-04	3.49E-02	-1.30E-04	-7.39E-12	3.50E-02
1.94E+00	6.02E-06	9.08E-04	1.23E-03	-1.23E-04	2.79E-02	-1.04E-04	-5.90E-12	2.79E-02
2.78E+00	4.38E-06	6.62E-04	1.23E-03	-1.23E-04	2.03E-02	-7.54E-05	-4.30E-12	2.04E-02
4.17E+00	2.76E-06	4.16E-04	1.23E-03	-1.23E-04	1.28E-02	-4.75E-05	-2.71E-12	1.29E-02
5.56E+00	1.87E-06	2.82E-04	1.23E-03	-1.23E-04	8.65E-03	-3.21E-05	-1.83E-12	8.74E-03
8.33E+00	9.74E-07	1.47E-04	1.23E-03	-1.23E-04	4.51E-03	-1.68E-05	-9.55E-13	4.68E-03
1.11E+01	5.69E-07	8.58E-05	1.23E-03	-1.23E-04	2.64E-03	-9.79E-06	-5.58E-13	2.91E-03
1.39E+01	3.77E-07	5.69E-05	1.23E-03	-1.23E-04	1.75E-03	-6.49E-06	-3.70E-13	2.14E-03
1.67E+01	2.88E-07	4.34E-05	1.23E-03	-1.23E-04	1.33E-03	-4.95E-06	-2.82E-13	1.82E-03
1.94E+01	2.47E-07	3.73E-05	1.23E-03	-1.23E-04	1.14E-03	-4.25E-06	-2.42E-13	1.68E-03
2.22E+01	2.29E-07	3.45E-05	1.23E-03	-1.23E-04	1.06E-03	-3.94E-06	-2.24E-13	1.63E-03

Time (Hour)	A.26	A.27	A.28	A.29	A.30
1.67E-02	8.13E-06	-2.10E-05	1.73E-03	-4.80E-04	1.79E-03
2.78E-01	7.84E-06	-2.02E-05	1.54E-03	-4.62E-04	1.60E-03
5.56E-01	7.51E-06	-1.94E-05	1.36E-03	-4.43E-04	1.43E-03
0.00E+00	7.17E-06	-1.85E-05	1.21E-03	-4.23E-04	1.28E-03
1.11E+00	6.82E-06	-1.76E-05	1.07E-03	-4.02E-04	1.14E-03
1.39E+00	6.47E-06	-1.67E-05	9.53E-04	-3.82E-04	1.03E-03
1.94E+00	5.76E-06	-1.49E-05	7.61E-04	-3.40E-04	8.33E-04
2.78E+00	4.72E-06	-1.22E-05	5.55E-04	-2.78E-04	6.21E-04
4.17E+00	3.21E-06	-8.30E-06	3.50E-04	-1.89E-04	3.98E-04
5.56E+00	2.12E-06	-5.47E-06	2.38E-04	-1.25E-04	2.69E-04
8.33E+00	1.00E-06	-2.59E-06	1.27E-04	-5.92E-05	1.41E-04
1.11E+01	6.46E-07	-1.67E-06	7.93E-05	-3.81E-05	8.80E-05
1.39E+01	5.42E-07	-1.40E-06	5.83E-05	-3.20E-05	6.65E-05
1.67E+01	5.13E-07	-1.33E-06	4.95E-05	-3.03E-05	5.80E-05
1.94E+01	5.05E-07	-1.30E-06	4.59E-05	-2.98E-05	5.47E-05
2.22E+01	5.03E-07	-1.30E-06	4.43E-05	-2.96E-05	5.33E-05

Time (Hour)	A.31	A.32	A.33				A.34
1.67E-02	1.59E-02	2.22E-06	6.02E-01				6.03E-01
2.78E-01	1.57E-02	2.20E-06	5.55E-01				5.55E-01
5.56E-01	1.55E-02	2.17E-06	5.11E-01				5.11E-01
0.00E+00	1.54E-02	2.15E-06	4.72E-01				4.72E-01
1.11E+00	1.52E-02	2.12E-06	4.39E-01				4.39E-01
1.39E+00	1.50E-02	2.09E-06	4.10E-01				4.10E-01
1.94E+00	1.45E-02	2.03E-06	3.63E-01				3.63E-01
2.78E+00	1.38E-02	1.93E-06	3.14E-01				3.14E-01
4.17E+00	1.26E-02	1.76E-06	2.69E-01				2.69E-01
5.56E+00	1.13E-02	1.58E-06	2.48E-01				2.48E-01
8.33E+00	9.40E-03	1.31E-06	2.27E-01				2.27E-01
1.11E+01	8.42E-03	1.18E-06	1.98E-01				1.98E-01
1.39E+01	8.06E-03	1.13E-06	1.70E-01				1.71E-01
1.67E+01	7.95E-03	1.11E-06	1.55E-01				1.55E-01
1.94E+01	7.92E-03	1.11E-06	1.48E-01				1.48E-01
2.22E+01	7.91E-03	1.11E-06	1.45E-01				1.45E-01
Time (Hour)	A.35	A.36	A.37	A.38	A.39	A.40	A.41
1.67E-02	1.07E+03	7.47E+01	6.26E+02	-6.26E+01	-1.29E+02	3.82E+02	1.31E+03
2.78E-01	8.80E+02	6.65E+01	6.20E+02	-6.20E+01	-1.14E+02	3.37E+02	1.14E+03
5.56E-01	7.16E+02	5.89E+01	6.14E+02	-6.14E+01	-9.99E+01	2.95E+02	9.97E+02
0.00E+00	5.87E+02	5.22E+01	6.07E+02	-6.07E+01	-8.75E+01	2.58E+02	8.91E+02
1.11E+00	4.85E+02	4.63E+01	5.99E+02	-5.99E+01	-7.68E+01	2.27E+02	8.10E+02
1.39E+00	4.03E+02	4.12E+01	5.91E+02	-5.91E+01	-6.74E+01	1.99E+02	7.49E+02
1.94E+00	2.85E+02	3.29E+01	5.74E+02	-5.74E+01	-5.22E+01	1.54E+02	6.65E+02
2.78E+00	1.80E+02	2.40E+01	5.46E+02	-5.46E+01	-3.62E+01	1.07E+02	5.89E+02
4.17E+00	9.68E+01	1.51E+01	4.96E+02	-4.96E+01	-2.07E+01	6.11E+01	5.12E+02
5.56E+00	6.04E+01	1.02E+01	4.47E+02	-4.47E+01	-1.26E+01	3.73E+01	4.55E+02
8.33E+00	2.88E+01	5.33E+00	3.71E+02	-3.71E+01	-5.46E+00	1.61E+01	3.75E+02
1.11E+01	1.47E+01	3.11E+00	3.32E+02	-3.32E+01	-2.86E+00	8.44E+00	3.35E+02
1.39E+01	8.38E+00	2.06E+00	3.18E+02	-3.18E+01	-1.81E+00	5.35E+00	3.20E+02
1.67E+01	5.82E+00	1.57E+00	3.14E+02	-3.14E+01	-1.36E+00	4.03E+00	3.15E+02
1.94E+01	4.77E+00	1.35E+00	3.13E+02	-3.13E+01	-1.17E+00	3.45E+00	3.14E+02
2.22E+01	4.32E+00	1.25E+00	3.12E+02	-3.12E+01	-1.08E+00	3.19E+00	3.14E+02

Time (Hour)	A.42	A.43	A.44	A.45	A.46
1.67E-02	8.22E+01	-8.73E-01	-4.75E+00	4.75E-01	8.24E+01
2.78E-01	8.02E+01	-9.36E-01	-5.72E+00	5.72E-01	8.04E+01
5.56E-01	7.95E+01	-1.00E+00	-6.92E+00	6.92E-01	7.98E+01
0.00E+00	8.01E+01	-1.07E+00	-8.32E+00	8.32E-01	8.06E+01
1.11E+00	8.21E+01	-1.13E+00	-9.92E+00	9.92E-01	8.27E+01
1.39E+00	8.52E+01	-1.19E+00	-1.17E+01	1.17E+00	8.61E+01
1.94E+00	9.48E+01	-1.29E+00	-1.59E+01	1.59E+00	9.61E+01
2.78E+00	1.15E+02	-1.38E+00	-2.33E+01	2.33E+00	1.18E+02
4.17E+00	1.59E+02	-1.35E+00	-3.64E+01	3.64E+00	1.63E+02
5.56E+00	2.09E+02	-1.19E+00	-4.73E+01	4.73E+00	2.15E+02
8.33E+00	3.30E+02	-8.96E-01	-6.84E+01	6.84E+00	3.37E+02
1.11E+01	5.05E+02	-8.85E-01	-1.16E+02	1.16E+01	5.18E+02
1.39E+01	7.28E+02	-1.07E+00	-2.11E+02	2.11E+01	7.59E+02
1.67E+01	9.41E+02	-1.31E+00	-3.39E+02	3.39E+01	1.00E+03
1.94E+01	1.09E+03	-1.50E+00	-4.50E+02	4.50E+01	1.18E+03
2.22E+01	1.18E+03	-1.61E+00	-5.22E+02	5.22E+01	1.29E+03
Time (Hour)	A.47	A.48	A.49		A.50
1.67E-02	5.23E+00	1.86E+01	-5.92E-01		1.94E+01
2.78E-01	5.11E+00	1.85E+01	-5.86E-01		1.92E+01
5.56E-01	5.07E+00	1.83E+01	-5.80E-01		1.90E+01
0.00E+00	5.12E+00	1.81E+01	-5.73E-01		1.88E+01
1.11E+00	5.25E+00	1.78E+01	-5.66E-01		1.86E+01
1.39E+00	5.47E+00	1.76E+01	-5.59E-01		1.84E+01
1.94E+00	6.10E+00	1.71E+01	-5.43E-01		1.82E+01
2.78E+00	7.47E+00	1.63E+01	-5.16E-01		1.79E+01
4.17E+00	1.04E+01	1.48E+01	-4.69E-01		1.81E+01
5.56E+00	1.36E+01	1.33E+01	-4.23E-01		1.91E+01
8.33E+00	2.14E+01	1.10E+01	-3.51E-01		2.41E+01
1.11E+01	3.29E+01	9.89E+00	-3.14E-01		3.43E+01
1.39E+01	4.82E+01	9.47E+00	-3.01E-01		4.91E+01
1.67E+01	6.35E+01	9.34E+00	-2.96E-01		6.42E+01
1.94E+01	7.50E+01	9.30E+00	-2.95E-01		7.56E+01
2.22E+01	8.18E+01	9.29E+00	-2.95E-01		8.23E+01
	A.51	A.52			A.53
	1.64E-04	-4.37E-04			4.67E-04

Time (Hour)	A.54			A.55
1.67E-02	-7.15E+01			7.15E+01
2.78E-01	-7.08E+01			7.08E+01
5.56E-01	-7.00E+01			7.00E+01
0.00E+00	-6.94E+01			6.94E+01
1.11E+00	-6.87E+01			6.87E+01
1.39E+00	-6.81E+01			6.81E+01
1.94E+00	-6.71E+01			6.71E+01
2.78E+00	-6.62E+01			6.62E+01
4.17E+00	-6.68E+01			6.68E+01
5.56E+00	-7.06E+01			7.06E+01
8.33E+00	-8.95E+01			8.95E+01
1.11E+01	-1.28E+02			1.28E+02
1.39E+01	-1.83E+02			1.83E+02
1.67E+01	-2.39E+02			2.39E+02
1.94E+01	-2.81E+02			2.81E+02
2.22E+01	-3.07E+02			3.07E+02
Time (Hour)	A.56	A.57	A.58	A.59
1.67E-02	3.29E-02	-7.45E-06	-3.28E-03	3.30E-02
2.78E-01	3.29E-02	-1.27E-04	-3.16E-03	3.30E-02
5.56E-01	3.29E-02	-2.59E-04	-3.03E-03	3.30E-02
0.00E+00	3.29E-02	-3.95E-04	-2.89E-03	3.30E-02
1.11E+00	3.29E-02	-5.35E-04	-2.75E-03	3.30E-02
1.39E+00	3.29E-02	-6.77E-04	-2.61E-03	3.30E-02
1.94E+00	3.29E-02	-9.65E-04	-2.32E-03	3.30E-02
2.78E+00	3.29E-02	-1.38E-03	-1.90E-03	3.30E-02
4.17E+00	3.29E-02	-1.99E-03	-1.30E-03	3.30E-02
5.56E+00	3.29E-02	-2.43E-03	-8.54E-04	3.30E-02
8.33E+00	3.29E-02	-2.88E-03	-4.05E-04	3.30E-02
1.11E+01	3.29E-02	-3.03E-03	-2.61E-04	3.30E-02
1.39E+01	3.29E-02	-3.07E-03	-2.19E-04	3.30E-02
1.67E+01	3.29E-02	-3.08E-03	-2.07E-04	3.30E-02
1.94E+01	3.29E-02	-3.08E-03	-2.04E-04	3.30E-02
2.22E+01	3.29E-02	-3.09E-03	-2.03E-04	3.30E-02

Time (Hour)	A.60	A.61	A.62	A.63	A.64
1.67E-02	-5.82E-03	7.85E+00	2.73E-01	7.83E-05	7.86E+00
2.78E-01	-6.04E-03	7.77E+00	2.35E-01	7.83E-05	7.78E+00
5.56E-01	-6.31E-03	7.69E+00	1.92E-01	7.83E-05	7.70E+00
0.00E+00	-6.60E-03	7.62E+00	1.48E-01	7.84E-05	7.62E+00
1.11E+00	-6.94E-03	7.55E+00	1.01E-01	7.84E-05	7.55E+00
1.39E+00	-7.31E-03	7.49E+00	5.14E-02	7.84E-05	7.49E+00
1.94E+00	-8.22E-03	7.38E+00	-5.44E-02	7.85E-05	7.38E+00
2.78E+00	-1.00E-02	7.29E+00	-2.32E-01	7.86E-05	7.29E+00
4.17E+00	-1.48E-02	7.37E+00	-5.82E-01	7.88E-05	7.39E+00
5.56E+00	-2.25E-02	7.81E+00	-1.02E+00	7.91E-05	7.87E+00
8.33E+00	-4.77E-02	9.94E+00	-2.21E+00	7.97E-05	1.02E+01
1.11E+01	-7.43E-02	1.42E+01	-3.95E+00	8.01E-05	1.48E+01
1.39E+01	-8.87E-02	2.04E+01	-6.10E+00	8.02E-05	2.13E+01
1.67E+01	-9.38E-02	2.67E+01	-8.17E+00	8.03E-05	2.79E+01
1.94E+01	-9.54E-02	3.14E+01	-9.68E+00	8.03E-05	3.29E+01
2.22E+01	-9.58E-02	3.43E+01	-1.06E+01	8.03E-05	3.59E+01

Time (Hour)	A.65	A.66	A.67	A.68(ω_α)	α	% Difference
1.67E-02	2.11E-05	7.48E-07	-1.98E-08	2.11E-05	3.80E-05	5.56E+01
2.78E-01	1.25E-06	4.51E-08	-7.17E-11	1.26E-06	2.29E-06	5.47E+01
5.56E-01	6.21E-07	2.27E-08	-1.80E-11	6.21E-07	1.15E-06	5.38E+01
0.00E+00	4.10E-07	1.53E-08	-8.07E-12	4.10E-07	7.75E-07	5.29E+01
1.11E+00	3.04E-07	1.15E-08	-4.57E-12	3.05E-07	5.85E-07	5.20E+01
1.39E+00	2.42E-07	9.29E-09	-2.95E-12	2.42E-07	4.72E-07	5.12E+01
1.94E+00	1.70E-07	6.75E-09	-1.53E-12	1.70E-07	3.43E-07	4.96E+01
2.78E+00	1.18E-07	4.87E-09	-7.72E-13	1.18E-07	2.47E-07	4.76E+01
4.17E+00	7.95E-08	3.42E-09	-3.62E-13	7.96E-08	1.74E-07	4.58E+01
5.56E+00	6.35E-08	2.71E-09	-2.15E-13	6.35E-08	1.38E-07	4.61E+01
8.33E+00	5.48E-08	1.99E-09	-1.05E-13	5.48E-08	1.01E-07	5.43E+01
1.11E+01	5.96E-08	1.57E-09	-6.23E-14	5.96E-08	7.97E-08	7.48E+01
1.39E+01	6.87E-08	1.28E-09	-4.07E-14	6.87E-08	6.51E-08	1.06E+02
1.67E+01	7.51E-08	1.07E-09	-2.84E-14	7.51E-08	5.46E-08	1.38E+02
1.94E+01	7.58E-08	9.23E-10	-2.09E-14	7.58E-08	4.69E-08	1.62E+02
2.22E+01	7.23E-08	8.08E-10	-1.60E-14	7.23E-08	4.10E-08	1.76E+02